Signal Processing Based on Irregular Sampling: Reconstruction, Compression, and Signal Transformation

Jorge Arturo Romero-Chacon

A Thesis

in

The Department

of

Electrical and Computer Engineering

Presented in Partial Fulfillment of the Requirements

for the Degree of Doctor of Philosophy at

Concordia University

Montréal, Québec, Canada

June 1996

ISBN 0-612-18431-5

ABSTRACT

Signal Processing Based on Irregular Sampling: Reconstruction, Compression, and Signal Transformation

Jorge Arturo Romero-Chacón, Ph. D.
Concordia University, 1996

Signal recovery from nonuniformly spaced samples and nonuniform sampling techniques are two topics, belonging to the wider area of sampling theory, that are addressed in this thesis. With respect to signal recovery, a series of sampling expansions, whose coefficients are signal samples located at the root loci of orthogonal polynomials, are produced from a combination of Kramer's generalized sampling theorem and the theory of reproducing kernels. These sampling expansions are actually derived from the reproducing kernels of finite signal spaces defined by the discrete transformations used in calculating the coefficients of orthonormal series expansions. The reproducing kernels and the sampling expansions are then employed in the extension of two methods of signal recovery for short length intervals to transformed domains other than Fourier: one based on the singular value decomposition (SVD) and the other on the solution of a system of linear equations (SLE). The extension implies the substitution of the sinc function and the infinite sampling expansion from the Whittaker-Kotel'nikov-Shannon theorem, by the respective reproducing kernel and related sampling expansion corresponding to the transformed domain. The applicability of the singular value decomposition method is later expanded from short length intervals to longer ones with the help of an on-line iterative procedure, which decomposes the input sequence of nonuniform samples into overlapping blocks. According to the study performed in this thesis, the procedure works very well for jitter values up to 3, after which other methods have to be used. For certain cases where the jitter is greater than 3, a predetermined nonuniform sampling technique is proposed,

and its usefulness depends on the proximity of the sampling points to the root loci of orthogonal polynomials which the technique relies upon. The on-line iterative procedure can be adapted to this last case, and a relative jitter parameter to measure the temporal deviation from a predetermined nonuniform sampling pattern is used, instead of the parameter employed for the case of uniform sampling with jitter.

With respect to the second topic addressed in this thesis, examples of the application of the nonuniform sampling technique, based on the root loci of orthogonal polynomials are shown in the following areas: signal compression, design of FIR digital filters, signal recovery from nonuniform samples, and representation of burst type signals. Also, the technique known as time warping is shown to provide a way to either enhance or suppress an AM/FM or an AM signal by employing a multirate nonuniform sampling approach. This same technique facilitates the representation of a signal in terms of another (unrelated to the first) by using a finite sum of weighted sinc functions centered at nonuniform time instants. These nonuniform points are obtained from information provided by both signals, and the expansion weights are samples of the unrelated signal taken at the nonuniform points.

PARA FERNANDO, MARIA CECILIA Y ROSAURA

ACKNOWLEDGEMENTS

I would like to thank Dr. Eugene I. Plotkin for his guidance during these doctoral years, as well as Dr. M. N. S. Swamy for his guidance and outstanding example of personal integrity in the face of blatant injustice.

I would like to acknowledge the friendship, support and aid I have received from the other students at the Centre for Signal Processing and Communications: Ramesh, Maciej, Manuel, Rajeev, Manijeh, Jiajun, Branka, Hani, Manu, Vijay, Selva, Ali, Hyess, Tong, Adel, Khalil. To all of them, a big thanks.

To the people at the house where I have lived for more than four years (211 rue Centre), in particular Gérard Martineau, Guy Castonguay, Claude and Nicole Chatelois, Andre and Nicole West, Jean-Claude Maillé and Louise del Vecchio, Aline Raymond, Madeleine Richardson, Roméo Labre, Marc Beaupre, I thank them all for being so kind to me. To the rest of the residents, a big thanks.

To my parents and my sister, so far and yet so close, I thank them for their love and unbreakable support and confidence in me.

Una lobrega noche silenciosa
Iba un León horroroso
Con mesurado paso majestuoso
Por una selva, oyó una voz ruidosa,
Que con tono molesto y continuado
Llamaba la atención y aun el cuidado
Del rematado animal que no sabía
De qué bestia feroz quiza saldría
Aquella voz que tanto tráis sonaba,
Cuanto mas en silencio todo estaba.
Su majestad leonesa
La selva toda registrar procura,
Mas nada encuentra con la noche oscura
Hasta que pudo ver, ¡oh que sorpresa!
Que sale de un estanque a la mañana
La tal bestia feroz, y era una Rana.
Llamará la atencion de mucha gente
El charlatán con su mania loca:
Mas ¿que logra, si al fin verá el prudente
Que no es sino una Rana, todo boca?

Félix María Samaniego, *Fábula XVI*

TABLE OF CONTENTS

LIST OF FIGURES

LIST OF SYMBOLS AND ABBREVIATIONS

ABR	Auditory evoked Brainstem Response
AM	Amplitude Modulation
BL_2	Space of Bandlimited Finite Energy Signals
CANF	Constrained Adaptive Notch Filter
cps	Cycles Per Second
DFT	Discrete Fourier Transform
ECG	Electrocardiogram
FIR	Finite Impulse Response
$\mathcal{F}(\ldots)$	Fourier Transform of the Argument
$\mathcal{F}^{-1}(\ldots)$	Inverse Fourier Transform of the Argument
FM	Frequency Modulation
Hz	Hertz (Frequency Unit)
$I[\ .\ ]$	Smallest integer greater than or equal to the argument
$\Im\{\ldots\}$	Imaginary part of the argument
J	Jitter Parameter (with respect to Uniform Positions)
J_r	Relative Jitter Parameter
$J_\mu(\cdots)$	Bessel Function of Order μ of the Argument
LCD	Level Crossing Detector
MSE	Mean Square Error
PSE	Power Spectrum Estimate
$\Re\{\ldots\}$	Real part of the argument
$S_z(j\omega)$	Spectral density of function z
SLE	System of Linear Equations
SVD	Singular Value Decomposition
WKS	Whittaker-Kotel'nikov-Shannon
$\forall$	Symbol meaning *for all*
ω	Angular frequency (rad/sec)

Chapter 1

Introduction

Signal processing based on irregular sampling has had a long history that is not limited to the years after 1949, when Claude E. Shannon published his version of a sampling theorem applicable to bandlimited signals in the Fourier transform sense. The interest in irregular sampling has indeed escalated since then, but there has been antecedents in the mathematical literature since the first decades of the nineteenth century. The aspects in sampling theory which the present thesis addresses, signal recovery from nonuniformly spaced samples and nonuniform sampling techniques, have been considered for many years before the Shannon sampling theorem was published. With respect to the first aspect, irregularity in sampling is a common problem that appears in measurements taken under the influence of natural phenomena. These phenomena disrupts the frequency of the sampling. This disruption can make the sampling to highly deviate from the uniform sampling pattern, that according to the Shannon sampling theorem, is required to retrieve reliable information from the quantity of interest. Methods for signal recovery from nonuniformly spaced samples that handle this type of situations are very useful. With respect to the second aspect, the application of nonuniform sampling techniques based on time warping or in predetermined nonuniform sampling, can facilitate the processing of signals that treated otherwise with uniform sampling, would generate a lot of computational effort. For example, when analyzing transient signals, with variations characteristically concentrated towards the beginning of the observation interval, the use of a sampling pattern adapted to those variations is more efficient than using an uniform sampling pattern for the whole extension of the interval. For both problems of signal recovery from irregularly spaced samples and the application of nonuniform sampling techniques, jitter error reduction can be achieved by using iterative algorithms that can be on-line or not. The concept of on-line refers to the ability to start the recovery procedure without waiting for the totality of the samples to be available.

To trace the origins of the problem of recovering a signal from a given sample set, one has to consider contributions as early as the Lagrange interpolation formula (used already by Cauchy in 1831), which gives a polynomial taking the same values of an arbitrary function at given $x_1, x_2, \ldots, x_n$ points.

$$f(x) = f(x_1)\frac{(x-x_2)\cdots(x-x_n)}{(x_1-x_2)\cdots(x_1-x_n)} + \cdots + f(x_n)\frac{(x-x_1)\cdots(x-x_{n-1})}{(x_n-x_1)\cdots(x_n-x_{n-1})} \qquad (1.1)$$

If the arbitrary function, say $g(x)$, is a polynomial, $f(x)$ will provide an exact representation. If on the other hand, $g(x)$ is a different type of function, $f(x)$ will give only a general approximation to $g(x)$, but it will equal $g(x)$ at the known points $g(x_1), \ldots, g(x_n)$. The points do not have to be taken at equal distances. Cauchy in 1841 [1] presented several formulas, most of them deduced from Equation 1.1, applicable to the problem of interpolation. Two of these formulas will be shown next. Let $f(t)$ be an entire (analytic) function of $\sin(t)$ and $\cos(t)$, and let k be the degree of f. Consider the product $e^{kt\sqrt{-1}}f(t)$, a function of the trigonometric exponential $e^{t\sqrt{-1}}$. The product will obviously be an entire function of degree $2k+1$. If n values $t_1, t_2, \ldots, t_n$ are taken with $n \geq 2k+1$, and Equation 1.1 with $n = 2k+1$ is used, we get

$$\begin{aligned} f(t) \;=\; & f(t_1)\frac{\sin(\frac{t-t_2}{2})\sin(\frac{t-t_3}{2})\cdots\sin(\frac{t-t_n}{2})}{\sin(\frac{t_1-t_2}{2})\sin(\frac{t_1-t_3}{2})\cdots\sin(\frac{t_1-t_n}{2})} + \cdots \\ & \cdots + f(t_n)\frac{\sin(\frac{t-t_1}{2})\sin(\frac{t-t_2}{2})\cdots\sin(\frac{t-t_{n-1}}{2})}{\sin(\frac{t_n-t_1}{2})\sin(\frac{t_n-t_2}{2})\cdots\sin(\frac{t_n-t_{n-1}}{2})} \end{aligned} \qquad (1.2)$$

If the values $\{t_i\}$ follow the rule prescribed by the arithmetic progression $\tau, \tau + \frac{2\pi}{n}, \ldots \tau + (n-1)\frac{2\pi}{n}, \ldots$, and if $f(t)$ represents a real function of t, it follows that

$$f(t) = \frac{1}{2k+1}\sum_{l=0}^{l=2k} \frac{\sin\left[(\frac{2k+1}{2})(t-\tau-\frac{2\pi l}{2k+1})\right]}{\sin\left[\frac{1}{2}(t-\tau-\frac{2\pi l}{2k+1})\right]} f(\tau + \frac{2\pi l}{2k+1}) \qquad (1.3)$$

The next important contribution in sampling theory is apparently due to the Belgian mathematician Charles-Jean Baron de la Vallée Poussin (1908) who was the first person to consider the sampling theorem for functions that are not necessarily band limited, by studying the particular case of duration-limited functions [2]. His work was continued by M. Theis (1919) and J. M. Whittaker (1927) [2]. The next important contribution to sampling theory was put forward by Shannon in the shape of what is today generally called the WKS sampling theorem [3, 4]. This theorem states that if a function f contains no frequencies higher than W Hz, it is completely determined by giving its ordinates at a series of points spaced $\frac{1}{2W}$ seconds apart,

$$f(t) = \sum_{n=-\infty}^{\infty} f(\frac{n}{2W}) \frac{\sin[\pi(2Wt - n)]}{[\pi(2Wt - n)]} \tag{1.4}$$

The qualitative difference between Cauchy's efforts and Shannon's is in the goal of each analysis: the first remains in the interpolation field, while the second states clearly the method by which a bandlimited signal is to be recovered exactly. Cauchy's analysis is applicable to points taken arbitrarily in time, but the sampling theorem strictly requires uniformly distributed time positions and uniformly spaced samples. What originally justified the study of signal processing based on irregular sampling was the impossibility under many practical situations of maintaining or obtaining uniform samples from the signal of interest. This particular problem gives origin to the widely studied topic of signal reconstruction from nonequispaced samples.

Signal recovery from nonuniform samples has been treated by Yen [5] who examined some special nonuniform sampling processes and derived some properties of bandlimited signals. His main results are contained in four theorems, three dealing with nonuniform sample point distributions having simple reconstruction formulas, and a fourth theorem dealing with a new class of signals which he named *minimum-energy* signals, a concept which would be taken up years later under the context of the application of the SVD technique to signal reconstruction [6]. The nonuniform sampling distributions considered are: (1) migration of a finite number of sample points in a uniform distribution, (2) shifting of half the uniform sample points, say, all those with $t > 0-$ by an equal amount with respect to the rest, and (3) a recurrent nonuniform distribution, like for instance, when the sample points are divided into groups of N points each, and the groups have a recurrent period of $\frac{N}{2W}$ seconds. For any of the above distributions, Yen proved that the bandlimited signal remains uniquely defined, so it could be reconstructed from its samples. The following theorem by Yen defines the minimum-energy signals: If the sample values at a finite set of arbitrarily distributed sample points $t = \tau_p$, $p = 1, 2, \ldots, N$ are given, a signal $f(t)$ with no frequency component above W cps is defined uniquely under the condition that the *energy* of the signal $\int_{-\infty}^{\infty} f^2(t)dt$ is a minimum. Moreover, the reconstruction of the signal is

$$f(t) = \sum_{p=1}^{N} f(\tau_p)\Psi_p(t) \tag{1.5}$$

where

$$\Psi_p(t) = \sum_{q=1}^{N} a_{qp} \frac{\sin(2\pi W(t-\tau_q))}{2\pi W(t-\tau_q)} \tag{1.6}$$

The coefficients a_{qp} are the coefficients of the inverse of a matrix whose elements are

$$\frac{\sin(2\pi W(\tau_p - \tau_q))}{2\pi W(\tau_p - \tau_q)}, \qquad p, q = 1, 2, \ldots, N$$

This minimum-energy signal can be employed as one of many approximations to a sampled signal in an interval T.

Several authors have addressed the issue of randomly sampled random processes, for which reconstruction theorems have been proved [7–13]. Among these contributions, Beutler [7] has provided a unified approach to sampling theorems for wide sense stationary random processes $x(t)$. This approach, based upon Hilbert space concepts, gives the following results: (i) a way to recover the process $x(t)$ from nonperiodic samples, or when any finite number of samples are deleted, (ii) conditions for obtaining $x(t)$ when only the past is sampled, (iii) a criterion for restoring $x(t)$ from a finite number of consecutive samples, and (iv) a minimum mean square error estimate of $x(t)$ based on any (possibly nonperiodic) set of samples. A proof of the WKS sampling theorem for wide sense stationary random processes is derived using integration theory, properties of trigonometric series, and Hilbert space ideas.

For bandlimited signals, Yao and Thomas [14] have established the conditions for the existence of stable sampling expansions of the Lagrange interpolation type. A collateral problem that is also addressed is the so-called expansion stability when small corruptions in the amplitudes of sample values may not lead to small changes in the reconstructed signal. A stable sampling expansion with respect to a class of sampling sequences $\{< t_n,\ n \in I >\}$ [1] of a class of functions B_γ (bandlimited to γ radians per second), rests upon the existence of a positive finite absolute constant C (C independent of $f \in B_\gamma$ and $< t_n,\ n \in I >$), such that

[1] I is an index set of integers fixed for each admissible class of sampling sequence

$$\int_{-\infty}^{\infty} |f(t)|^2\,dt \le C\sum_{n\in I} |f(t_n)|^2$$

is valid for each sampling sequence and each f. A stable Lagrange interpolation sampling expansion is defined by the following theorem, due to Yao and Thomas: The class of functions f bandlimited to π rad/s B_π possesses a sampling expansion given by

$$f(t) = \sum_{n=-\infty}^{\infty} f(t_n)\Psi_n(t) \tag{1.7}$$

with respect to each sampling sequence $< t_n,\ n \in I >$ from the class $|t_n - n| \le d < \frac{1}{4}$, with $n \in I = \{0, \pm 1, \pm 2, \ldots\}$, and

$$\Psi_n(t) = \frac{G(t)}{(t - t_n)G'(t_n)}$$

where $G(z)$ is an entire function of exponential type with indicator $H_G(\theta)$ [2] and with its zeros equal to the sampling sequence. In particular, if $d = 0$, the theorem reduces to the Shannon sampling expansion, each composing function is given by $\Psi_n(t) = \frac{\sin(\pi(t-n))}{\pi(t-n)}$, the constant C for stability becomes unity and the following identity is obtained (Parseval's relation):

$$\int_{-\infty}^{\infty} |f(t)|^2\,dt = \sum_{n=-\infty}^{\infty} |f(t_n)|^2 \tag{1.8}$$

It follows from the theorem that for $d > \frac{1}{4}$, it is not possible to obtain a sampling expansion for B_π. However, some of the properties implied by the theorem are still valid for $B_{\pi-\epsilon}$, where $0 < \epsilon \le \pi$. Higgins [15] has presented similar results except that his approach is rooted in the theory of reproducing kernel Hilbert spaces and their bases.

Willis [16] has proposed a method for the spectral estimation and interpolation of a bandlimited function when there are small perturbations (jitter) in sample location. This work is related to [6].

[2] Let $G(z)$ be an entire function of finite order $\rho > 0$ and finite type $\sigma \ge 0$. The function

$$H_G(\theta) = \overline{\lim}_{r\to\infty} \frac{\ln|G(re^{i\theta})|}{r^\rho}$$

which measures the growth of $|G(z)|$ along the ray making the angle θ with the positive real axis, is called the indicator function of $G(z)$

Iterative procedures for the recovery of bandlimited signals from unequally spaced samples have been treated in [17–26], and all these methods depend for their convergence and optimum performance on the constraint imposed on the data sets of the minimum distance known as the Nyquist interval. This interval comes from the Nyquist rate, which is the minimum rate at which a signal can be sampled and still be recovered. The violation of this requirement makes it impossible for any realistic signal recovery.

A definite approach to treat all cases of signal recovery from nonuniform samples in a uniform way has not been achieved owing to the large variety of environments and conditions. On the other hand, and from a different perspective, the application of a nonuniform sampling scheme can be found to be advantageous under some circumstances, when for instance, the signal bandwidth changes with time and in this case, a varying sampling rate would be more efficient to use than a uniform one [27]. In other applications, the inclusion of a nonuniform grid of points in the design of particular systems provide better results than designs based on a uniform grid of points.

Nonuniform sampling techniques have received attention in many fields prompted by the unavoidable alteration of the uniform sampling patterns out of the control of the designer or the observer. Such is the case in astronomy [28, 29], the construction of far field patterns for antennas [30], and system identification [31]. Consider the case of astronomy. It is important in this field to perform photometric observations of stellar objects. These observations cover usually a long period of time in order to obtain an accurate estimation of the main peak, corresponding to the stellar object, in a power spectral window, for example. Secondary peaks could appear, with the rest of the spectral window values very close to zero. Some of the secondary peaks can be justified in the following way: any astronomical object has a seasonal appearance in the sky, which implies that one year periodicity is bound to come up in any long series of astronomical observations; photometric observations can only be made during the dark period of the Moon, and of course, the observations follow the civil calendar in their scheduling of observing time. All these observations are nonuniform in nature, because, apart from the phenomena that appear in the observations and which have been mentioned before, the influence of the Sun has to be taken into account also. A Fourier transform theory is developed in [28] that is valid for arbitrary data spacing. The resulting transform is used in power

spectrum analysis with results that are comparable to an analysis performed with equal data spacing; the important point is that in this case aliasing can not be predicted in advance as it happens for equally spaced data, but has to be analyzed after the fact, in terms of the time spacings employed and the resultant spectral window. One of the main results of [28] is that the observed Fourier transform, denoted by $F_N(\nu)$, is the convolution of the true Fourier transform $F(\nu)$ with a spectral window, $\delta_N(\nu)$, which is obtainable as a function of ν and the times of observation. The problem of the processing of astronomical data is also studied in [29], where an exact nonuniform sampling scheme is proposed based on Cauchy's residue theorem, and the class of signals the study considers can be described by an inverse discrete Fourier transform:

$$f(t) = \frac{1}{2N} \sum_{k=0}^{N} \left[\mathrm{Re}_k \cos\left(\frac{2\pi tk}{2N}\right) + \mathrm{Im}_k \sin\left(\frac{2\pi tk}{2N}\right) \right]$$

A general nonuniform sampling formula is used for the reconstruction of the uniform samples and the DFT of a bandwidth limited signal. The method is successful if as many nonuniform samples are taken during one fundamental period of the signal as are needed for the uniform Shannon sampling theorem; also, the nonuniform kernels work best in situations where an equidistant sampling strategy is disturbed. The same results can be used in the error correction of high frequency network analyzers.

In other fields, the use of nonuniform sampling schemes has been found to be more useful under certain conditions than the normally used uniform sampling scheme, or they have provided a more attractive alternative than the traditional methods from different points of view (computational complexity, sampling efficiency, design characteristics achieved, among others). Such is the case in spectrum analysis [32–36], transient analysis [37], analog-to-digital conversion [38], discrete representation of signals [39, 40], digital encoding of analog sources [41], nonuniform decimation of bandlimited signals [25], digital synthesis of sinusoids [42–46], and FIR digital filter design [47–49]. As an example, consider the field of transient analysis. The study of the transient response of a linear system is based on the characterization of the impulse response by a sum of weighted complex exponentials, and a subsequent estimation of the parameters of the modelled signal. In the determination of the parameters of a complex signal consisting of nonharmonically related damped sinusoids, a nonuniform sampling scheme, found from data adaptation,

could be chosen over uniform sampling. The reasons to use a nonuniform sampling scheme could be the reduction of the effect of measurement noise on estimation, the achievement of sampling efficiency, etc. The chosen nonuniform sampling scheme depends on different criteria of the signal involved, and so, a preprocessing of the data by orthogonal polynomial approximation together with a minimum variance criterion takes place. This allows the reconstruction of the signal at uniform spacings. The statistical characterization of error in the reconstructed signal values is used in an approximate maximum likelihood estimator, which leads to accurate results in the study of transient response in noise [37].

In this thesis, several additions are made to both areas of research in irregular sampling theory, the signal recovery from nonuniform samples and the application of nonuniform sampling techniques. The following outline identifies these contributions:

- Based on Kramer's generalized sampling theorem and the theory of reproducing kernel Hilbert spaces, a set of sampling expansions are obtained whose coefficients depend on the root loci of orthogonal polynomials. The integral transformations derived from orthonormal series expansions (Laguerre, Jacobi, Hermite, Bessel) form the cornerstone of the procedure that combines the theory of reproducing kernels and Kramer's theorem, as explained in Chapter 2.

- Extension of two existing methods for signal recovery, SVD [6] and SLE [21, 26], to other transformed domains and sampling expansions, as well as the recognition and study of areas where a nonuniform sampling technique based on the root loci of orthogonal polynomials could be applied. Chapter 3 presents some of these areas: signal compression, FIR digital filter design, signal recovery from nonuniform samples, and signal representation with its relationship to signal compression.

- Use of the SVD method in conjunction with an on-line iterative procedure for the signal recovery from nonuniform samples. As seen in Chapter 4, this technique is very attractive up to values of the jitter parameter J less than 3. For greater jitter values, and a nonuniform sampling scheme close to the root loci of an orthogonal polynomial, the procedure is adapted to employ recovery methods for short length intervals modified to use reproducing kernels (SVD method) or sampling expansions (SLE method) belonging to finite signal spaces (see Chapter 2).

- Use of nonuniform sampling strategies as a signal transformation tool, for the enhancement or suppression of an AM/FM or an AM signal. This kind of transformation, known as time warping, has also applications in representing a signal in terms of a finite sum of weighted sinc functions centered at nonuniform positions. Several examples in Chapter 5 will help explain these ideas.

The conclusions in Chapter 6 will summarize the highlights of this thesis, as well as provide a view to research areas where additional work can be done to extend and improve the results achieved.

Chapter 2

Reproducing Kernels and Sampling Expansions

2.1 Reproducing kernels for some finite signal spaces

2.1.1 Introductory definitions

The theory of reproducing kernels has originated in the work of mathematicians like G. Szegö (1921) and S. Bergman (1922) [50]. Several definitions are necessary before stating its relationship with sampling theory.

Definition 2.1 Let V be a linear space. A *norm on* V is a rule γ that assigns a real number $\gamma(\phi)$ to each $\phi \in V$ and which satisfies the following axioms ($\phi, \psi \in V$, α any complex number):

1. $\gamma(\alpha\phi) = |\alpha|\gamma(\phi)$
2. $\gamma(\phi + \psi) \leq \gamma(\phi) + \gamma(\psi)$
3. $\gamma(\phi) = 0$ implies that $\phi = 0$ (0 is the zero element in V)

Definition 2.2 Let I denote any open interval $a < x < b$ on the real axis. A function $f(x)$ is said to be quadratically integrable on I if it is a locally integrable function on I such that

$$\alpha_0(f) = \left[\int_a^b |f(x)|^2 dx\right]^{\frac{1}{2}} \tag{2.1}$$

with $\alpha_0(f) < \infty$. This definition defines a complete linear space $L_2(I)$, and its zero element is the class of all functions that are equal to zero almost everywhere on I; α_0 is a norm on $L_2(I)$.

Definition 2.3 An inner product is a rule assigning a complex number (f, g) to each ordered pair f, g of elements in $L_2(I)$ defined by

$$(f, g) = \int_a^b f(x)\overline{g(x)}dx \tag{2.2}$$

where $\overline{g(x)}$ denotes the complex conjugate of $g(x)$. From the concept of inner product follows the concept of completeness. The completeness of a set of orthonormal functions $\{v_n\}$ means that every $f \in L_2(I)$ can be expanded into the series

$$f = \sum_{n=0}^{\infty} (f, v_n) v_n \tag{2.3}$$

which converges in $L_2(I)$, that is

$$a_0 \left(f - \sum_{n=0}^{N} (f, v_n) v_n \right) \to 0$$

as $N \to \infty$. Equation 2.3 is known as the orthonormal series expansion of f with respect to $\{v_n\}$.

Definition 2.4 An inner product space over C (the set of complex numbers) or R (the set of real numbers) which is complete with respect to the norm induced by the inner product is called a complex (or respectively, real) Hilbert space.

With the brief background provided by the above definitions, the concept of a reproducing kernel can be introduced

Definition 2.5[51] Let $\aleph$ be a class of functions defined in I, forming a Hilbert space (complex or real). The function $K(x, y)$ of x and y in I is called a reproducing kernel of $\aleph$ if

1. For every y, $K(x, y)$ as function of x belongs to $\aleph$.

2. The reproducing property: for every $y \in E$ and every $f \in \aleph$,

$$f(y) = (f(x), K(x, y))_x$$

The subscript x indicates that the scalar product applies to functions of x

2.1.2 The calculation of reproducing kernels for some finite signal spaces

The reproducing kernel, when it exists, is unique for a Hilbert space [51]. It will now be calculated for finite spaces that originate from transformations implicit in some orthonormal series expansions.

Given a set of orthonormal functions $\{v_n\}$, every $f \in L_2(I)$ (the set of finite energy signals defined on the interval I) is expressed in the form

$$f = \sum_{n=0}^{N} (f, v_n) v_n = \sum_{n=0}^{N} F(n) v_n \tag{2.4}$$

The coefficients $F(n)$ are obtained according to the relation

$$F(n) = \int_I f(x)\psi_n(x)dx \tag{2.5}$$

where I denotes the interval on $\mathcal{R}$ (the real line) where the orthonormality exists. $F(n)$ is the result of the inner product of each orthonormal function with f. $F(n)$ can assume any value, but only at the discrete points n; this is the main feature of a *discrete* transformation. Consider the following correspondence between Equation 2.4 and a Fourier series expansion for a periodic signal. When the Fourier transform of a Fourier series for a periodic signal is calculated, a sequence of impulses is obtained, with the impulses centered at points separated by a distance which is inversely proportional to the period of the signal. This sequence of impulses defines the *line spectrum* of the periodic signal [52]. The amplitude of each impulse is given by the corresponding coefficient in the expansion. When the periodic signal decomposes into a finite number of harmonics, the Fourier series expansion reduces to a finite sum. Similarly, assume f in Equation 2.4 as being decomposable into a finite sum of $N+1$ basis functions, so that f can be said to be of finite support N on the discrete set of points $\{n\}$, which means, for values $n > N$, $F(n) = 0$. This can be regarded as the discrete counterpart of the concept of bandlimited signals for the Fourier transform domain. An extension of this concept for an integral transformation which produces a continuous spectrum for a continuous variable λ, implies that the finite support is over a bounded, and "continuous" set of values of the variable λ. Other definitions of a bandlimited signal are found in [53]. For the case of signals with finite support N on a discrete transform domain,

$$f = \sum_{n=0}^{N} F(n)\psi_n(x) \tag{2.6}$$

The reproducing kernel $K(x,y)$ corresponding to the signal space under consideration has the following expansion coefficients according to Equation 2.5:

$$K(n,y) = \int_I K(x,y)\psi_n(x)dx \tag{2.7}$$

which is equal, due to the reproducing property of the reproducing kernel, to $\psi_n(y)$. Expanding $K(x,y)$ in terms of the set $\{\psi_n\}$,

$$K(x,y) = \sum_{n=0}^{N} K(n,y)\psi_n(x) = \sum_{n=0}^{N} \psi_n(y)\psi_n(x) \tag{2.8}$$

The set $\{\psi_n\}$ of orthonormal functions is now identified as originating from the classical orthogonal polynomials (Jacobi, Hermite, Laguerre), which define integral transformations corresponding to the orthonormal series expansions. For each of these integral transformations, any member of the set $\{\psi_n\}$ is written as [54]

$$\psi_n(x) = p_n(x)\left[\frac{w(x)}{h_n}\right]^{\frac{1}{2}} \tag{2.9}$$

where $p_n(x)$ is the n^{th} order polynomial, $w(x)$ is the weight function which defines orthogonality on the interval I, and h_n is the normalizing factor for orthonormality on I. Substituting in Equation 2.8:

$$K(x,y) = [w(x)w(y)]^{\frac{1}{2}} \sum_{n=0}^{N}\left[\frac{p_n(x)p_n(y)}{h_n}\right] \tag{2.10}$$

Applying the Christoffel-Darboux identity [55, 56],

$$K(x,y) = [w(x)w(y)]^{\frac{1}{2}}\left\{\frac{k_N}{k_{N+1}}\right\}\left\{\frac{p_{N+1}(x)p_N(y) - p_N(x)p_{N+1}(y)}{h_N(x-y)}\right\} \tag{2.11}$$

where k_N is the highest coefficient of the orthogonal polynomial of order N, and h_N is the normalizing factor corresponding to that polynomial. Appendix A sets out the values of the constants k_N and h_N corresponding to the classical orthogonal polynomials, as well as the values for the generalized Bessel polynomials [57]. The Bessel polynomials behave in a way similar to the classical orthogonal polynomials, the only difference being that their orthogonality is achieved on a trajectory around the unit circle. The reproducing kernels for the aforementioned four examples are given below:

1. Laguerre Transformation: This transformation is defined in the interval $[0,\infty)$. It is based on the generalized Laguerre polynomials, L_n^{α}, of order n and parameter $\alpha > -1$.

$$K(x,y) = (xy)^{\frac{\alpha}{2}}\exp(-\frac{(x+y)}{2})\frac{\Gamma(N+2)}{\Gamma(N+\alpha+1)} \times \left\{\frac{L_N^{\alpha}(x)L_{N+1}^{\alpha}(y) - L_{N+1}^{\alpha}(x)L_N^{\alpha}(y)}{x-y}\right\} \tag{2.12}$$

2. Jacobi Transformation: It is defined in the interval $[-1, 1]$. The Jacobi transformation has as particular cases, the Legendre, the Chebyshev, and the Gegenbauer transformations. The Jacobi polynomials $P_n^{(\alpha,\beta)}$ have order n and parameters $\alpha, \beta > -1$.

$$K(x,y) = [w(x)w(y)]^{\frac{1}{2}} \frac{2^{-\alpha-\beta}}{2N+\alpha+\beta+2} \frac{\Gamma(N+2)}{\Gamma(N+\alpha+1)} \frac{\Gamma(N+\alpha+\beta+2)}{\Gamma(N+\beta+1)} \times \left\{ \frac{P_{N+1}^{(\alpha,\beta)}(x)P_N^{(\alpha,\beta)}(y) - P_N^{(\alpha,\beta)}(x)P_{N+1}^{(\alpha,\beta)}(y)}{x-y} \right\} \tag{2.13}$$

where

$$w(x) = (1-x)^{\alpha}(1+x)^{\beta}$$

3. Hermite Transformation: This transformation is defined in $(-\infty, \infty)$. The Hermite polynomials H_n are characterized by their order n.

$$K(x,y) = \frac{\exp(-\frac{x^2+y^2}{2})}{\sqrt{\pi}} \frac{H_{N+1}(x)H_N(y) - H_N(x)H_{N+1}(y)}{2^{N+1}N!(x-y)} \tag{2.14}$$

4. Bessel Transformation: In a merely formal way, the generalized Bessel polynomials can be stated to form an orthonormal set with weight function $\rho(x)$ and a unit circle path of integration.

$$K(x,y) = \frac{(-1)^{N+1}[\rho(x)\rho(y)]^{\frac{1}{2}}\Gamma(N+a)[y_{N+1}(x)y_N(y) - y_N(x)y_{N+1}(y)]}{(2N+a)N!\Gamma(a)(x-y)} \tag{2.15}$$

where y_N denotes the generalized Bessel polynomial $y_N(x,a,b)$ of variable x, parameters a and b, and order N [57].

Several authors have proposed to modify the transformations defined in Equation 2.5, so that they no longer depend on a discrete index. The definition of continuous versions and the corresponding inverse transformations, along with the derivation of sampling theorems (in the transform domain) similar to the Shannon sampling theorem, are some of the modifications proposed [58-60].

2.2 Sampling Expansions from Reproducing Kernels

The reproducing kernel Hilbert spaces associated with the Fourier, Hankel-Bessel, sine and cosine transformations can be shown to produce sampling expansions [61]. These transformations are functions of a continuous variable, and each of them has an associated space of finite energy bandlimited signals. Next, sampling expansions will be derived from the reproducing kernels presented in the previous section.

For the discrete transformations under consideration, the application of Kramer's generalized sampling theorem [62] will result in a sampling expansion for the functions f which have finite support N in the transform domain [63].

Let $f(t)$ be a signal of finite support N. The basic assumption of the Kramer's generalized sampling theorem is the existence of a finite energy signal $g(t)$ related to $f(t)$ by a kernel function $R(t,x)$. Consider the particular case when $g(t) = f(t)$, and $R(t,x) = K(t,x)$. With these modifications, it follows that, if,

$$f(t) = \int_I R(t,x)g(x)dx = \int_I K(t,x)f(x)dx \tag{2.16}$$

and if there is a set $E = \{t_n\}$ such that $\{K(t_n,x)\}$ is a complete orthogonal set on $L_2(I)$, then

$$f(t) = \lim_{N\to\infty} \sum_{|n|\le N} f(t_n)S_n(t) = \sum_{|n|\le N} f(t_n)S_n(t) \tag{2.17}$$

with

$$S_n(t) = \frac{\int_I K(t,x)K^*(t_n,x)dx}{\int_I |K(t_n,x)|^2 dx} \tag{2.18}$$

where $K^*(t_n,x)$ denotes the complex conjugate of $K(t_n,x)$. To illustrate how to find the set $\{t_n\}$, consider the Laguerre transformation with the Laguerre polynomial of order N and parameter α. For this case, the reproducing kernel is

$$K(x,y) = (xy)^{\alpha/2}\exp(-\frac{x+y}{2})\frac{\Gamma(N+2)}{\Gamma(N+\alpha+1)}\left[\frac{L_N^\alpha(x)L_{N+1}^\alpha(y) - L_{N+1}^\alpha(x)L_N^\alpha(y)}{x-y}\right] \tag{2.19}$$

Let $t_1, t_2 \in I, t_1 \neq t_2$,

$$\begin{aligned}\int_0^{\infty} K(x,t_1)K(x,t_2)dx &= K(t_1,t_2) \\ &= (t_1t_2)^{\alpha/2}e^{-\frac{t_1+t_2}{2}}\frac{\Gamma(N+2)}{\Gamma(N+\alpha+1)} \quad \times \\ &\quad \left[\frac{L_N^{\alpha}(t_1)L_{N+1}^{\alpha}(t_2)-L_{N+1}^{\alpha}(t_1)L_N^{\alpha}(t_2)}{t_1-t_2}\right]\end{aligned}$$

To make $K(x,t_1), K(x,t_2)$ orthogonal, the following equality has to be fulfilled:

$$L_N^{\alpha}(t_1)L_{N+1}^{\alpha}(t_2)-L_{N+1}^{\alpha}(t_1)L_N^{\alpha}(t_2)=0$$

With f of finite support N, there are $\frac{(N-1)N}{2}$ equations similar to the above equation. One obvious choice to satisfy these equations at the same time, is to choose the $t_i's$ to be the $N+1$ roots of the Laguerre polynomial $L_{N+1}^{\alpha}(x)$. With this choice, the set of functions expressed by

$$\begin{aligned}K(x,t_i) &= (xt_i)^{\alpha/2}\exp(-\frac{x+t_i}{2})\frac{\Gamma(N+2)}{\Gamma(N+\alpha+1)}\left\{\frac{L_N^{\alpha}(x)L_{N+1}^{\alpha}(t_i)-L_{N+1}^{\alpha}(x)L_N^{\alpha}(t_i)}{x-t_i}\right\} \\ &= (xt_i)^{\alpha/2}\exp(-\frac{x+t_i}{2})\frac{\Gamma(N+2)}{\Gamma(N+\alpha+1)}\left\{\frac{-L_{N+1}^{\alpha}(x)L_N^{\alpha}(t_i)}{x-t_i}\right\} \qquad (2.20)\end{aligned}$$

with $i=1,\ldots,N+1$, forms an orthogonal set of functions. Note that the choice is partly justified by the number of orthonormal functions in the expansion of f with finite support N. Therefore,

$$f(t)=\sum_{k=1}^{N+1} f(t_k)S_k(t) \qquad (2.21)$$

where $\{t_k\}$ are the roots of the Laguerre polynomial $L_{N+1}^{\alpha}(x)$, and

$$S_k(t)=\frac{\int_0^{\infty}K(x,t)K(x,t_k)dx}{\int_0^{\infty}|K(x,t_k)|^2dx}$$

Using the fact that t_k is a root of L_{N+1}^{α}, the denominator simplifies in the following way:

$$\int_0^{\infty}|K(x,t_k)|^2dx = \lim_{t_j\to t_k}\int_0^{\infty}K(x,t_j)K(x,t_k)dx$$

$$
\begin{aligned}
&= \frac{\Gamma(N+2)}{\Gamma(N+\alpha+1)} \lim_{t_j \to t_k} (t_j t_k)^{\alpha/2} \exp(-\frac{t_j+t_k}{2}) \frac{-L_{N+1}^{\alpha}(t_j) L_N^{\alpha}(t_k)}{t_j - t_k} \\
&= \frac{\Gamma(N+2)}{\Gamma(N+\alpha+1)} \exp(-t_k) t_k^{\alpha} \left\{ \frac{d}{dt_j} [-L_{N+1}^{\alpha}(t_j) L_N^{\alpha}(t_k)] \right\}_{t_j = t_k} \\
&= \frac{\Gamma(N+2)}{\Gamma(N+\alpha+1)} \exp(-t_k) t_k^{\alpha} (-L_N^{\alpha}(t_k)) \quad \times \\
&\quad \left\{ \frac{(N+1) L_{N+1}^{\alpha}(t_k) - (N+\alpha+1) L_N^{\alpha}(t_k)}{t_k} \right\} \\
&= t_k^{\alpha-1} \exp(-t_k) \frac{\Gamma(N+2)}{\Gamma(N+\alpha+1)} (N+\alpha+1) [L_N^{\alpha}(t_k)]^2
\end{aligned}
$$

The identity [56]

$$
t \frac{dL_{N+1}^{\alpha}(t)}{dt} = (N+1) L_{N+1}^{\alpha}(t) - (N+\alpha+1) L_N^{\alpha}(t)
$$

has been used. Now, for the numerator,

$$
\begin{aligned}
\int_0^{\infty} K(x,t) K(x,t_k) dx &= K(t,t_k) \\
&= (tt_k)^{\alpha/2} \exp(-\frac{t+t_k}{2}) \frac{\Gamma(N+2)}{\Gamma(N+\alpha+1)} \frac{-L_{N+1}^{\alpha}(t) L_N^{\alpha}(t_k)}{(t-t_k)}
\end{aligned}
$$

The final expression for the composing functions in the sampling expansion is:

$$
\begin{aligned}
S_k(t) &= \frac{t^{\alpha/2} (t_k)^{1-\frac{\alpha}{2}} \exp(-\frac{t-t_k}{2}) [-L_{N+1}^{\alpha}(t)]}{(t-t_k)(N+\alpha+1) L_N^{\alpha}(t_k)} \\
&= \frac{t_k (t/t_k)^{\alpha/2} \exp(-\frac{t-t_k}{2}) [-L_{N+1}^{\alpha}(t)]}{(t-t_k)(N+\alpha+1) L_N^{\alpha}(t_k)}
\end{aligned} \tag{2.22}
$$

This example given for the Laguerre transformation may be generalized for the other transformations as well. Equation 2.20 that sets up the condition under which a set of values $\{t_n\}$ defines a set of orthogonal functions, is generalized for the other transformations considered here, by substituting the variables t_1 and t_2 for x and y respectively, in Equations 2.13, 2.14, and 2.15. For those three transformations and for any values $t_1, t_2, t_1 \neq t_2$:

$$
P_{N+1}^{(\alpha,\beta)}(t_1) P_N^{(\alpha,\beta)}(t_2) - P_N^{(\alpha,\beta)}(t_1) P_{N+1}^{(\alpha,\beta)}(t_2) = 0 \tag{2.23}
$$

$$H_{N+1}(t_1)H_N(t_2) - H_N(t_1)H_{N+1}(t_2) = 0 \tag{2.24}$$

$$y_{N+1}(t_1)y_N(t_2) - y_N(t_1)y_{N+1}(t_2) = 0 \tag{2.25}$$

For each transformation, the composing functions of the sampling expansions before normalization are:

$$K(x,t_i) = (w(x)w(t_i))^{\frac{1}{2}} \frac{2^{-\alpha-\beta}}{2N+\alpha+\beta+2} \frac{\Gamma(N+2)}{\Gamma(N+\alpha+1)} \times \frac{\Gamma(N+\alpha+\beta+2)}{\Gamma(N+\beta+1)} \frac{P_{N+1}^{(\alpha,\beta)}(x)P_N^{(\alpha,\beta)}(t_i)}{x-t_i} \tag{2.26}$$

$$K(x,t_i) = \frac{e^{-\frac{x^2+t_i^2}{2}}}{\sqrt{\pi}} \frac{H_{N+1}(x)H_N(t_i)}{2^{N+1}N!(x-t_i)} \tag{2.27}$$

$$K(x,t_i) = \frac{(-1)^{N+1}[\rho(x)\rho(t_i)]^{\frac{1}{2}}\Gamma(N+a)y_{N+1}(x)y_N(t_i)}{(2N+a)N!\Gamma(a)(x-t_i)} \tag{2.28}$$

The respective composing functions for each of the above transformations, in the same order, are:

$$S_k(t) = \frac{2[w(t)]^{\frac{1}{2}}P_{N+1}^{(\alpha,\beta)}(t)}{(t-t_k)[w(t_k)]^{\frac{1}{2}}(N+2+\alpha+\beta)P_N^{(\alpha+1,\beta+1)}(t_k)} \tag{2.29}$$

$$S_k(t) = \frac{\sqrt{\pi}\exp(-\frac{t^2-t_k^2}{2})H_{N+1}(t)}{2(t-t_k)(N+1)H_N(t_k)} \tag{2.30}$$

$$S_k(t) = \frac{[\rho(t)/\rho(t_k)]^{\frac{1}{2}}\, y_{N+1}(t)t_k[2(N+1)+a-2]}{(t-t_k)y_N(t_k)b(N+1)} \tag{2.31}$$

The intermediate algebraic operations corresponding to the last results can be found in Appendix D.

In summary, for a signal f of finite support N, there is an expansion based on $N+1$ orthonormal functions $\psi_n(x)$ obtained by choosing the set $\{t_n\}$ equal to the $N+1$ roots of the polynomials $L_{N+1}^{\alpha}(x)$, $P_{N+1}^{(\alpha,\beta)}(x)$, $H_{N+1}(x)$, and $y_{N+1}(x)$. This expansion results from evaluating Equation 2.21.

Chapter 3

Nonuniform Sampling: Methods, Strategies and Applications

3.1 The SVD method and its relationship with reproducing kernels

The singular value decomposition (SVD) method for the recovery of signals from nonuniform samples has been introduced by D. J. Wingham [6]. This approach, originally proposed for bandlimited signals in the Fourier transform sense, uses the reproducing property of the sinc function to set up an algorithm based on the singular value decomposition of a matrix whose entries are given by the sinc function evaluated at the known nonuniform time instants. An expansion based on multiples of the sinc function and centered at the nonuniform time instants, is used to reconstruct the original signal. The number of composing functions of the expansion equals the number of nonuniform samples. These composing functions are linearly independent but not necessarily orthogonal. The expansion coefficients are calculated from the nonuniform sample values, and from the eigenvectores and eigenvalues of the singular value decomposition.

This method guarantees that the values of the reconstructed signal equal the nonuniform samples at the known nonuniform time instants. The reconstruction so provided constitutes the minimum norm solution to the recovery problem, and from this point of view, it is equivalent to Yen's solution [5].

There are two ways to implement the SVD method, but the final result is the same. The following is the description of the algorithm, showing both versions.

First version: Let $\{t_i\}$ be the set of nonuniform time instants with $i = 1, 2, \ldots, m$, $\{y(t_i)\}$ be the set of nonuniform samples, $\{s_k\}$ be the set of uniform time instants (or any other set of points where the signal has to be known) with $k = 1, 2, \ldots, p$, and $\{h(s_k)\}$ be the set of samples to recover.

1. Construct the matrix A whose entries are given by

$$a_{ik} = \frac{\sin[2\pi f_0(t_i - s_k)]}{[2\pi f_0(t_i - s_k)]}$$

In general, A is a rectangular matrix.

2. Find the singular value decomposition of A. This generates the left singular vectors $\{v_i(n)\}$ with $n = 1, 2, \ldots, m$ and size $m \times 1$, the right singular vectors $\{u_i(s_k)\}$ of size $p \times 1$, and the singular values $\{\lambda_i\}$.

3. Compute

$$\gamma_i = \lambda_i^{-1} \sum_n y(t_n) v_i(n)$$

where $n = 1, 2, \ldots, m$.

4. Compute

$$h(s_k) = \sum_i \gamma_i u_i(s_k)$$

Second version: Let $\{t_i\}$, $\{y(t_i)\}$, $\{s_k\}$, $\{h(s_k)\}$ be defined as before.

1. Form matrix B, whose entries are given by

$$b_{ij} = \frac{\sin[2\pi f_0(t_i - t_j)]}{[2\pi f_0(t_i - t_j)]}$$

where $i, j = 1, 2, 3, \ldots, m$. Notice that B is formed using only the nonuniform time instants $\{t_i\}$.

2. Obtain eigenvectors and eigenvalues of B. Let the eigenvectors be denoted as $\{v_i(n)\}$ with $n = 1, 2, \ldots, m$, and the eigenvalues as λ_i^2, where λ_i's are also the singular values of the SVD decomposition of the kernel

$$K(n, t) = \frac{\sin[2\pi f_0(t_n - t)]}{[2\pi f_0(t_n - t)]}$$

3. Evaluate

$$u_i(s_k) = \lambda_i^{-1} \sum_n v_i(n) \frac{\sin[2\pi f_0(s_k - t_n)]}{[2\pi f_0(s_k - t_n)]}$$

where $n = 1, 2, \ldots, m$. $\{u_i(s_k)\}$ are the right singular vectors and $\{v_i(n)\}$ are the left singular vectors of the SVD decomposition of $K(n, t)$.

4. Evaluate

$$\gamma_i = \lambda_i^{-1} \sum_n y(t_n) v_i(n)$$

where $n = 1, 2, \ldots, m$.

5. Evaluate

$$h(s_k) = \sum_i \gamma_i u_i(s_k)$$

Even though the SVD method is concerned with bandlimited signals in the Fourier transform domain, the reproducing property of the sinc function opens up the possibility of extending the method to other transform domains. Hilbert spaces with a reproducing kernel, in particular those where orthogonal transforms can be defined, can then have their own version of the SVD method. Within the transform domains, the set of signals for which the method would be applicable are those with finite support in the corresponding transform domain. For the Fourier transform domain, these finite support signals are the commonly known bandlimited signals.

The main reason for extending the results obtained for the Fourier domain to other domains is the possible optimization of signal processing: useful characteristics not shown in the Fourier domain but existing in another transform domain, can be exploited [64, 65]. If a signal reconstruction is attempted, it would be based on composing functions which are also of finite support in the transform domain under consideration. Functions which are not of finite support in any domain can always get a reconstruction based on finite support functions. In this case, the reconstruction would be somewhat affected by the finite number of composing functions (one composing function for each given nonuniform sample). An additional advantage of having a reproducing kernel-based procedure for a given transform domain is the certainty that the reconstruction achieves the minimum-norm solution to the problem.

The changes that have to be made to adapt the SVD method to other Hilbert spaces with reproducing kernel $K(x, y)$, are minimal. For the first version of the method, make

$$a_{ik} = K(t_i, s_k)$$

The second version requires some more changes. Make

$$\begin{aligned} b_{ij} &= K(t_i, t_j) \\ K(n, t) &= K(t_n, t) \\ u_i(s_k) &= \lambda_i^{-1} \sum_n v_i(n) K(s_k, t_n) \end{aligned}$$

Once these changes are made for the respective Hilbert space and transformation, the algorithm is ready for use. Several examples will be presented to illustrate this theory.

This general approach based on the SVD method, once extended to other reproducing kernel Hilbert spaces, justifies the name of *reproducing kernel approach* for the whole procedure [63].

3.1.1 Reproducing kernel approach: examples

Consider the Hankel, sine, and cosine transformations. The expressions for the corresponding reproducing kernels have been already obtained in [61] under different considerations.

(a) Hankel transformation

Let H_h be the class of $L_2([0,\infty[)$ functions f such that their Hankel transforms of order ν, $\nu \geq -\frac{1}{2}$

$$F(\lambda) = \int_0^{\infty} (\lambda t)^{\frac{1}{2}} J_\nu(\lambda t) f(t) dt$$

vanish almost everywhere outside of $[0, B_h]$. The corresponding inverse Hankel transform is given by

$$f(t) = \int_0^{B_h} (\lambda t)^{\frac{1}{2}} J_\nu(\lambda t) F(\lambda) d\lambda$$

with $t \geq 0$, $F \in L_2([0, B_h])$. H_h is a reproducing kernel Hilbert space on $E_h = [0, \infty[$. The unique reproducing kernel is given by

$$\begin{aligned} K_h(x,y) &= \frac{B_h (yx)^{\frac{1}{2}}}{2(x^2 - y^2)} [y J_\nu(xB_h)\{J_{\nu-1}(yB_h) - J_{\nu+1}(yB_h)\} - \\ &\quad x J_\nu(yB_h)\{J_{\nu-1}(xB_h) - J_{\nu+1}(xB_h)\}] \end{aligned} \tag{3.1}$$

(b) Sine transformation

Let H_s be the class of $L_2([0,\infty[)$ f functions such that their sine transforms

$$F(\beta) = \left(\frac{2}{\pi}\right)^{\frac{1}{2}} \int_0^{\infty} \sin(\beta t) f(t) dt$$

vanish almost everywhere outside of $[0, B_s]$. The corresponding inverse sine transform is given by

$$f(t) = \left(\frac{2}{\pi}\right)^{\frac{1}{2}} \int_0^{B_s} \sin(\beta t) F(\beta) d\beta$$

with $t \geq 0$, $F \in L_2([0, B_s])$. H_s is a reproducing kernel Hilbert space on $E_s = [0, \infty[$. The unique reproducing kernel is given by

$$K_s(x, y) = \frac{1}{\pi} \left\{ \frac{\sin((y-x)B_s)}{y-x} - \frac{\sin((y+x)B_s)}{(y+x)} \right\} \tag{3.2}$$

(c) Cosine transformation

Let H_c be the class of $L_2([0, \infty[)$ f functions such that their cosine transforms

$$F(\gamma) = \left(\frac{2}{\pi}\right)^{\frac{1}{2}} \int_0^{\infty} \cos(\gamma t) f(t) dt$$

vanish almost everywhere outside of $[0, B_c]$. The corresponding inverse cosine transform is given by

$$f(t) = \left(\frac{2}{\pi}\right)^{\frac{1}{2}} \int_0^{B_c} \cos(\gamma t) F(\gamma) d\gamma$$

with $t \geq 0$, $F \in L_2([0, B_c])$. H_c is a reproducing kernel Hilbert space on $E = [0, \infty[$. The unique reproducing kernel is given by

$$K_c(x, y) = \frac{1}{\pi} \left\{ \frac{\sin(B(y+x))}{y+x} + \frac{\sin(B(y-x))}{y-x} \right\} \tag{3.3}$$

3.1.2 A triangular function: recovery from nonuniform samples

As a practical example of the application of the reproducing kernel approach, consider a train of three triangular pulses. If the bandwidth of this signal is defined as the frequency at which 90 per cent of the signal energy is contained, then 19 is the number of samples necessary to reconstruct the signal according to the sampling theorem. This number of samples comes after some calculations involving the square power of the magnitude of the FFT of the signal.

Figure 3.1 shows the results of signal recovery after 20 uniform samples have been given as input to four different variations of the SVD method. Each of these variations includes a reproducing kernel analyzed already in the last section.

Figure 3.2 shows the signal recovery after 20 uniform samples with jitter have been given as input to four different variations of the SVD method. The jitter parameter[1] is

[1] J is the parameter used to define the interval $[-\frac{JT}{2}, \frac{JT}{2}]$, on which the random variable δt is uniformly distributed. T is the sampling period. The random variable defines the set $\{\tau_k\}$ of nonuniform time instants, $\tau_k = kT + \delta t$, where kT is the uniform time instant.

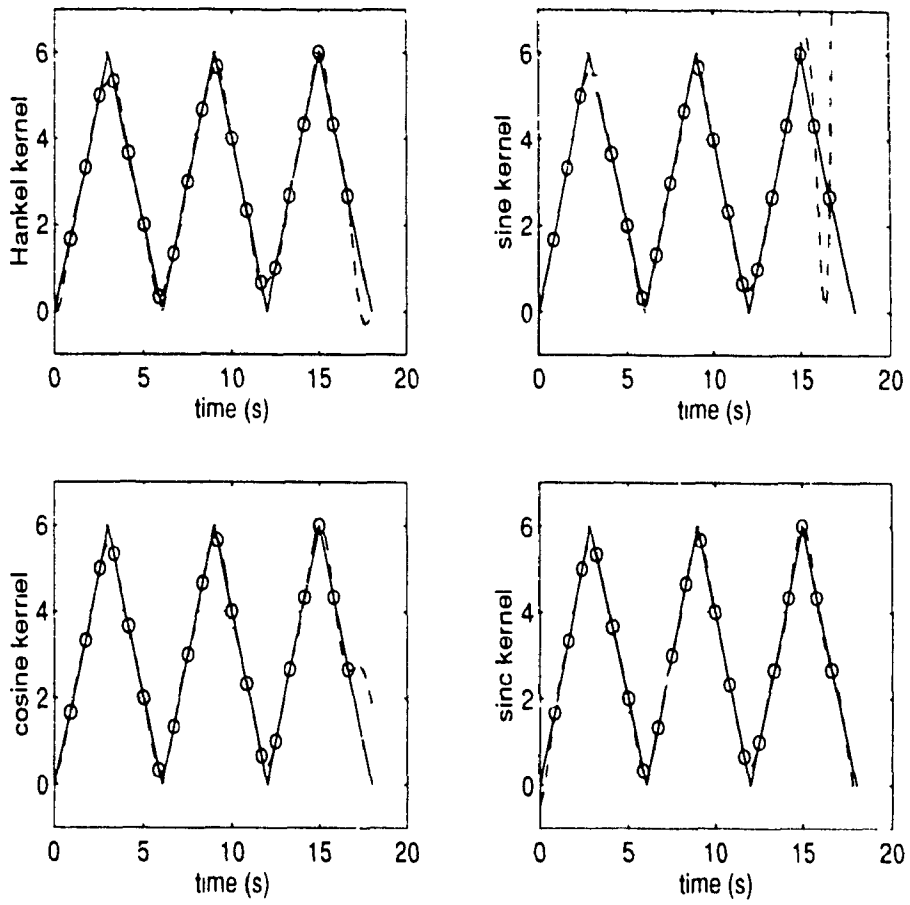

Figure 3.1: Recovery of a train of three triangular pulses using the SVD method. Each of the graphs corresponds to a different reproducing kernel. The first corresponds to the Hankel-transformed domain, the second to the sine-transformed domain, the third to the cosine-transformed domain, and the last to the Fourier-transformed domain, where the sinc function is the corresponding reproducing kernel.

$J = 0.6$.

Figure 3.3 shows the signal recovery when $J = 1.2$. For this particular example, the method with the sinc kernel seems to provide the best solution when the jitter increases.

The SVD method can also be adapted to the finite signal spaces with reproducing kernels obtained in Chapter 2. The special case when $x = y$ for those kernels is considered in Appendix D. The recovery from nonuniform samples using the SVD method with those reproducing kernels will be treated later in this chapter.

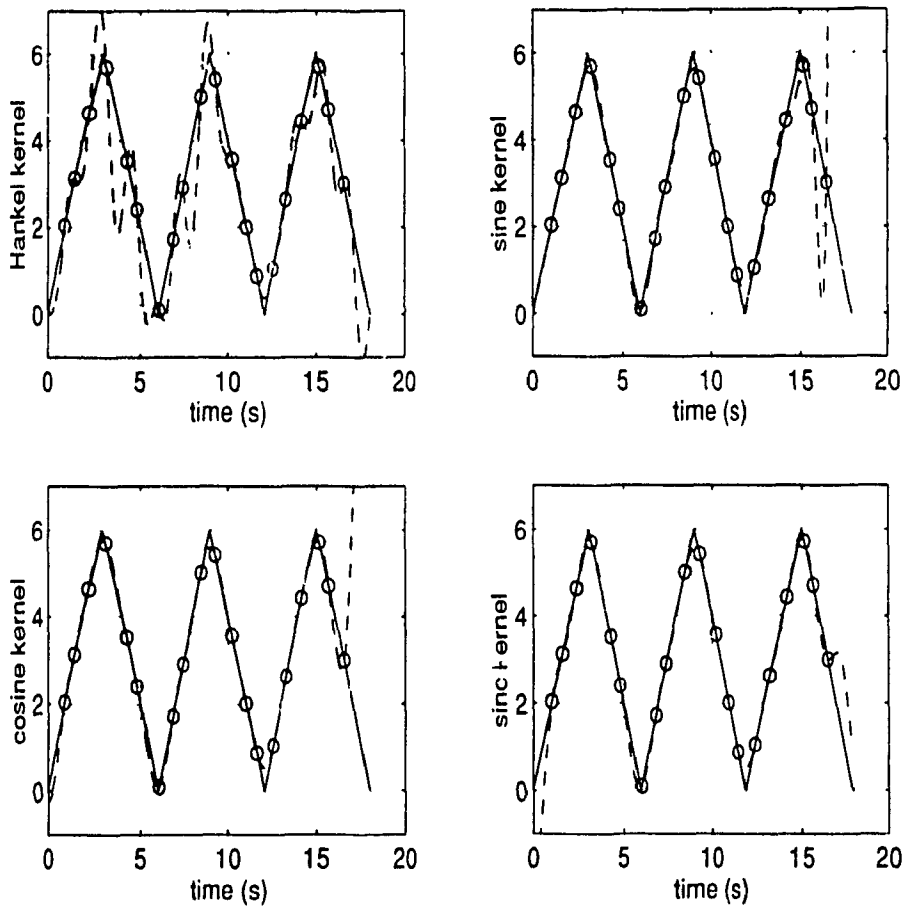

Figure 3.2: Recovery of a train of triangular pulses using the SVD method with $J = 0.6$.

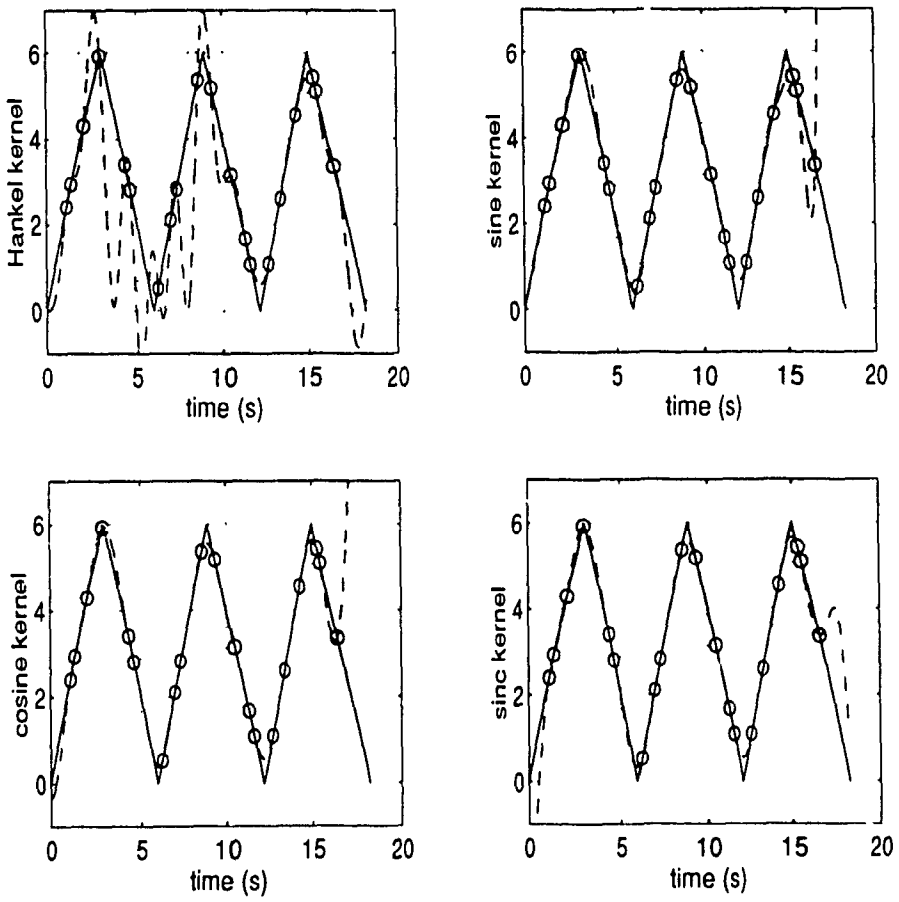

Figure 3.3: Recovery of a train of triangular pulses using the SVD method with $J = 12$.

3.1.3 Other examples

Figure 3.4 shows three different examples of signal recovery using the reproducing kernel approach. The recovery is performed from a set of eight nonuniform samples, which are positioned in the time instants indicated by a circle ('o'). In (a), the recovery takes place in the Hankel transformed domain, where the signal

$$f(t) = \frac{AB_h t^{\frac{1}{2}}}{2(1-t^2)} \{t(J_{\nu-1}(B_h t) - J_{\nu+1}(B_h t))J_\nu(B_h) - (J_{\nu-1}(B_h) - J_{\nu+1}(B_h))J_\nu(B_h t)\}$$

is bandlimited to B_h in the Hankel transform sense. Note in this case that the signal and the reconstruction are indistinguishable from one another. In (b), the recovery this time takes place in the cosine transformed domain, where the signal

$$f(t) = A\sqrt{\frac{2}{\pi}}\frac{\sin(B_c t)}{t}$$

is bandlimited to B_c in the cosine transform sense. The match between the reconstruction and the original signal seems to be very good. Finally, in (c), the signal reconstruction takes place in the sine transformed domain, where the signal

$$f(t) = \frac{2A}{t}\sqrt{\frac{2}{\pi}}\sin^2(\frac{B_s t}{2})$$

is bandlimited to B_s in the sine transform sense. The reconstruction is not good at the end of the observation interval, due to: (1) the positiveness of the original signal and that the composing functions of the expansion used in the reconstruction can take any value positive or negative, and (2) there is not enough information at the end of the interval for the reconstruction to match the signal variations.

3.2 Sampling expansions and the SLE method

To determine a finite-energy signal $x(t)$, bandlimited to $|f| \leq f_0$, from its samples $\{x(nT)\}$ sampled at or above the Nyquist rate $(1/2f_0)$, an infinite series has to be used. This infinite series is stated in the sampling theorem (also known as the WKS sampling theorem, for Whittaker, Kotel'nikov, and Shannon [3]). Instead of using an infinite series, a truncated version can be used, giving the value of $x(t)$ at any instant t_m, as

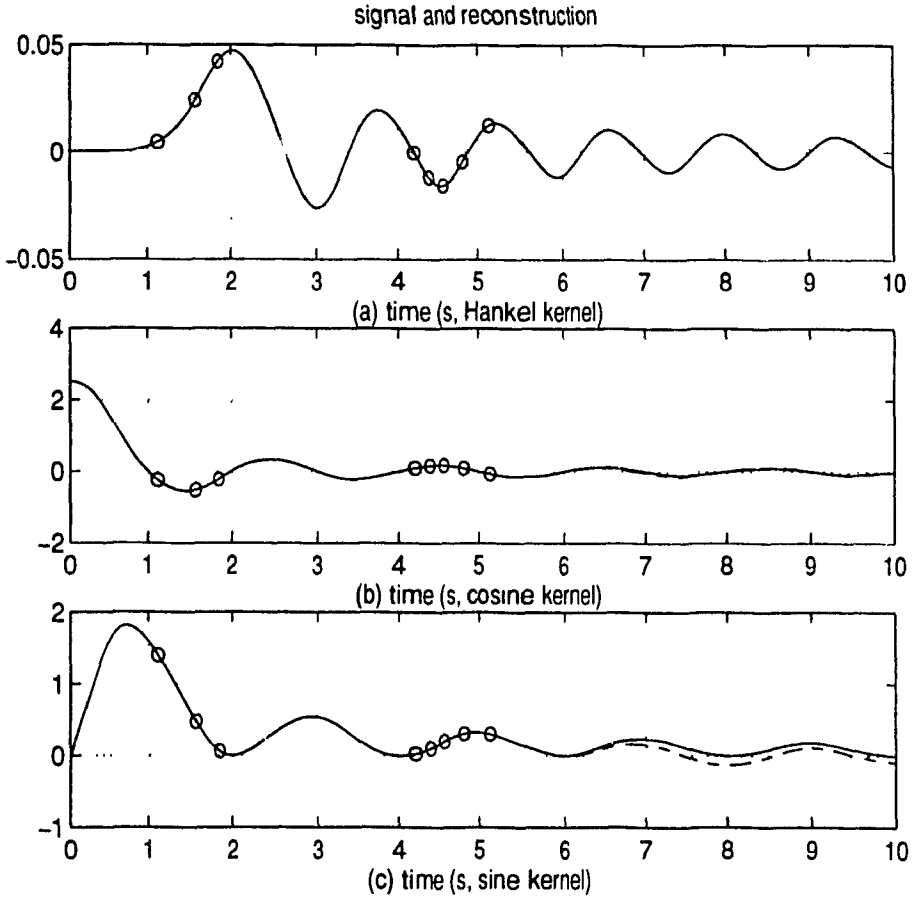

Figure 3.4: The continuous line represent the original signal, and the dashes represent the recovery. In (a), the recovery is performed in the Hankel transformed domain. In (b), it is performed in the cosine transformed domain, and in (c), it is performed in the sine transformed domain.

$$\underline{x}(t_m) = A\underline{x}(nT) \tag{3.4}$$

where $T = 1/2f_s$, f_s is the sampling frequency, $\underline{x}(t_m)$ is the vector of reconstructed samples, and A is a $N \times N$ matrix with entries defined by

$$a_{mn} = \frac{\sin[2\pi f_s(t_m - nT)]}{[2\pi f_s(t_m - nT)]} \tag{3.5}$$

with $m, n = 1, 2, \ldots, N$, and $\underline{x}(nT) = [x(T), x(2T), \ldots, x(NT)]^T$ is a set of equally spaced samples. Note that Equation 3.4 is a system of N equations for N unknowns. To reduce the error caused by the substitution of the infinite series by its truncated version, the order N of the system should be taken exceptionally large. The solution of the system, in consequence, represents a straightforward solution to the problem but becomes meaningless due to its large size. In [24] it was suggested that a set $\underline{x}(\tau_m)$ of nonuniform samples at time instants $\{\tau_m\}$ could be used in Equation 3.4 because $\underline{x}(t_m)$ represents any arbitrary set of samples. The relationship between $\underline{x}(\tau_m)$ and $\underline{x}(nT)$ is then given by the Equation 3.4 where A is the composing matrix with elements

$$a_{mn} = \frac{\sin[2\pi f_s(\tau_m - nT)]}{2\pi f_s(\tau_m - nT)} \tag{3.6}$$

with $m, n = 1, 2, \ldots, N$, and $\tau_m = mT + \delta t$. δt is a random variable distributed in the interval $[-\frac{JT}{2}, \frac{JT}{2}]$, where J has been already defined as the jitter parameter. The uniform sample vector $\underline{x}(nT)$ is found by solving the system of linear equations. This method, which will be called SLE (for System of Linear Equations) can be extended also to other types of sampling expansions, infinite or not.

Sampling expansions can be derived from the reproducing kernels examined in Section 3.1.1 by following a path similar to the one already described in Chapter 2 for finite signal spaces related to discrete transformations derived from orthonormal series expansions. These sampling expansions are calculated by an alternate way in [61, 66]. The extension of the SLE method to other sampling expansions has the effect of mapping the set of nonuniform samples given into another set of nonuniform samples of a known time instants pattern. The original signal is thereby restored using the new set of nonuniform samples and the respective sampling expansion [63].

A comparison between the SVD and SLE methods points out several differences. Firstly, the kind of expansion used in the SLE method is based on a set of orthonormal functions, while reconstruction using the SVD method is based on linearly independent functions that are not necessarily orthogonal. Secondly, the expansion coefficients in the second method are signal samples, while the coefficients in the first method depend on, but are not restricted to, the nonuniform samples given. Thirdly, the coefficient matrix of the system of linear equations uses two sets of time instant points, while the matrix in one of the two versions of the first method uses only one set. Fourthly, the reconstruction using the SVD method is guaranteed to produce the minimum-norm solution to the problem of recovery from nonuniform samples. A fifth observation concerns the computational complexity of both the methods: the SLE method is much less computationally expensive than the SVD method. In this regard, see Appendix F. Finally, a sixth observation will be made in Chapter 4 with respect to the robustness of the methods in the presence of jitter.

Examples where the generalized SLE method is employed will be shown in the next section.

3.3 Signal recovery from nonuniform samples in short intervals

The two methods of signal recovery from nonuniform samples, SVD and SLE, have been presented and extended to transform domains other than Fourier in the two first sections of this chapter. The reproducing kernels and sampling expansions obtained in Chapter 2 can also be included in the generalization of the SVD and SLE methods [67].

The collection of sampling expansions from Chapter 2 are characterized by coefficients dependent on unique sets of sampling points $\{t_n\}$ (the roots of orthogonal polynomials). Suppose that a set of nonuniform samples and its attached nonuniform time instants are provided, and the original signal is to be recovered from this information. Out of the collection of sets $\{t_n\}$, the set *that is closest to the given set of nonuniform time instants* is selected. The signal is then restored using the sampling expansion or the reproducing kernel corresponding to that set by applying the generalized version of the SLE or SVD

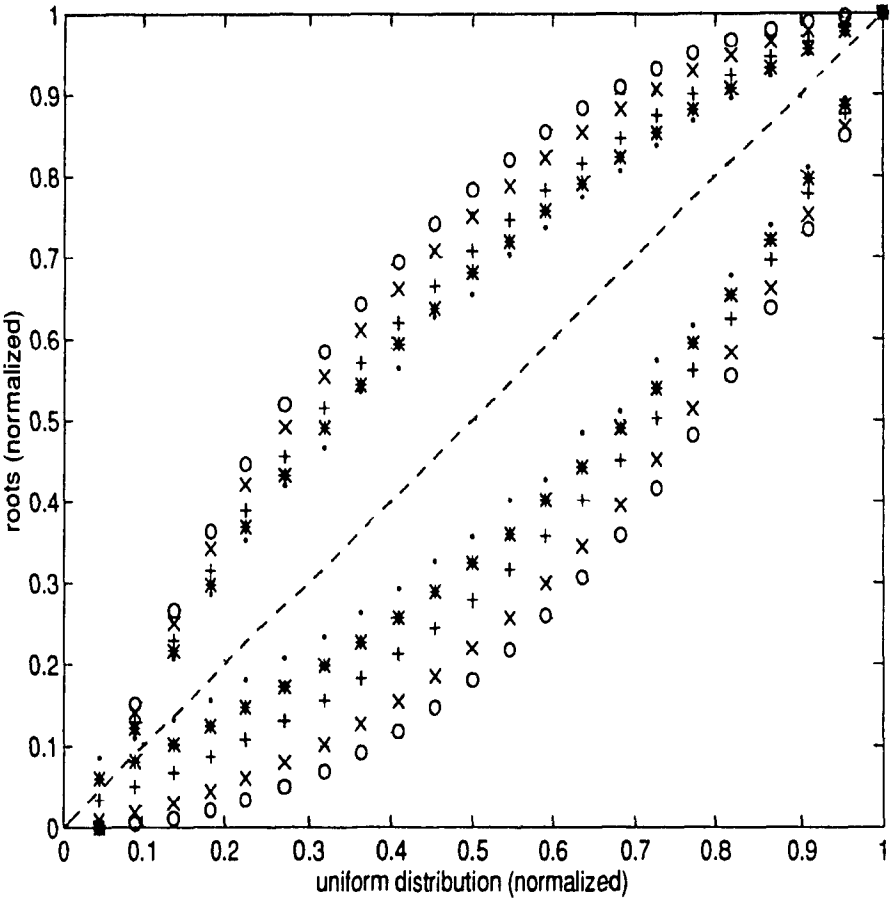

Figure 3.5: Root loci of the Laguerre and modified Laguerre polynomials of order 22 with varying parameter α against uniform distribution of points. The parameter takes the following values: (o): 0, (x): 5, (+): 15, (*): 25, (.): 35.

methods, respectively [63]. Thus, from this perspective, the problem of signal recovery from nonuniform samples can be seen as a problem of mapping a set of nonuniform time instants into a set of predetermined nonuniform time instants.

To show the relevance of the sets $\{t_n\}$ to the recovery problem, consider the root pattern of the Laguerre polynomials in Figure 3.5. With the variation of the parameter α, the polynomial roots change position. A parabola-shaped curve is obtained with each parameter value. The Laguerre polynomial produces the curves in the lower half of the plot; a modified Laguerre polynomial, $R_n^\alpha(x) = L_n^\alpha(\nu_n - x)$, produces the set of curves in the upper half, where ν_n is the largest root of $L_n^\alpha(x)$. The modified Laguerre polynomials are treated in Appendix E. Both the polynomials, the original and the modified, are orthogonal, although over different intervals. The modified polynomial is orthogonal over the interval $(-\infty, \nu_n]$. These loci are convenient for those sampling schemes where the samples are concentrated either at the beginning or at the end of the observation interval. Particular situations where those sampling schemes are useful arise in transient analysis and in biological systems, where burst signals have their information concentrated at the beginning of the observation interval.

As an example of signal recovery from nonuniform samples, consider Figure 3.6, where a random signal with a maximum frequency of 1911 Hz is nonuniformly sampled according to the root pattern of a Laguerre polynomial of order 22 with parameter $\alpha = 0$. Plots (a) and (b) in the figure respectively show the signal reconstruction using the SLE and SVD methods in the absence of jitter. The SLE method uses the Laguerre-based sampling expansion known from Chapter 2. The SVD method uses the reproducing kernel deducted from the discrete Laguerre transformation. Plots (c) and (d) correspond to the cases shown in the first two plots, but with a relative jitter parameter, J_r, of 0.85 added to the samples.

The jitter parameter mentioned in the last paragraph is defined as follows. Let $\{t_k\}$ be a sequence of nonuniform time instants, and $\{\tau_k\}$ be the same sequence but with jitter. Let $\alpha_k = t_{k+1} - t_k$. Then $\tau_k = t_k + \delta t$, where δt is a random variable, uniformly distributed in the interval $[-(\frac{\bar{p}\alpha_{k-1}}{2})J_r, (\frac{p\alpha_k}{2})J_r]$, where J_r is a scalar called the relative jitter parameter (relative to the nonuniform positions), p is a random variable that takes the values 1 or 0, with probability $Q(p)$ for a 1, and probability $R(p) = 1 - Q(p)$ for a 0.

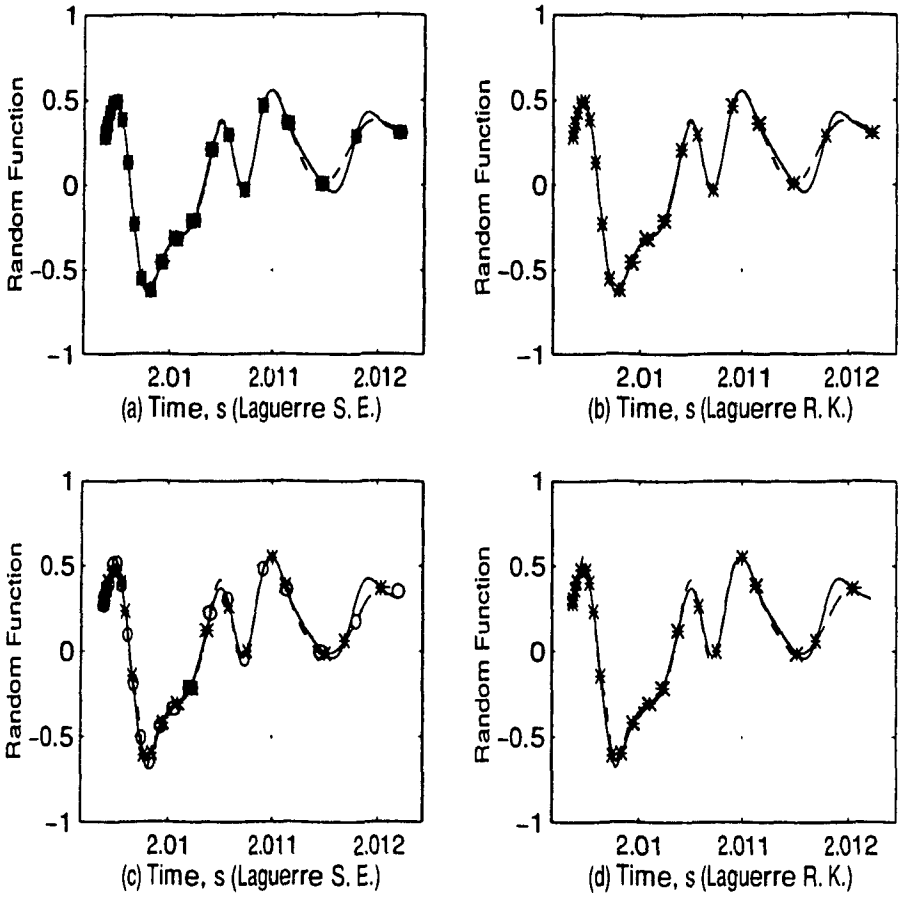

Figure 3.6: Reconstruction of a random signal with a maximum frequency of 1944 Hz. The symbology used means: (*): signal sample, (o): value obtained by recovering method corresponding to the position of the coefficient of the sampling expansion. S. E. stands for sampling expansion, and R. K. for reproducing kernel. The original signal is depicted using a continuous line, and its reconstructions with dashes.

and $\overline{p} = 1 - p$.

Figure 3.6 pinpoints the similarity in the results of both SVD and SLE methods. Appendix B shows that, in fact, both are equivalent under the conditions of the example.

Note that time scaling has been used in the plots so that the relative position of the polynomial roots is preserved. Given an observation interval of duration T, a simple linear transformation is used to map the roots of the orthogonal polynomial into the observation interval. Let y_2 be the last point of the interval, y_1 be the first point, x_1 be the first root, x_2 be the last root, and $\underline{x}$ be a vector containing the roots. Then the new locations $\underline{y}$ of

the roots are given by

$$\underline{y} = \frac{(y_2 - y_1)}{(x_2 - x_1)}\underline{x} + \frac{(y_1 x_2 - y_2 x_1)}{(x_2 - x_1)} \tag{3.7}$$

This expression and its equivalent, which maps the roots back into their original positions, have to be considered in the application of the SVD and SLE methods because the arguments of the sampling expansion and the reproducing kernel have to be values within the same scale as the roots. In other words, before using any of the signal recovery methods, the values of the observation interval have to be mapped into the interval defined by the first and the last roots of the orthogonal polynomial, by using a linear transformation analogous to Equation 3.7.

The SLE and SVD methods that respectively use a truncated sampling expansion and a reproducing kernel based on the sinc function [6, 26], fail to reconstruct the random signal given the set of nonuniform samples in Figure 3.6. This is due to the ill-conditioning[2] of the coefficient matrices employed in those methods. For the example considered, the estimated reciprocals of the condition number of the coefficient matrices employed in the abovementioned methods, oscillate between 3.077×10^{-15} for the smallest, and 1.7574×10^{-14} for the largest, making the signal reconstruction absolutely impossible. The problem of ill-conditioning appears as a direct effect of the violation of the known rule that a stable signal reconstruction cannot be achieved when the sampling is performed at a rate lower than the Nyquist rate (usually measured in Hz) [70], which implies that the gaps between samples cannot exceed a precise quantity also known as the Nyquist interval. Many methods of signal reconstruction from unequally spaced samples have as a basic assumption that the maximum gap between two samples does not exceed the Nyquist interval [71, 17, 18, 72, 73]. For these methods, when in the sampling set there are sampling gaps larger than the Nyquist interval, the result is either divergence or a very slow convergence in the method [71]. Due to the different nature of the extended methods, the assumption mentioned before is not necessary.

[2] A matrix is ill-conditioned if the reciprocal of its condition number approaches the computer's floating point precision (for instance, less than 10^{-6} for single precision or 10^{-12} for double). The condition number is defined as the ratio (in magnitude) of the largest to the smallest singular value of the matrix [68]. The values of the reciprocal condition number given here come from the use of the software package MATLAB, which bases its calculations on LINPACK [69].

The implicit limitation in the number of roots that can be calculated with accuracy when increasing the order of a polynomial, imposes a practical bound in the order of the orthogonal polynomials that form the basis of the generalized SVD and SLE methods. This implies that only small sampling sets can be analyzed at a time. For larger sampling sets, an on-line iterative procedure [74, 75] that decomposes the incoming set of nonuniform samples into overlapping blocks of a chosen minimum size, can be used, and within each block, the SLE and SVD methods proposed can be applied as long as the signal characteristics allow it. This iterative procedure will be presented in Chapter 4.

3.4 Signal compression

The search for techniques applicable to signal compression has been a very important area of research for years. The simple compression technique of varying the sampling rate of a signal that presents variations in frequency with interlacing intervals of slow and fast change, has the overall effect of producing a signal sampled nonuniformly. Another example of the application of a nonuniform sampling approach for compression consists in the cascading of a level crossing detector (LCD) and an interval encoder. The LCD produces a sample whenever its input crosses a threshold level, and the interval encoder, by assigning binary strings to the time between level crossings and to the directions of the crossings, codifies the information about the source signal; along with the addition of run-length encoding and prediction, the compression ratio would improve depending on the source [41]. An immediate application of this type of encoding is to analog-to-digital conversion [38].

The possibility of representing most of the information carried by a signal by using few coefficients of the signal representation in a transform domain, constitutes another way to achieve signal compression. Such is the case when dealing with image processing, where it is possible to preserve only 12.4% of Fourier transform coefficients of an image, and there is still enough information to be able to clearly distinguish the basic features of the image [76].

A decrease in the number of coefficients necessary for a signal representation could be achieved when representing the signal in a transform domain other than the Fourier

transform domain. This implies compression by reducing the number of coefficients that store the signal information. The following example will show that representing a signal using its samples taking according to the root locus of an orthogonal polynomial, could provide significant savings in the number of samples needed to recover the signal [77].

A linear FM signal with a maximum frequency of 18245 Hz is generated by placing its peaks at the time instants given by the root loci of the polynomials $L_n^{\alpha}(x)$ and $R_n^{\alpha}(x)$ of order 15 and parameter $\alpha = 0$. Figure 3.7 shows the relevant plots for this example. A power spectrum estimate (PSE) of the signal is shown in (a). The variation of the mean square error (MSE) with respect to the number of samples used in the reconstruction is shown in (b). Curve 1 corresponds to a signal recovery by the combination of a Laguerre-based and a modified Laguerre-based sampling expansions, whose coefficients are nonuniform samples centered at the root loci of the orthogonal polynomials. Curve 2 corresponds to a signal recovery based on the WKS sampling expansion whose coefficients are uniform samples. In (c), a reconstruction using 32 nonuniform samples and the two sampling expansions is shown, with each expansion occupying half of the curve. The nonuniform samples are placed at the root loci of the polynomials $L_n^{\alpha}(x)$ and $R_n^{\alpha}(x)$, of order 16 and $\alpha = 0$. For comparison, a reconstruction for the same FM signal is shown in (d), but it is based on the WKS sampling expansion using 32 uniform samples.

For this example, the WKS sampling theorem stipulates a minimum of 147 uniform samples to recover the signal, for the observation interval and bandwidth given. However, a very good reconstruction is achieved using only 32 nonuniform samples and the two sampling expansions proposed, leading to a compression index of 4.6.

3.5 Design of a linear phase FIR digital filter in the frequency domain using nonuniform samples

The dependency of the root locus of an orthogonal polynomial on the values of a parameter (or parameters, according to the case) can be exploited in digital filter design to define frequency response values in certain points like cutoff frequencies.

There has been much interest in the use of nonuniform samples in digital filter design [47,48,78–82], and two of the reasons for it have been: (1) the search for a technique

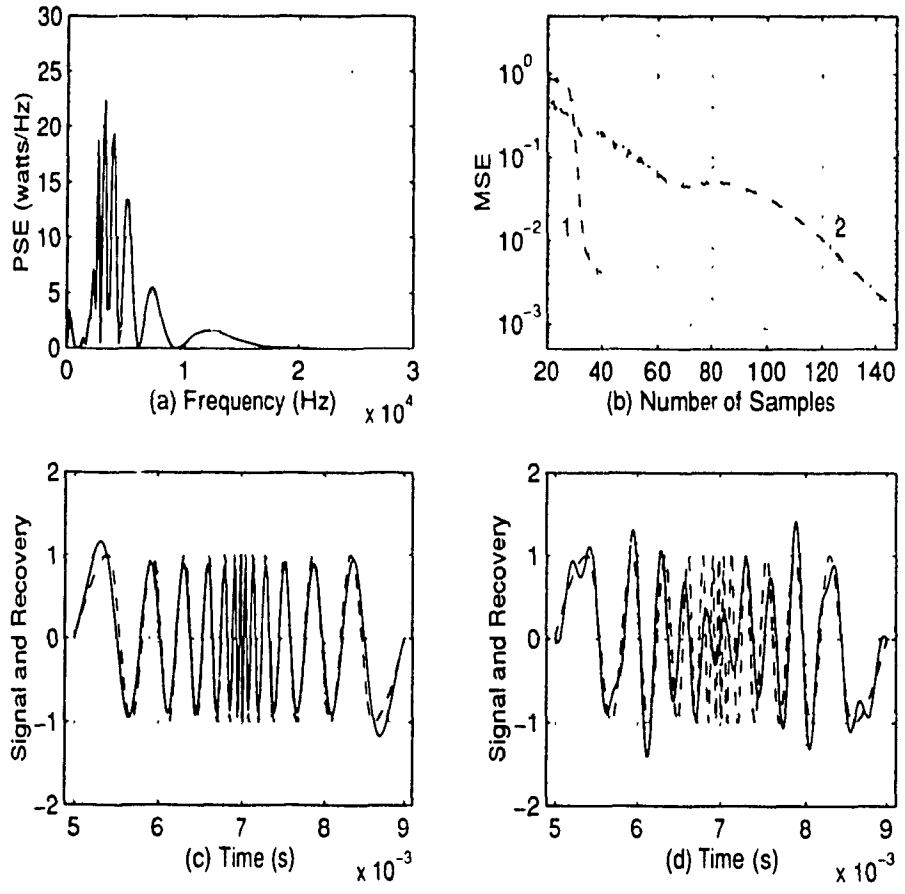

Figure 3.7: Signal compression for a linear FM signal with a maximum frequency of 18245 Hz. The reconstructions for the FM signal in (c) and (d) are shown with a continuous line, and the original signal is described by dashes.

that provides a way to place frequency response values in particularly chosen places not necessarily situated on a grid of equispaced frequencies [77], and (2) the design of efficient FIR filters requiring fewer arithmetic operations than the conventional filters.

The design procedure proposed for an FIR digital filter using nonuniform samples starts by considering

$$H(e^{j\omega T}) = \sum_{n=0}^{M} h(n) e^{-j\omega nT} \equiv H(\omega)$$

which is known as the frequency response of the filter, and where $h(n)$ is the impulse response, T the sampling period, and ω the frequency in radians per second. For a linear phase design, the frequency response should be made symmetrical or antisymmetrical about a midpoint, and for each of these two cases, M could be odd or even [83]. For a symmetrical design with M even,

$$H(\omega) = \sum_{n=0}^{\frac{M}{2}-1} h(n) e^{-j\omega nT} + h(\frac{M}{2}) e^{-\frac{M}{2}\omega T} + \sum_{n=\frac{M}{2}+1}^{M} h(n) e^{-j\omega nT} \tag{3.8}$$

which after some algebra and the use of symmetry, changes to,

$$H(\omega) = e^{-j\omega\frac{M}{2}T} \left\{ h(\frac{M}{2}) + 2 \sum_{i=0}^{\frac{M}{2}-1} h(i) \cos[(\frac{M}{2} - i)\omega T] \right\} \tag{3.9}$$

For a symmetrical design with M odd,

$$H(\omega) = 2e^{-j\omega\frac{M}{2}T} \sum_{i=0}^{\frac{M-1}{2}} h(i) \cos[(\frac{M-2i}{2})\omega T] \tag{3.10}$$

Both Equations 3.9,3.10 have the form

$$H(\omega) = A(\omega) e^{-j\omega\frac{M}{2}T} \tag{3.11}$$

where $A(\omega)$ is a real function of the variable ω, and it is expressed in terms of the unknown impulse response $h(n)$. Because $A(\omega)$ is real, it can be approximated by any of the finite sampling expansions from Chapter 2:

$$A(\omega) = \sum_{n=1}^{N+1} f(\gamma_n) S_n(\omega, \gamma_n) \tag{3.12}$$

The values $\{\gamma_n\}$ are the roots of orthogonal polynomials where the frequency response can be made to take specific values. By varying the parameters associated with the orthogonal polynomials, the root locus changes, and with it, the position of the samples.

To design a linear phase lowpass filter symmetrical about its midpoint with M even, the following equation is established,

$$\sum_{n=1}^{N+1} f(\gamma_n) S_n(\omega, \gamma_n) = h(\frac{M}{2}) + 2 \sum_{i=0}^{\frac{M}{2}-1} h(i) \cos[(\frac{M}{2} - i)\omega T] \tag{3.13}$$

On the right there are $\frac{M}{2} + 1$ unknowns, and on the left $N + 1$ operands. So, $\frac{M}{2} = N$. By extending the last equation to L frequencies $\{\omega\}$, the resulting overdetermined system of linear equations is solved by using singular value decomposition (SVD), which provides a linear least square solution for the impulse response $h(n)$. The impulse response (filter coefficients) will then have a minimum norm in the Euclidean sense [84]. The number L of frequencies has to be greater than or equal to $\frac{M}{2} + 1$. The overdetermined system of equations is written as $B\underline{h} = \underline{d}$, where $\underline{h}$ is the vector of filter coefficients, $\underline{d}$ is the vector of values of the sampling expansion, and B is the matrix originating from the evaluation of the cosine function in Equation 3.13, and characterized by entries of the form

$$2\cos[(\frac{M}{2} - i)\omega_j T]$$

where $j = 1, \ldots, L$ and $i = 0, \ldots, \frac{M}{2} - 1$. The solution of the system is obtained in terms of the right singular vectors $\underline{v}$, and the singular values $\{\sigma_i\}$ corresponding to the singular value decomposition of B:

$$\underline{h} = \sum_{i=1}^{W} \frac{1}{\sigma_i^2} \underline{v_i v_i}^T B^T \underline{d} \tag{3.14}$$

where W is the rank of B, defined as the number of linearly independent columns of the matrix. In this case, the solution is consistent because W equals the number of elements of $\underline{h}$.

This design method differs from other design approaches in the use of an expansion that completely specifies the frequency response in the frequency domain, and as a consequence, in the inclusion of a smooth transition band which reduces the approximation ripple [85, 86].

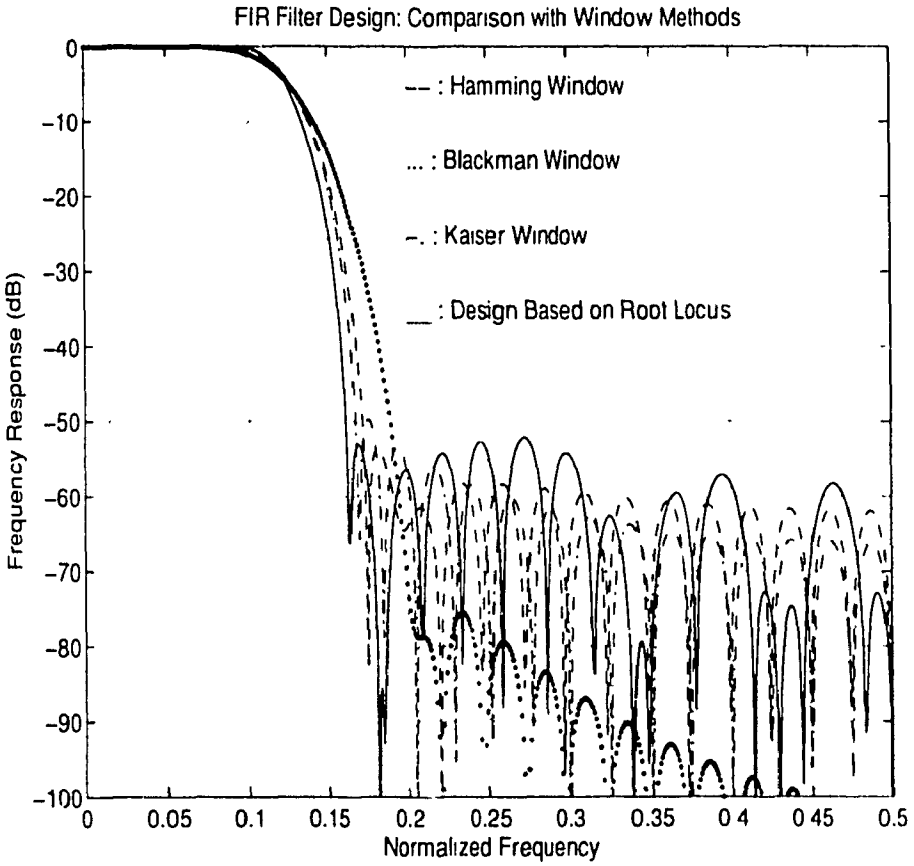

Figure 3.8: FIR lowpass filter with cutoff frequency at 0.1 (normalized). Three window based design methods are compared against the method proposed.

Figure 3.8 shows four different designs for a lowpass digital filter with cutoff frequency 0.1 (normalized), a minimum attenuation of 50 dB in the stopband, and twenty distinct coefficients for each design. Note the significant improvement that in the transition band the method proposed achieves with respect to the other methods. The sampling expansion for this design used a Laguerre polynomial of order 20 and parameter $\alpha = 9.89$.

Another example will be provided to illustrate the design technique proposed. The design of a linear phase bandstop filter presents a double symmetry, one about $\frac{M}{2}$, and another about $\frac{M}{4}$, for M even. To find the corresponding design equations, the frequency response is rewritten in the following way:

$$\begin{aligned} H(\omega) &= \sum_{n=0}^{M} h(n)e^{-j\omega nT} \\ &= h(0) + \sum_{n=1}^{\frac{M}{4}-1} h(n)e^{-j\omega nT} + h(\frac{M}{4})e^{-j\omega\frac{M}{4}T} + \sum_{\frac{M}{4}+1}^{\frac{M}{2}-1} h(n)e^{-j\omega nT} + \\ &\quad h(\frac{M}{2})e^{-j\omega\frac{M}{2}T} + \sum_{\frac{M}{2}+1}^{\frac{3M}{4}-1} h(n)e^{-j\omega nT} + h(\frac{3M}{4})e^{-j\omega\frac{3M}{4}T} + \\ &\quad \sum_{\frac{3M}{4}+1}^{M-1} h(n)e^{-j\omega nT} + h(M)e^{-j\omega MT} \end{aligned} \tag{3.15}$$

which after some algebra reduces to

$$\begin{aligned} H(\omega) &= e^{-j\omega\frac{M}{2}T}\{h(0)[1+2\cos(\omega\frac{M}{2}T)] + \sum_{i=1}^{\frac{M}{4}-1} 2h(i)[\cos[(\frac{M}{2}-i)\omega T] + \cos(i\omega T)] + \\ &\quad 2h(\frac{M}{4})\cos(\omega\frac{M}{4}T)\} \end{aligned} \tag{3.16}$$

The last expression presents the same form as in Equation 3.11. The reasoning can then proceed as above,

$$\begin{aligned} A(\omega) &= h(0)[1+2\cos(\omega\frac{M}{2}T)] + \sum_{i=1}^{\frac{M}{4}-1} 2h(i)[\cos[(\frac{M}{2}-i)\omega T] + \cos(i\omega T)] + \\ &\quad 2h(\frac{M}{4})\cos(\omega\frac{M}{4}T) \end{aligned} \tag{3.17}$$

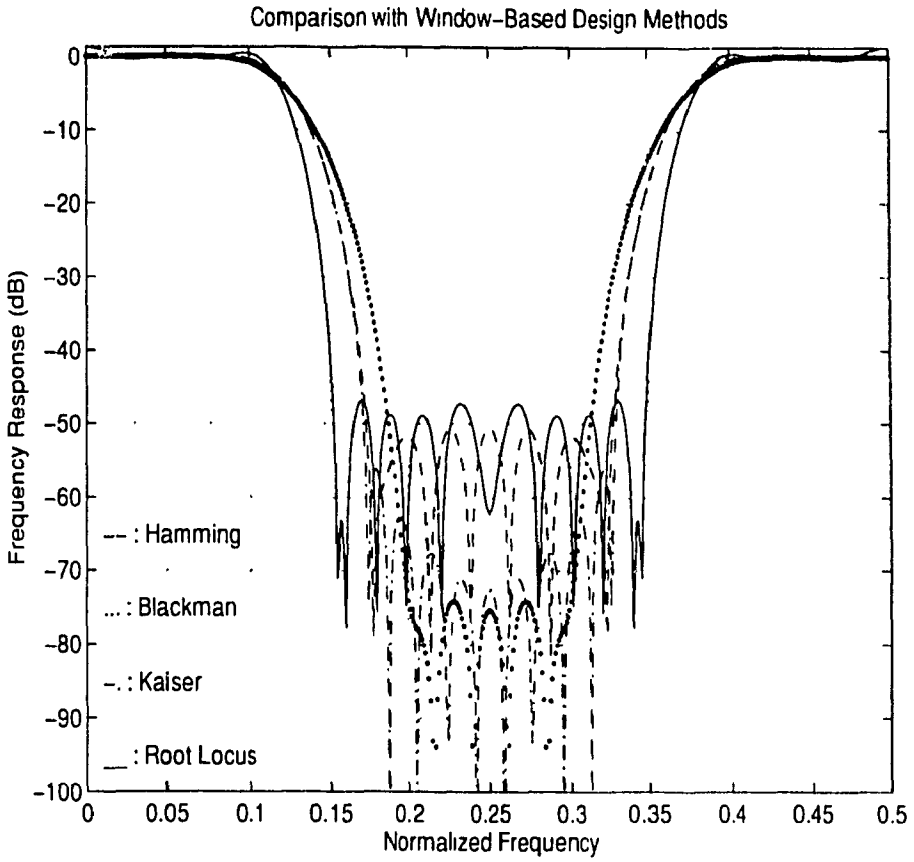

Figure 3.9: Bandstop filter with cutoff frequencies at 0.1 and 0.1. Three window-based methods are compared against the method proposed.

On the right side of the last expression there are $\frac{M}{4}+1$ unknowns, and on the left there are $N+1$ operands. So, $\frac{M}{4} = N$, with M an even number. By establishing again an overdetermined system of linear equations, a linear least square solution for $h(n)$ is calculated.

Figure 3.9 presents the results of designing an FIR bandstop filter with cutoff frequencies at 0.1 and 0.4, with a minimum attenuation in the stopband of 50 dB. Using 21 distinct coefficients in the design, the transition band is shorter for the method proposed than for the other methods shown, but the minimum attenuation goal is missed by approximately 2 dB. The sampling expansion used a Laguerre polynomial of order 11 and parameter $\alpha = 202$.

A comparison with window-based methods is shown in both figures of this section.

The design method proposed is interactive, and involves a series of trials to achieve the desired features. Not any nonuniform placement of samples provides an optimum design that satisfies the requirements of minimum attenuation and cutoff frequencies [77]. In both examples, two of the nonuniform samples were placed in the transition band to eliminate the approximation ripples in the stopband. For the lowpass design, one transition sample was given the value 0.69, and the other 0.18. For the bandstop design, the values for the transition samples were 0.92, and 0.23. The rest of the samples took the values 1 or 0. The approximation ripples in the passband for both designs were lower than 2 dB.

3.6 Signal representation by nonuniform sampling

The application of Kramer's generalized sampling theorem to finite signal spaces has produced sampling expansions whose coefficients are signal samples taken according to the root loci of orthogonal polynomials. The root loci are functions of the parameters that characterize the polynomials, and they can assume many different shapes with the variation of these parameters. The parabolic shape of the Laguerre polynomials, for instance, makes the corresponding sampling expansion suitable to represent signals showing fast variation at the beginning, and slow variations at the end of an observation interval. Such is the case for the so-called burst signals. The opposite case, wherein a signal varies slowly at the beginning and faster at the end of the interval, corresponds to a sampling expansion based on mirrored images of the Laguerre polynomials, the $R_n^{\alpha}(x)$ polynomials. A signal with maximum variation at the center of the interval can be represented by a combination of two sampling expansions, one based on Laguerre polynomials and the other on their mirrored images (see Section 3.4).

A signal representation can be assigned to a burst signal such as the transient auditory evoked brainstem response (ABR, [87]). A simulated ABR signal is shown in Figure 3.10, along with a corresponding signal reconstruction based on a Laguerre-based sampling expansion ($\alpha = 5$). The number of coefficients in the signal representation is $N + 1 = 24$, while the more typical Shannon sampling expansion employs 41 uniform samples. This signal representation produces a compression ratio of 1.7.

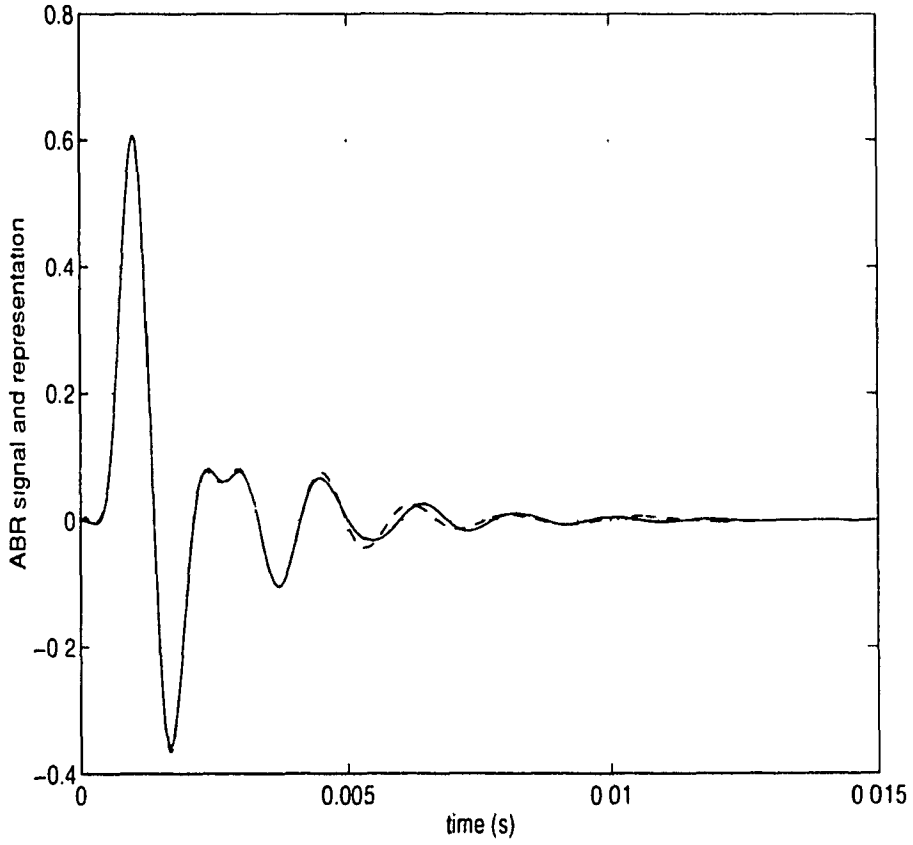

Figure 3.10: ABR signal (-) and its corresponding representation (- -) using a Laguerre based sampling expansion.

Chapter 4

On-Line Iterative Recovery of Nonuniformly Sampled Signals

In this chapter, an on-line iterative procedure for signal recovery from nonuniform samples will be presented. This procedure will extend the use of the two methods examined before, the SVD and SLE methods, to long intervals with large sets of signal samples. The procedure avoids the restraint imposed by the size of the sample set in other methods by rearranging the set into smaller jointly overlapping blocks. The procedure has also the advantage of being on-line, which means that the signal processing can start even before all samples have been received.

The procedure proposed constitutes an improvement over the existing methods due to its on-line nature, and it offers the possibility of using iterations to ameliorate the results. It is a much less complicated technique from the point of view of mathematical tools employed (compared with [20, 22]).

The on-line iterative procedure will be applied in this chapter to two different cases: (1) the first case involves the conversion from nonuniform sampling to uniform sampling, that is, from a set of nonuniform samples to a set of uniform samples, and (2) the conversion from nonuniform sampling to a predetermined nonuniform sampling, which means, from a set of nonuniform samples to a set of samples positioned at the root loci of orthogonal polynomials. The first type of conversion is the most common, because the set of uniform samples is then used with the WKS sampling theorem to reconstruct the signal. For this conversion, the cases of small jitter ($J < 1$) and of medium jitter ($1 < J < 3$) will be studied and a comparison made between the results obtained by using the SLE and the SVD methods of signal recovery. The second type of conversion relies on the proximity of the sampling to any of the root loci of orthogonal polynomials, and it corresponds to the case where $J > 3$. For this second type of transformation, the concept of relative jitter (J_r, defined with respect to nonuniform samples) is then applicable.

The description of the on-line iterative procedure for the conversion from nonuniform samples to uniform samples requires the following definitions. Let M be the minimum block length, P be the number of overlapping uniform points between consecutive blocks, N be the total number of samples in the input sequence, Q be the number of points used in obtaining an estimate of the nonuniform samples from the estimated uniform samples, and $\{\tau_m\}$ be the nonuniform time instants. Refer to Figure 4.1 for an illustration of the definitions of M, P, and N.

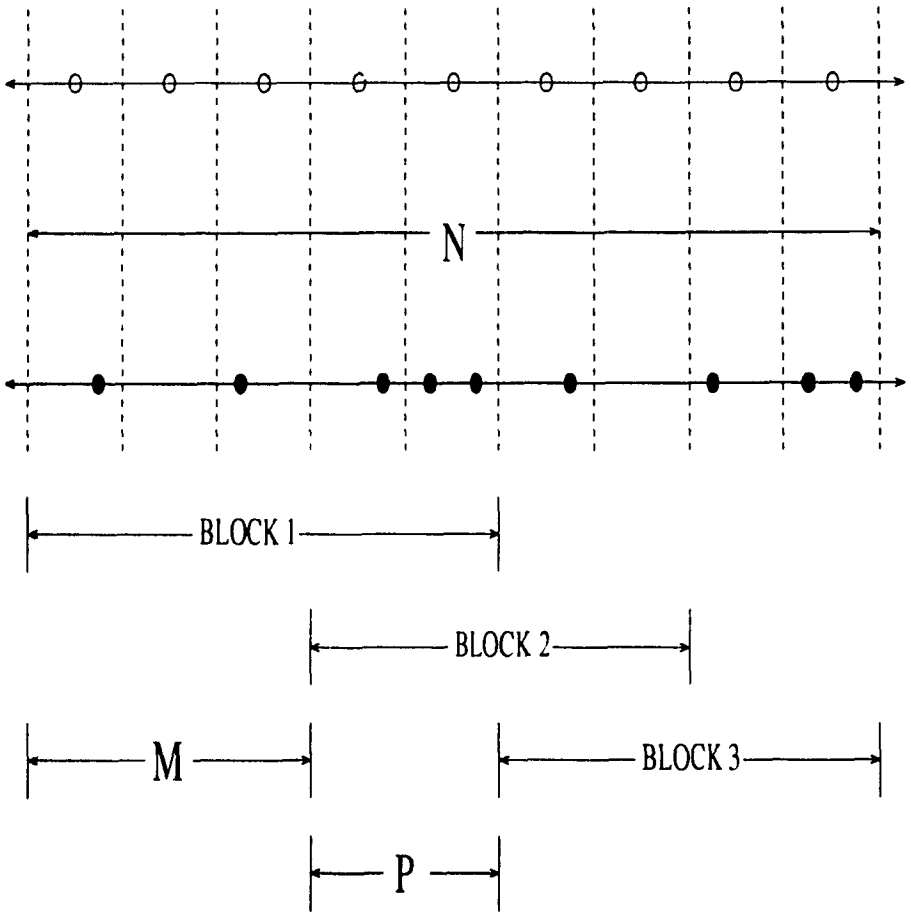

Figure 4.1: Block rearrangement of the sequence of nonuniform samples. The first sequence corresponds to the uniform points, and the second to the nonuniform points. The uniform points are supposed to be synchronized with respect to the nonuniform points.

The following steps define the procedure.

1. Choose values of M and P where M is an odd number (> 1) and P is an even number (≥ 2). This particular choice for the values of M and P is made to favor symmetry and simplify processing. Perform a partition of the sequence in blocks according to M and P as seen in Figure 4.1. Each block has to have as many uniform as nonuniform points. For Figure 4.1, the values chosen for M and P are 3 and 2, respectively.

2. Estimate uniform samples corresponding to the nonuniform samples included in each block. The estimation is performed using either the SLE or the SVD method. Let $\underline{\hat{x}}_1(nT)$ be the vector of estimated uniform samples (before iterations), and T the sampling period. After the estimation, discard the estimated uniform samples corresponding to the P points on the edges of the block. For example, if the block includes 5 points and $P = 2$, five uniform samples will be estimated but two of them will be discarded, one at each point on the edge of the block.

3. Once the uniform samples have been estimated over the sequence of N samples, calculate an estimate of the nonuniform samples using the expression

$$\underline{\hat{x}}(\tau_m) = \sum_{n=1}^{Q} \underline{\hat{x}}_1(nT) sinc[\omega_0(\tau_m - nT)] \tag{4.1}$$

where $Q \leq N - P$. Subtract these values from the known nonuniform samples, $\underline{x}(\tau_m)$, thereby generating the error

$$\underline{\epsilon}(\underline{\hat{x}}(\tau_m)) = \underline{x}(\tau_m) - \underline{\hat{x}}(\tau_m) \tag{4.2}$$

4. $\underline{\epsilon}(\underline{\hat{x}}(\tau_m))$ is used to calculate the error in the uniform samples, $\underline{\epsilon}(\underline{\hat{x}}_1(nT))$, by using $\underline{\epsilon}(\underline{\hat{x}}(\tau_m))$ as input to the SLE or SVD method. The block rearrangement is again used in this calculation.

5. Use $\underline{\epsilon}(\underline{\hat{x}}_1(nT))$ to improve estimation of the uniform samples.

$$\underline{\hat{x}}_2(nT) = \underline{\hat{x}}_1(nT) + \underline{\epsilon}(\underline{\hat{x}}_1(nT)) \tag{4.3}$$

6. Repeat steps 2 thru 5, to perform successive iterations.

Several remarks concerning this algorithm can be made [75].

- The number of samples involved in the computation decreases slightly with each iteration because the samples corresponding to the points on the edges of the sequence are discarded.

- The reason behind the elimination of the abovementioned samples is to decrease the influence of the truncation error, which is unavoidable when dealing with a truncated version of the WKS sampling expansion [88]. This will become clearer when examining the examples.

- With respect to the step 3 of the procedure, Q could be made less than N to reduce processing delay and computational complexity. In simulations, the value $Q = v \times M$ could be used, where v is a scalar conveniently chosen.

- To keep constant the number of points under analysis, so that there is no loss from iteration to iteration, the samples estimated corresponding to the outer edges of the first and last blocks of the sequence are to be retained, not discarded.

- A particular problem implicit in the procedure is the placement of the sequence of uniform points with respect to the sequence of nonuniform points, whose positions are known. The uniform points cannot be placed arbitrarily with respect to the nonuniform points because the deviation of the nonuniform points from the uniform points is not guaranteed to be a minimum (the same for the recovery error). The identification of the proper locations for the uniform points is called synchronization.

To explain how synchronization can be accomplished, consider the following reasoning. Let $\{\tau(i)\}$, $i = 1, \ldots, L$ be the nonuniform sample positions, and T the sampling interval. The uniform positions are located at $\{t(i)\}$, $i = 1, \ldots, L$ such that

$$t(i) = \tau(1) + (i-1)T + \delta t \tag{4.4}$$

where $|\delta t| < T$. Choose $\{t(i)\}$ such that the average jitter,

$$\overline{J} = \frac{1}{L}\sum_{i=1}^{L}[t(i) - \tau(i)]^2 \tag{4.5}$$

is minimized over a length of data L. The set $\{t(i)\}$ reaches its optimum location if δt in Equation 4.4 minimizes the average jitter given by Equation 4.5. By differentiating Equation 4.5 with respect to δt,

$$\delta t_{opt} = \frac{1}{L}\sum_{i=1}^{L}[\tau(i) - \{\tau(1) + (i-1)T\}] \tag{4.6}$$

The second derivative of $\overline{J}$ shows that for this value δt_{opt}, the set $\{t(i)\}$ reaches its optimum location. To implement synchronization, find δt_{opt} and place the uniform points according to Equation 4.4. Now, several examples will be examined to show the performance of the method.

4.1 Performance of the method for a random signal

A random signal with a bandwidth of 2200 Hz, is sampled at a sampling rate of 1.2 times the Nyquist rate. The number of samples taken is $N = 370$. The sampling is affected by jitter between the values of $J = 0.1$ and $J = 2.5$. The noise that generates the jitter is uniformly distributed. Two different sets of experiments are performed, one with $M = 3$, $P = 2$, and the other one with $M = 5$, $P = 2$.

Figure 4.2 corresponds to the first case, and Figure 4.3 to the second case. In each figure, a comparison is made between the performance of the SLE and the SVD methods. With the increment of jitter, the mean square error increases faster when using the SLE method than when using the SVD method. The latter can accept larger values of jitter than the former. The reason is the interaction among the sample spacing, the Nyquist interval, and the ill-conditioning of matrices.

Figure 4.4 shows the reconstruction of the signal after three iterations of the method, for $J = 2.5$ and using the SVD method for the block processing. The first graph in the figure corresponds to the case $M = 3$, $P = 2$, and the second to the case $M = 5$, $P = 2$. The reconstruction is better in the second graph due to the decrement in truncation error with the increment in M.

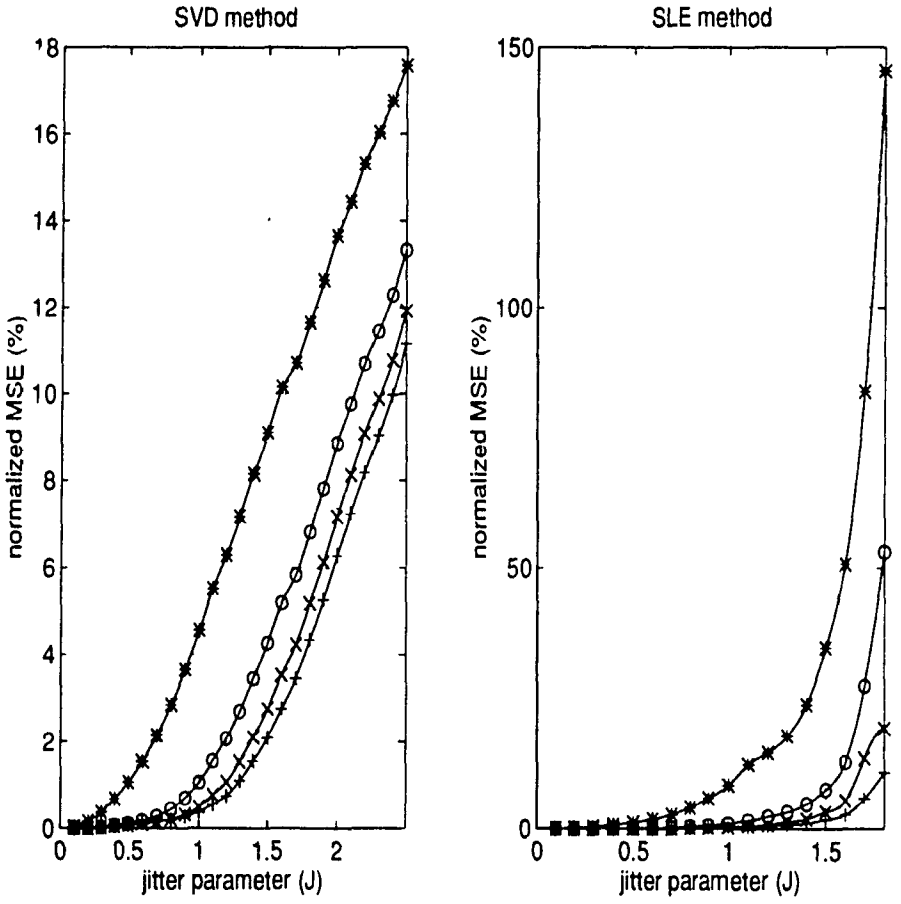

Figure 4.2: Results of the application of the on-line iterative method in the recovery of a random signal. The minimum block size is $M = 3$, and the number of overlapping uniform points between blocks is $P = 2$. The symbology for this and the following figures is: (*) zero iterations, (o) one iteration, (x) two iterations, (+) three iterations.

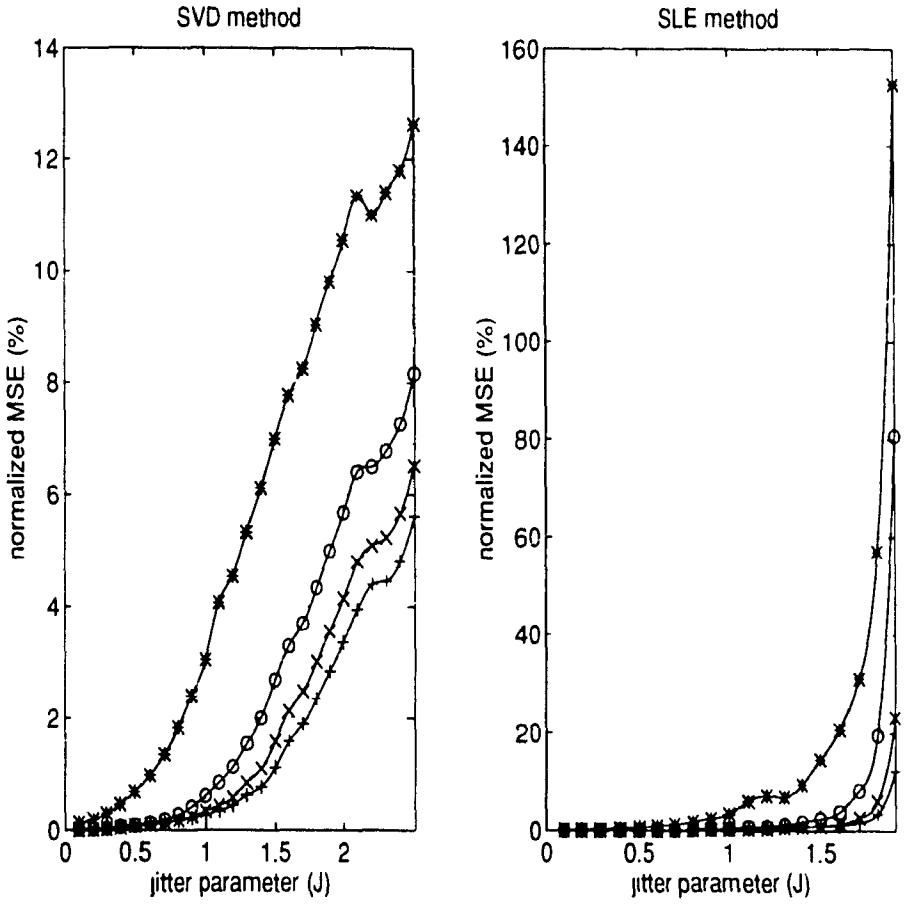

Figure 4.3: Results of the application of the on-line iterative method in the recovery of a random signal. The minimum block size is $M = 5$, and the number of overlapping uniform points between blocks is $I = 2$.

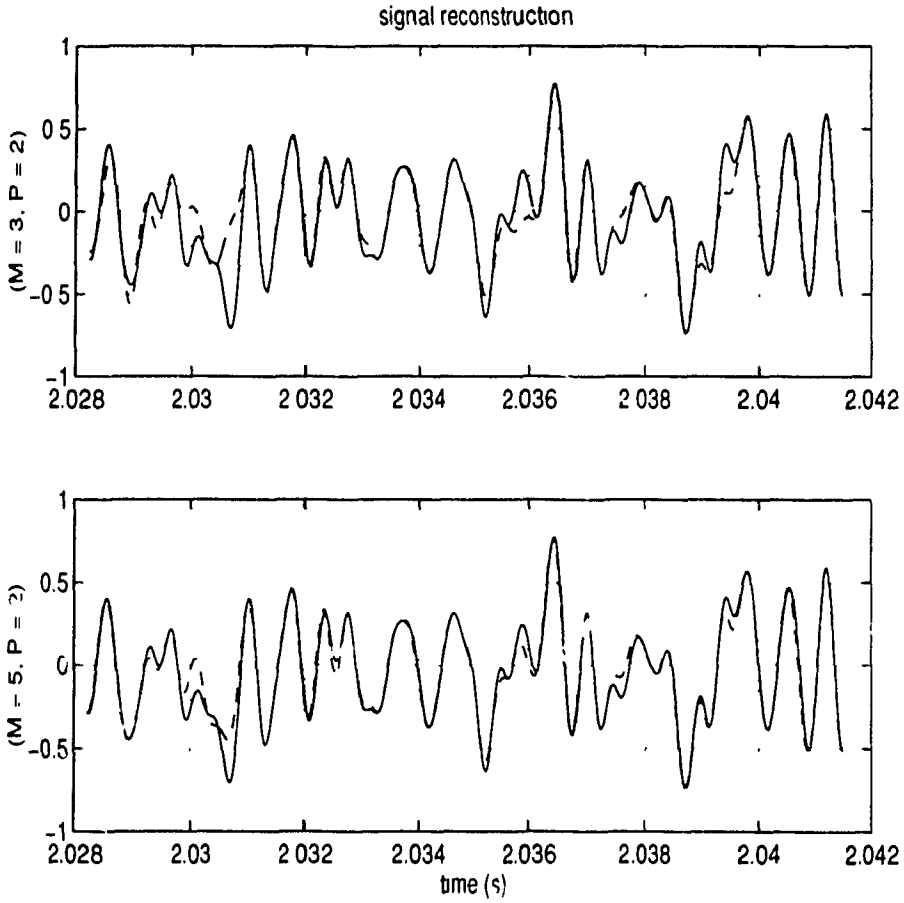

Figure 4.4: Reconstruction of a random signal. The first graph corresponds to the reconstruction obtained with the method parameters $M = 3$ and $P = 2$. The second corresponds to a reconstruction with $M = 5$ and $P = 2$. The original signal is represented with a continuous line, and the reconstruction with dashes.

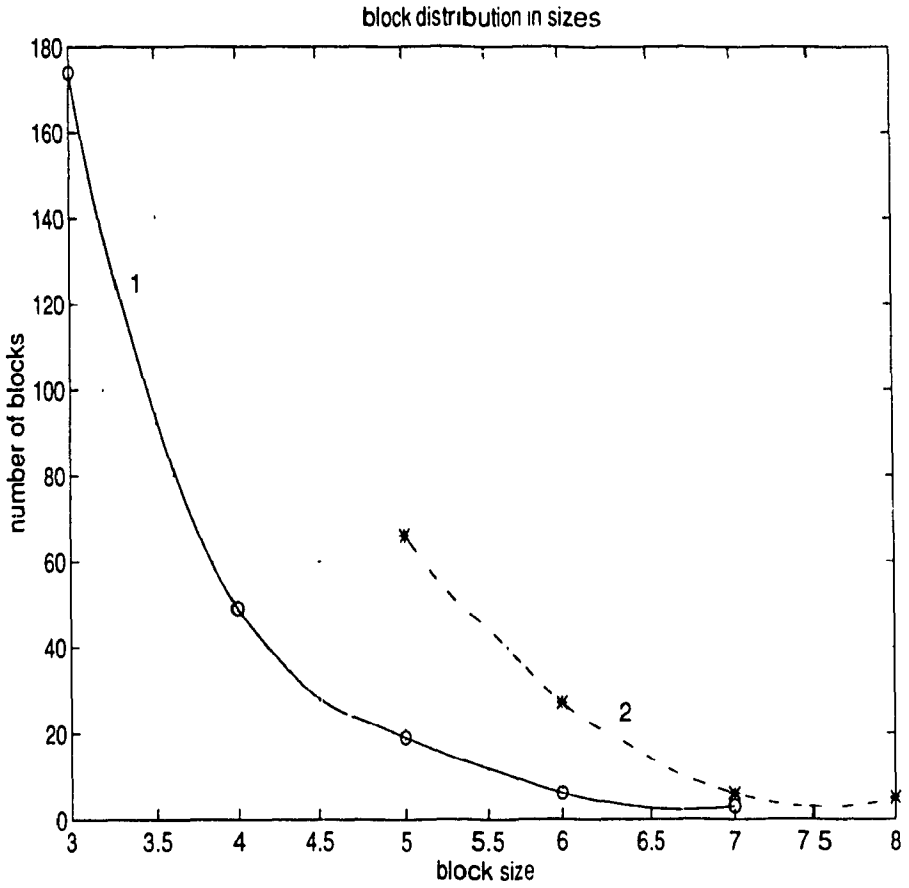

Figure 4.5: Number and sizes of blocks obtained for the example where a random signal is reconstructed from its samples. Curve 1 corresponds to the case where the method parameters are $M = 3$, $P = 2$, and curve 2 to the case where the parameters are $M = 5$, $P = 2$.

With respect to the computational complexity, the results of Appendix F will now be used. Refer to Figure 4.5 for a glimpse at the number and size of the blocks involved in the calculation for this example. The total number of multiplications for the case $M = 3$, $P = 2$ is, for the SLE method, 39284, and for the SVD method, 485724. The calculation does not consider the intermediate step 3 because it is common to both versions of the algorithm. For the second case, where $M = 5$, $P = 2$, for the SLE method there are 47548 multiplications, and for the SVD method, 688079 multiplications.

Some observations can be made at this point. The best overall results are achieved

with the combination of the on-line iterative method and the SVD method, but the computational complexity of this combination greatly exceeds that corresponding to the combination of the SLE method and the on-line iterative procedure. For small jitter ($J < 1$), the combination of the SLE method and the algorithm proposed is more convenient to use for the savings that are obtained in calculations, and for the results achieved. For medium jitter ($1 < J < 3$), the combination of the SVD method and the algorithm gives best results despite the number of operations involved [74].

4.2 Performance of the method for a speech signal

A speech signal with a bandwidth of 2536 Hz is sampled at 1.2 times the Nyquist rate. $N = 370$ samples are collected, and the on-line iterative method is used with the parameters $M = 3$ and $P = 2$. The results are shown in Figure 1.6, with J varying between 0.1 and 2.5. The comparison between the SVD and the SLE methods in that figure again shows that the overall performance of the former is better than the latter. Note that in the part of the figure corresponding to the SLE method, not all the values for the jitter are shown owing to the large increase in the mean square error after $J = 1.6$; if shown until $J = 2.5$, the MSE values would not be distinguishable for $J < 1$ due to scaling.

A small detail was mentioned when introducing the algorithm: it is the possibility of not using all the values ($N = 370$) of the sequence in step 3 to estimate nonuniform samples from the uniform samples estimated. Several simulations have been made to study how the value of r (in $Q = r \times M$) affects the results of the algorithm for the speech signal under study. Figure 4.7 presents the results of those simulations for three different values of jitter and for the SLE and SVD methods. The parameters M and P are the same. Note that $r = 15$ seems to mark the point where the mean square error stabilizes for the three examples. The expression *sliding window* describes the neighbourhood of points around a particular uniform point that is used to calculate an estimation of the nonuniform sample associated with the sample at that point.

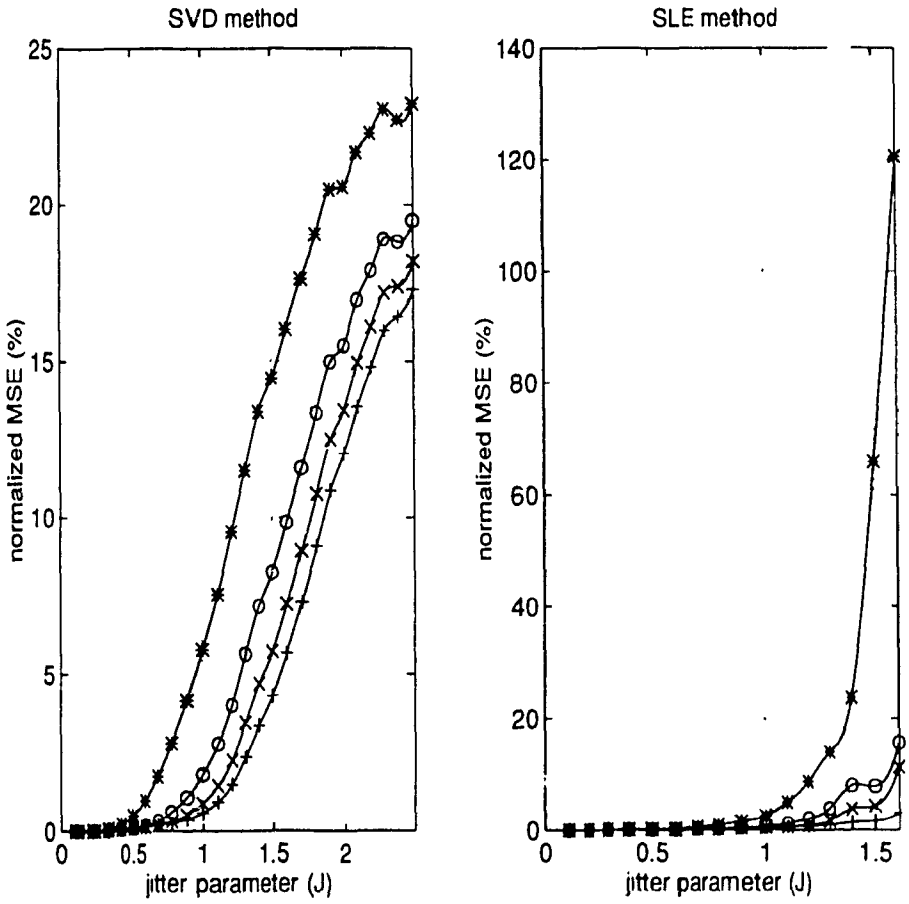

Figure 4.6: Results when a speech signal is recovered from its nonuniform samples, for varying jitter values and three iterations. The SVD method is compared with the SLE method.

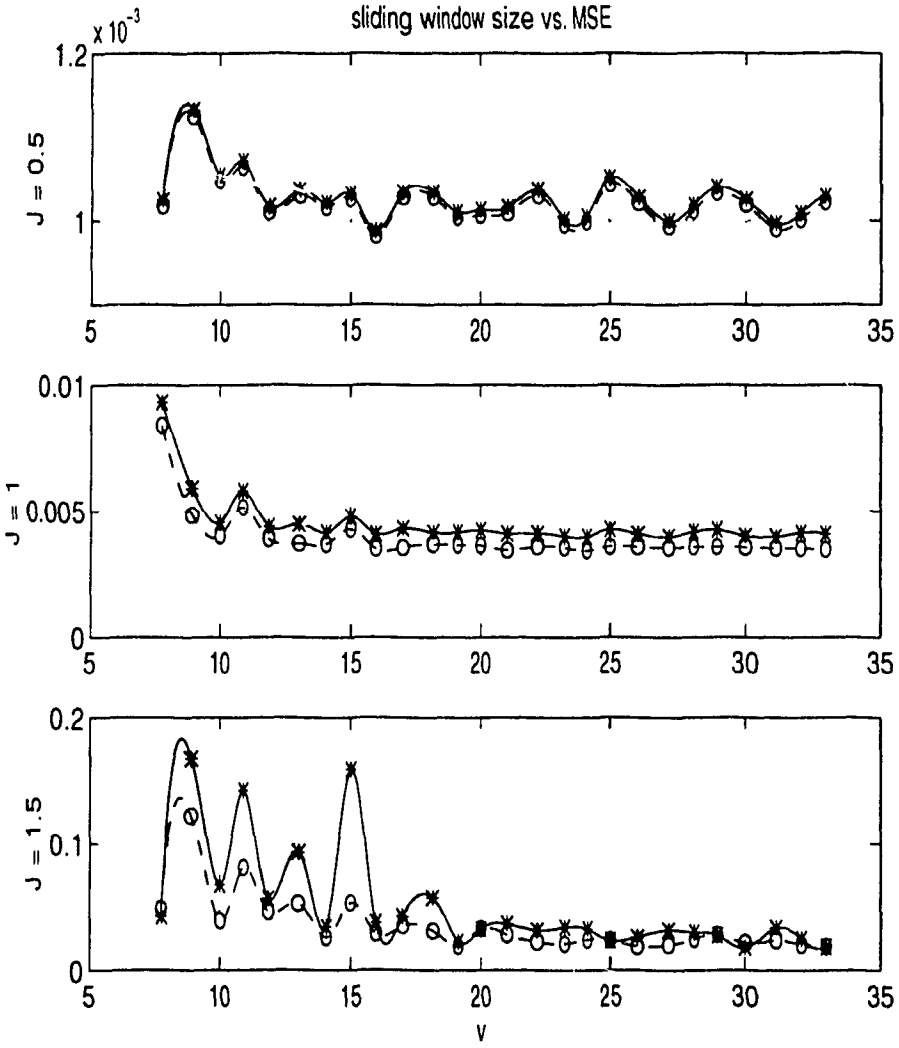

Figure 4.7: This figure shows how the variation in $Q = v \times M$ affects the performance of the algorithm. The value of v is plotted against the mean square error for three different values of J. Two curves are shown in each plot: one corresponds to the SLE method (*), and the other to the SVD method (o).

4.3 A statistical study of the method

An important aspect of the performance analysis of the method is its behaviour in the presence of jitter induced by a Gaussian noise source.

The following simulations were performed. Taking $M = 3$, $P = 2$, a random signal with a bandwidth of 2200 Hz was sampled at 1.2 times the Nyquist rate and a total of $N = 370$ samples were obtained. By varying the seed number of a random generator, 50 different realizations of jitter for a variance between 0.1 and 1.2 were obtained to produce two curves, one for the SLE method and the other for the SVD method. Figure 4.8 shows the dispersion of the results for the SLE method. Note the change in scaling to be able to present the results. Figure 4.9 shows the results for the SVD method. For small values of the variance (up to 0.5667), both methods offer a mean square error less than one percent. After that value, the error increases substantially faster for the SLE method than for the SVD method. The results reinforce the opinion of the robustness of the combination algorithm-SVD method when an increment in jitter is experimented.

4.4 Conversion from nonuniform sampling to predetermined nonuniform sampling

A nonuniform sampling scheme, based on the root loci of Laguerre polynomials, was proposed in Section 3.6 to provide a better adjustment of the sampling to signal characteristics than the provided by uniform sampling. The decrease in the amount of data necessary to store signal information is the direct effect of this new type of sampling scheme. There is also the possibility of more freedom in choosing design parameters for systems that have relied so far on uniform sampling.

An on-line iterative procedure for signal recovery from nonuniform samples will be proposed for the case of a nonuniform sampling scheme applied to a signal with the appropriate characteristics. The relative jitter, J_r, will be relevant in the discussion, and the jitter will be measured against a set of reference points, $\{t_k\}$, which are nonuniform and represent the roots of the Laguerre polynomial.

In general terms, the procedure about to be described follows the one already studied,

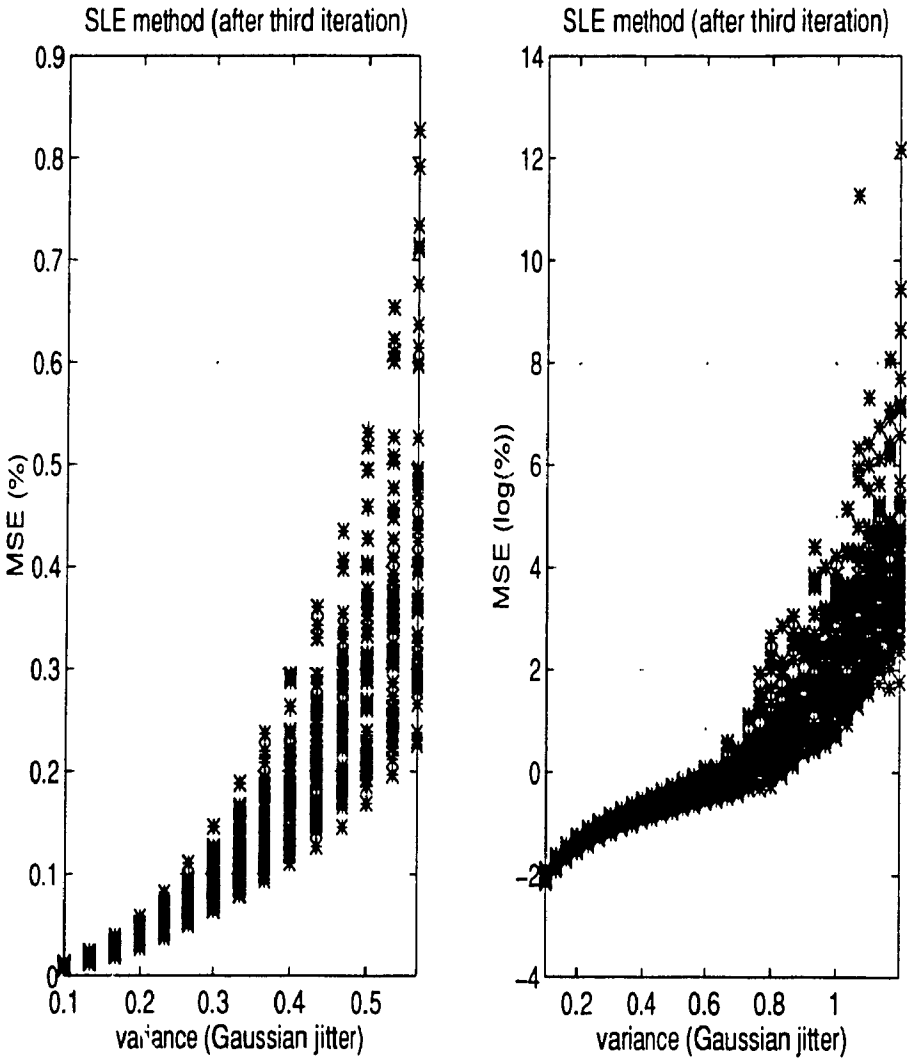

Figure 4.8: This figure shows the behaviour of the algorithm when using the SLE method. The figure is broken in two to be able to present the effect of small values of variance in the left side, and the overall performance in the right.

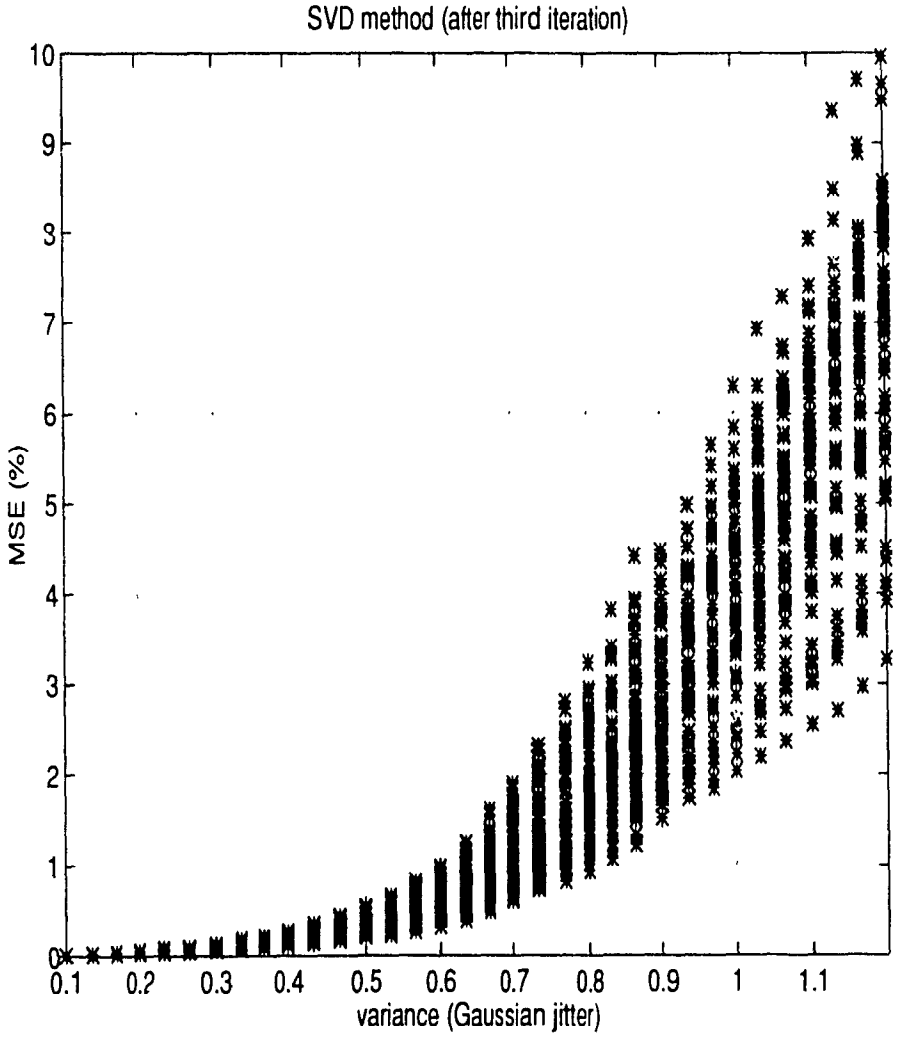

Figure 4.9: This figure shows the behaviour of the algorithm when using the SVD method.

with the obvious changes to account for the predetermined nonuniform samples which will now be the reference points (instead of the uniform points as before).

Assume that the signal has been effectively sampled using $N+1$ nonuniform samples, and that jitter has affected the sampling with a value J_r. The time instants given by the root locus of a Laguerre polynomial of order $N+1$ are termed the *reference points*, $\{t_k\}$. By *true* nonuniform samples or *reference* samples it will be understood to mean the signal samples at the reference points, $\{\underline{x}(t_k)\}$. The time positions $\{t_k\}$ with jitter are called *jittered points*, $\{\tau_k\}$, and the associated nonuniform samples, simply *samples*, $\{\underline{x}(\tau_k)\}$.

Let M be the minimum block length, P be the number of overlapping samples between consecutive blocks, and Q be the number of points used to obtain an estimate of the jittered nonuniform samples from the estimated reference samples.

The procedure is as follows.

1. Choose values of M and P where M is an odd number (> 1), and P is an even number (≥ 2). Perform a partition of the sequence in blocks according to M and P as shown in Figure 4.10. Each block has to have as many reference points as jittered points.

2. Estimate the signal samples corresponding to the reference points from the samples. This estimation is performed using either the SLE method or the SVD method, and it is performed block by block. For each block, discard the reference samples estimated corresponding to P points on the edges of the block. For example, if the block comprises six points and $P = 2$, then six samples will be estimated but two of them will be discarded (one on each edge). Let $\underline{\hat{x}}_1(t_k)$ be the vector of estimated reference samples.

3. Once the sample estimation has been completed for all the blocks, calculate an estimate of the samples $\underline{\hat{x}}_1(\tau_k)$ from the estimated reference samples, $\underline{\hat{x}}_1(t_k)$. This estimation involves Q points, and it is performed using the following expression:

$$\underline{\hat{x}}_1(\tau_k) = \sum_{k=k_1}^{k_2} \underline{\hat{x}}_1(t_k) \frac{t_k(\tau_k/t_k)^{\alpha/2} \exp(-\frac{\tau_k - t_k}{2})[-L_{N+1}^{\alpha}(\tau_k)]}{(\tau_k - t_k)(N+1+\alpha)L_n^{\alpha}(t_k)} \tag{4.7}$$

where $Q = k_2 - k_1 + 1$, which is the number of estimated samples in step 2 after discarding the estimated samples on the edges. k_1 indicates the first, and k_2 the last estimated sample.

4. Subtract $\underline{\hat{x}}_1(\tau_k)$ from the known samples, $\underline{x}(\tau_k)$, thereby generating the error

$$\underline{\epsilon}(\underline{\hat{x}}_1(\tau_k)) = \underline{x}(\tau_k) - \underline{\hat{x}}_1(\tau_k) \tag{1.8}$$

5. $\underline{\epsilon}(\underline{\hat{x}}_1(\tau_k))$ is used to calculate the error in the estimated reference samples $\underline{\epsilon}(\underline{x}_1(t_k))$ by using it as the input in either the SLE method or the SVD method. Then, use $\underline{\epsilon}(\underline{\hat{x}}_1(t_k))$ to improve the estimation of the reference samples,

$$\underline{\hat{x}}_2(t_k) = \underline{\hat{x}}_1(t_k) + \underline{\epsilon}(\underline{\hat{x}}_1(t_k)) \tag{1.9}$$

6. Repeat steps 2 thru 5, until a satisfactory error reduction is achieved.

Some observations are in order.

- The number of points involved in the computation decreases with each iteration because the samples on the edges of the sequence are discarded. To keep the number of points constant, the estimated reference samples at the outer edges of the first and last blocks are kept instead of being discarded.

- The SLE and SVD methods have been adapted to deal with the sampling scheme. For the SLE method, the system of linear equations is derived from a sampling expansion based on Laguerre-based composing functions, instead of the Shannon sampling expansion. For the SVD method, the original reproducing kernel (sinc function) has been replaced by a reproducing kernel corresponding to a finite signal space [63].

- Synchronization is an important issue. To place the sequence of reference points with respect to the nonuniform positions in such a way to reduce the overall jitter, the value δ needed to define the positions of the reference points can be found as follows.

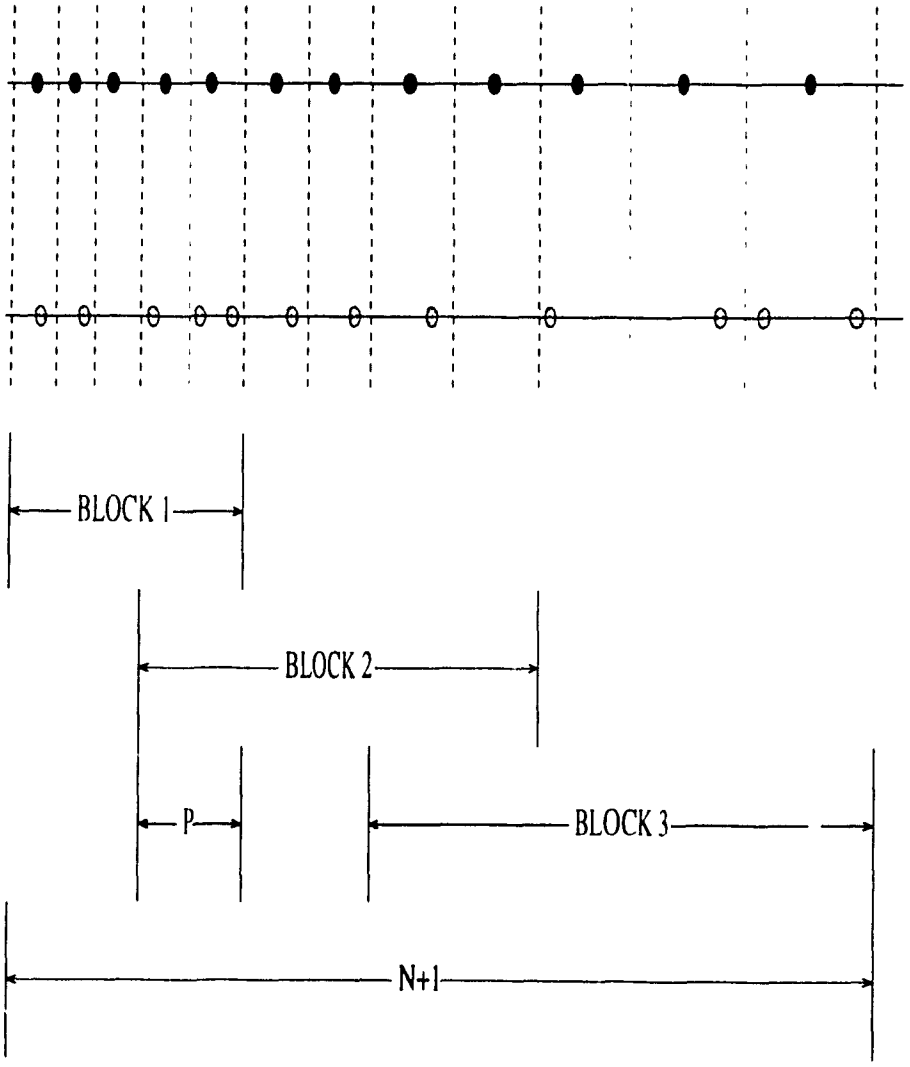

Figure 4.10: The sequence is rearranged in blocks. The first sequence corresponds to the reference points, and the second corresponds to the jittered points.

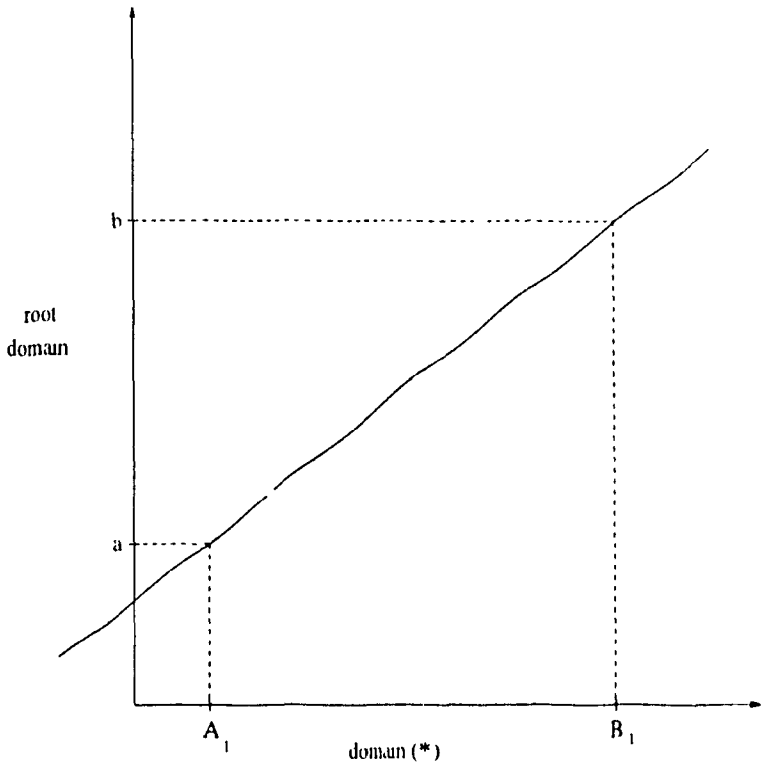

Figure 4.11: The axes relate the transformed domain (where the sampling takes place) and the root domain, where the polynomial roots are located. All operations have to refer to the root domain so that the Laguerre-based sampling expansions are valid.

The minimization of the overall jitter will take place in the original domain of the roots. Consider Figure 4.11. Let $\underline{z} = \{z_i\}$ be the Laguerre roots in domain (*). Let $A = \min\{z_i\}$, $B = \max\{z_i\}$, and $\{\gamma_i\}$ be the Laguerre roots. Let $a = \min\{\gamma_i\}$, $b = \max\{\gamma_i\}$, A_1 the minimum and B_1 the maximum of the transformed roots with jitter in domain (*).

From the domain (*) to the root domain, the following transformation is applied:

$$\underline{z}_T = \frac{b-a}{B_1 - A_1}\underline{z} + \frac{aB_1 - bA_1}{B_1 - A_1} \tag{4.10}$$

where the subscript T indicates transformation. Let $A_1 = A$, $B_1 = B$ [sic]. The goal of the analysis will be to find δ that minimizes the jitter as it appears in the transformed values. Replacing the values of A_1, B_1 in Equation 4.10,

$$\underline{z}_T = \frac{b-a}{B+\delta-A}\underline{z} + \frac{a(B+\delta) - bA}{B+\delta-A}$$

$$= \frac{(b-a)\underline{z} + a(B+\delta) - bA}{(B+\delta) - A} \tag{4.11}$$

The jitter expression that is to be minimized is

$$\begin{aligned} \overline{J} &= \frac{1}{N+1}\sum_{i=1}^{N+1}(\gamma_i - z_I(i))^2 \\ &= \frac{1}{N+1}\sum_{i=1}^{N+1}\left[\gamma_i - \left\{\frac{(b-a)z_i + a(B+\delta) - bA}{(B+\delta) - A}\right\}\right]^2 \end{aligned} \tag{4.12}$$

The differentiation will give

$$\frac{\partial \overline{J}}{\partial \delta} = \frac{1}{N+1}\sum_{i=1}^{N+1} 2\left[\frac{\gamma_i(B+\delta-A) - [(b-a)z_i + a(B+\delta) - bA]}{B+\delta-A}\right]\frac{(b-a)(z_i - A)}{(B+\delta-A)^2}$$

Now, equating to zero to find value of δ that minimizes $\overline{J}$:

$$\begin{aligned} \frac{1}{N+1}\sum_{i=1}^{N+1} 2\left[\frac{\gamma_i(B+\delta-A) - [(b-a)z_i + a(B+\delta) - bA]}{B+\delta-A}\right]\frac{(b-a)(z_i-A)}{(B+\delta-A)^2} &= 0 \\ \sum_{i=1}^{N+1}\{\gamma_i(B+\delta-A) - [(b-a)z_i + a(B+\delta) - bA]\}(z_i - A) &= 0 \\ \sum_{i=1}^{N+1}\{\gamma_i(B-A) - (b-a)z_i - aB + bA + \delta(\gamma_i - a)\}(z_i - A) &= 0 \end{aligned}$$

which gives finally,

$$\delta = \frac{-\sum_{i=1}^{N+1}[\gamma_i(B-A) - (b-a)z_i - aB + bA](z_i - A)}{\sum_{i=1}^{N+1}(\gamma_i - a)(z_i - A)} \tag{4.13}$$

The value δ is then used to place the reference points in an adequate position to decrease jitter.

Consider the following example that shows the method as applied to a transient signal. An ABR signal is nonuniformly sampled according to the root loci of the Laguerre polynomial of order 24 and parameter $\alpha = 5$. This means that 24 samples are obtained from the signal and used in its representation. The sampling is affected by jitter varying between $J_r = 0.1$ and $J_r = 1.8$. These jitter values correspond to $J > 3$. The results are shown for the SLE and the SVD methods in Figure 4.12. For this example, $M = 3$ and

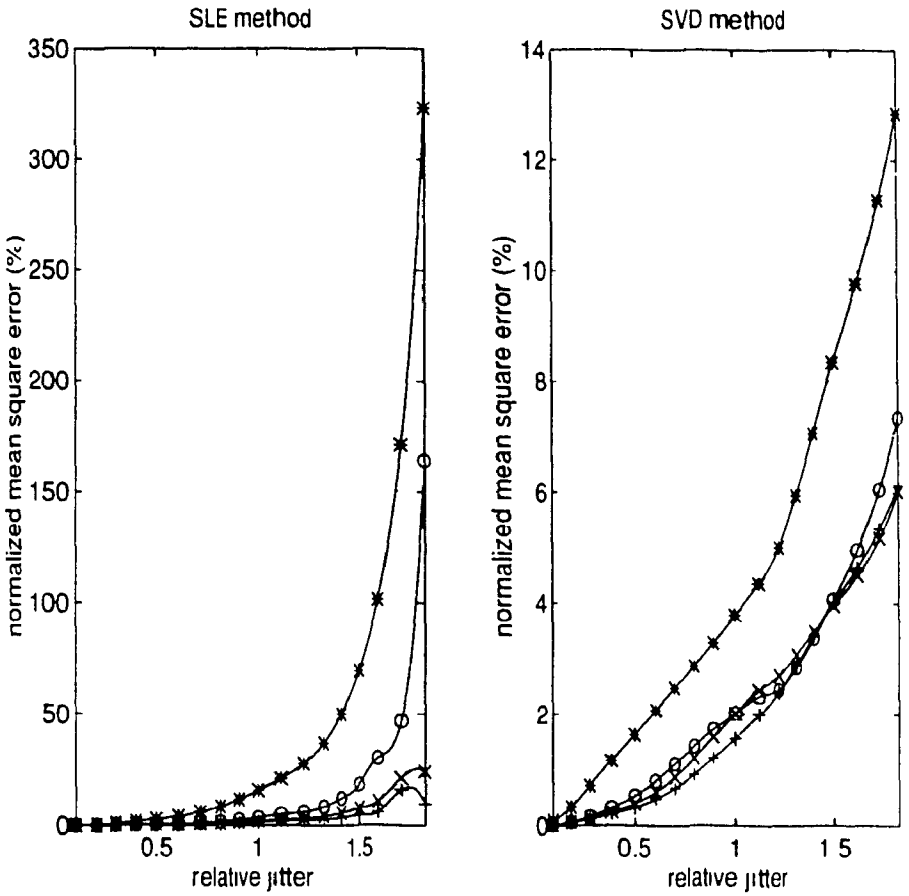

Figure 4.12: This figure shows the performance of the algorithm proposed when applied to the conversion from nonuniform sampling to a predetermined nonuniform sampling scheme. For this example, $M = 3$ and $P = 2$. Three iterations are used, with the following symbology: (*) 0 iterations, (o) 1 iteration, (x) 2 iterations, (+) three iterations. The relative jitter, J_r, occupies the horizontal axis.

$P = 2$. The SVD method provides the best overall performance. Figure 4.13 presents the signal reconstruction achieved after the use of the algorithm proposed and the SLE and SVD methods. The latter method seems to show a better recovery than the former.

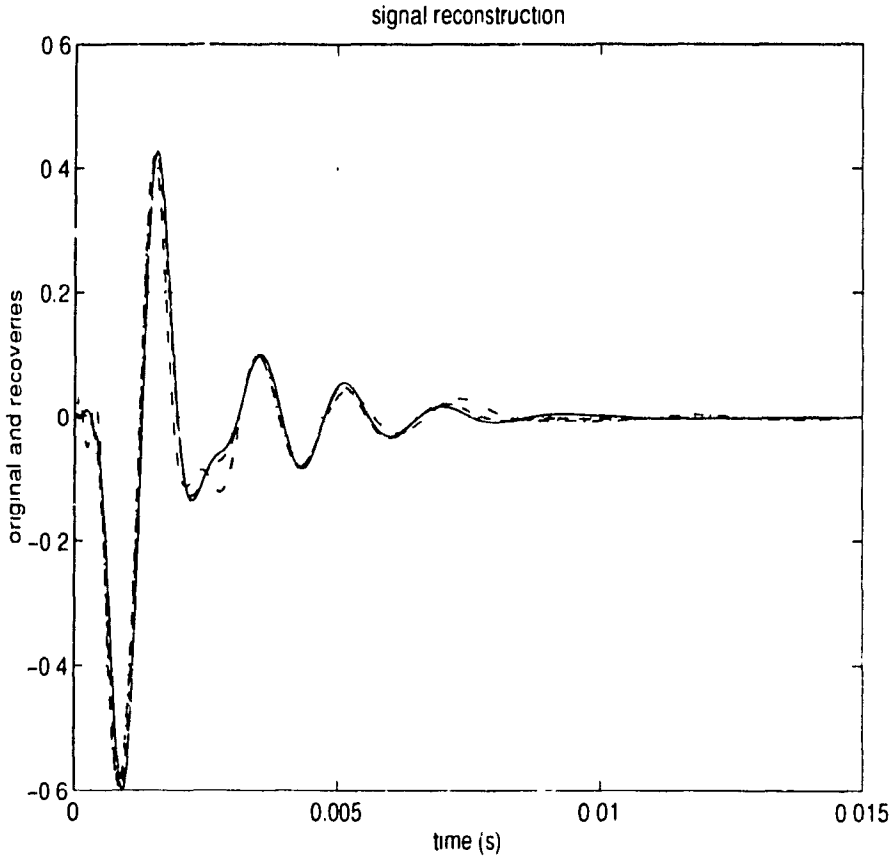

Figure 4.13: This figure shows the reconstruction of an ABR signal from the results provided by the algorithm using both the SLE and the SVD methods. The results are from the third iteration, and $\lambda_r = 1.8$. The original signal is represented by a continuous signal, the recovery using the SLE method by (-.-) and the recovery using the SVD method by (- -).

Chapter 5

Nonuniform Sampling as a Signal Transformation Tool

Several applications were examined in Chapter 3 showing that methods based on nonuniform sampling could be used with advantage under different circumstances over methods that traditionally rely on uniform sampling. An idea closely related to those methods and which has received special attention in the literature concerning potential applications for nonuniform samples schemes, has been the use of nonuniform sampling as a signal transformation tool. If a given signal can be transformed to a new domain and an analysis performed in a more convenient fashion than in the original domain, then the transformation applied to the signal should be encouraged. Such is the case of the Fourier transformation, where the transformed signal gives an insight into the frequency components that otherwise would not be evident.

With the simple example of the Fourier transformation in mind, an obvious question is where and how nonuniform sampling could be used for a signal transformation.

There are two different instances to be treated here where nonuniform sampling alters a signal and transforms it. The first approach deals with the transformation of an analytic signal, and the second with the representation of a signal in terms of a sum of weighted sinc functions centered at nonuniform positions.

5.1 Transformation of an analytic signal

The particular technique that is employed to perform a transformation on a signal involving nonuniform sampling is known as time warping. Under the same name, there are three techniques in different fields that share the warping effect with the method that will be proposed. The first technique is used in Medicine in the extraction or estimation of evoked potentials, and it involves the nonlinear extension and/or compression of the time axis of an initial evoked potential estimate [89-91]. The second technique, known as the time-warped polynomial coding method, is used for the coding of ECG, speech, and image line information, and is based on a general class of orthogonal transforms that rely on warping and weight functions [92, 93]. The third technique, more related to the topic of this chapter, appears in the sampling and reconstruction of bandlimited and non-bandlimited signals [91, 95]. This technique assumes the existence of an one-to one transformation applied to $f(t)$ (the sampled signal), denoted by $\tau = \gamma(t)$, such that another function $h(\tau)$

is obtained, with a sampling period of T units. If the transformation γ between t and τ is such that $c + nT = \gamma(t_n)$ for some arbitrary c and with $\{t_n\}$ a set of nonuniform time instants, then the samples of $h(\tau)$ will be uniformly spaced, and the WKS theorem can be used for the signal reconstruction. To get an exact reconstruction, $h(\tau)$ must be bandlimited to $\omega_0 = \pi/T$. With this, the transformation can be reversed, and $f(t)$ can be retrieved by using $f(t) = h(\gamma(t))$. Substituting this relationship in the WKS theorem with $\tau = \gamma(t)$,

$$f(t) = \sum_{n=-\infty}^{\infty} \frac{\sin[\omega_0(\gamma(t) - nT)]}{[\omega_0(\gamma(t) - nT)]} \tag{5.1}$$

To reconstruct $f(t)$ from its nonuniformly spaced samples $\{f(t_n)\}$, find the invertible and one-to-one function $\gamma(t)$ such that $\gamma(t_n) = nT$, and then use the Equation 5.1.

The time warping technique of interest in this section will transform an analytic signal into a sinusoid signal that will be enhanced or suppressed depending upon the application. By analytic signal is understood a signal of the form

$$v(t) = A(t)\cos(\Psi(t)) \tag{5.2}$$

where $A(t)$ is called envelope, and $\Psi(t)$ is called angle (or phase). In fact, $v(t) = \Re\{\tilde{v}(t)\}$, where $\tilde{v}(t)$ is called a complex-analytic signal [96], and whose imaginary part is the Hilbert transform of $v(t)$. There are three cases or combinations that will be mentioned and an example for each one of them will be given:

- $A(t)$: fixed-valued, $\Psi(t)$: time varying
- $A(t)$: time-varying, $\Psi(t)$: time varying
- $A(t)$: time-varying, $\Psi(t)$: fixed valued.

5.1.1 A fixed-valued envelope and a time-varying phase

The time warping technique may perform a transformation on an angle modulated signal, so that it can be rejected by two types of discrete linear time varying filters [97]. The angle modulated signal $v(t)$ can be written as

$$\begin{aligned} v(t) &= A_v \cos[\psi_v(t) + \phi_v] \\ &= A_v \cos[\omega_v t + \theta(t) + \phi_v] \end{aligned} \tag{5.3}$$

where A_v and $\Psi_v(t) = \psi_v(t) + \phi_v$ are the envelope and the angle (phase), $\omega_v t$ and $\theta(t)$ are the linear and nonlinear terms of the phase, respectively, and ϕ_v is the initial phase of $v(t)$. Suppose that $\Psi_v(t)$ is time varying (but can be known), while A_v and ϕ_v are unknown but fixed. Consider $\lambda(t) = \Psi_v(t)/\omega_v^*$, where ω_v^* is a scaling coefficient not necessarily equal to ω_v. For an appropriate choice of ω_v^*, the signal $v(t)$ becomes a function of the new variable λ:

$$v^*(\lambda) = A_v \cos[\omega_v^* \lambda + \phi_v] \tag{5.4}$$

where "*" indicates the time warping effect. The signal $v^*(\lambda)$ is a harmonic signal of frequency ω_v^* if λ is considered an independent variable. Therefore, the problem of filtering an angle modulated signal $v(t)$ transforms into the processing of a single sinusoidal signal of fixed frequency ω_v^* and a transformed time λ. There are two practical ways to perform the transformation, a nonuniform-to-uniform transformation and a uniform-to-nonuniform transformation. The interest here is centered in the former way. If the original angle modulated signal was mixed with an arbitrary signal $s(t)$,

$$u(t) = s(t) + v(t) \tag{5.5}$$

after having converted the angle modulated signal into a single sinusoid of a fixed frequency, it can be rejected using a constrained notch filter [98]. The mixture $u(t)$ can be nonuniformly sampled at the time instants $\{t_k\}$, defined by $\Psi_v(t_k) = \frac{2\pi k}{N}$. The constrained notch filter central frequency is then fixed at $\frac{2\pi}{N}$ (N being the number of samples during the time interval in which the phase $\Psi_v(t)$ advances by 2π radians). By making N large enough, it is possible to reconstruct $s(t)$ from the nonuniform samples, using any interpolation method. The time varying nature of the suppression of a FM interference (the time variance that characterizes the linear system that rejects the signal) has been eluded by means of a transformation by nonuniform sampling, and the relatively easy problem of

the design of a linear time-invariant system has replaced it. The synchronization problem (to extract $\Psi_v(t)$) has been considered in [99, 100]. An example, taken from [98], will illustrate this technique. Consider the signals,

$$s(t) = -\frac{\sin[1\pi(t-37.5)]}{4\pi(t-37.5)}\cos(2\pi 5t) \tag{5.6}$$

$$v(t) = 10\cos[2\pi 5t + 10\sin(2\pi 0.1t) + 7\sin(2\pi 0.3t)] \tag{5.7}$$

Figure 5.1 shows the signal $s(t)$ and the mixture $u(t)$, along with the power spectrum estimate (PSE) of $u(t)$ and $v(t)$. Note that the interference practically overwhelms the signal $s(t)$ as seen in plot (d). Figure 5.2 shows the power spectrum estimate of $s(t)$. The second plot in Figure 5.2 shows the effect of nonuniform sampling in the power spectrum of $u(t)$: a harmonic signal appears and it is suppressed by the CANF system as seen in the plot (c). The suppression takes place when the central frequency of the notch filter is fixed at the value of the sinusoid frequency. Plot (d) of the same figure shows the CANF output before interpolation: it is a plot of sample values against the sample index. Figure 5.3 shows the CANF output after interpolation: the original signal is present as well as the system transient. Plot (b) in that figure compares the original signal and the CANF output after interpolation. The recovery is very good.

5.1.2 A time-varying envelope and phase

The following procedure is proposed to deal with this case. Both envelope and phase are time varying but known. The aim of the transformation will be to transform the AM/FM signal into a single sinusoid for enhancement or annihilation. An example will illustrate the steps to be taken in the transformation.

Consider the following envelope and phase functions,

$$A(t) = \frac{2t}{(1+t^2)^2} \tag{5.8}$$

$$\Psi(t) = 2\pi 5t + 10\sin(2\pi 0.1t) + 7\sin(2\pi 0.3t) \tag{5.9}$$

Figure 5.4 shows the integral of the envelope, as well as $A(t)$, the signal and its PSI

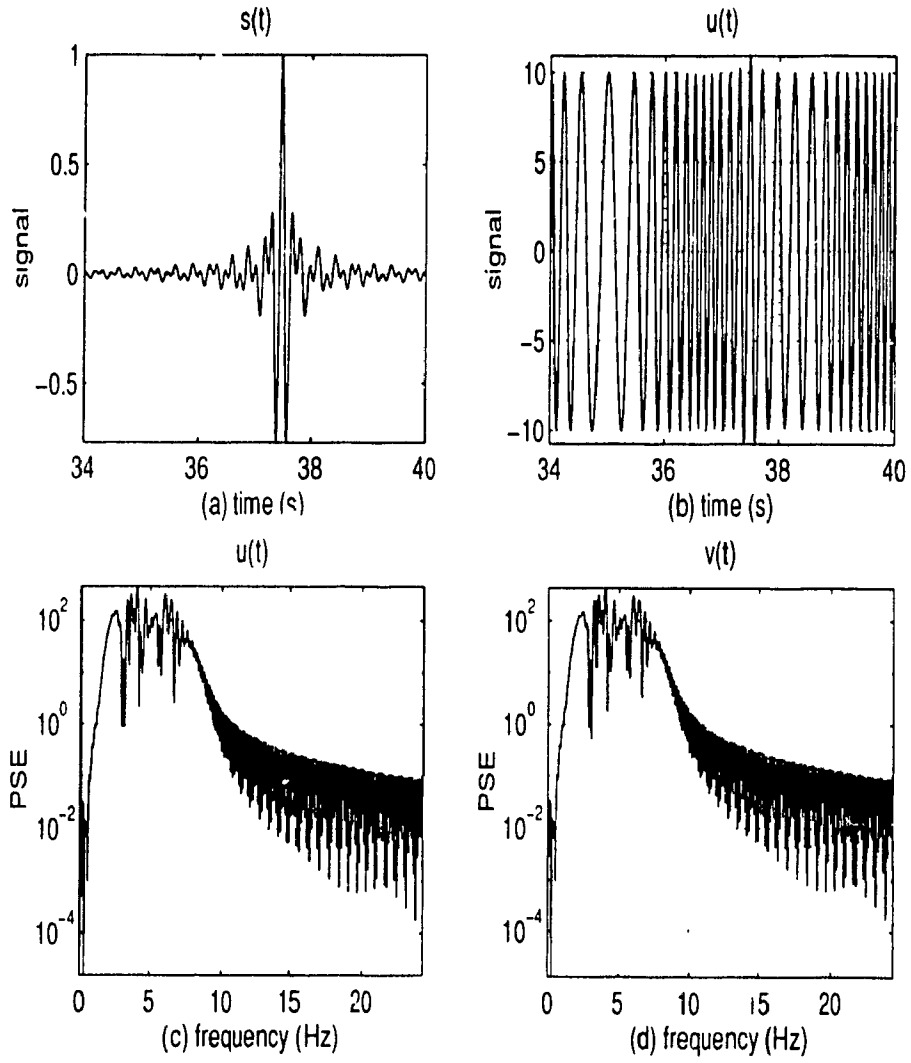

Figure 5.1: This figure shows the signal $s(t)$ and the mixture $u(t)$, along with the power spectrum estimates of $u(t)$ and $v(t)$.

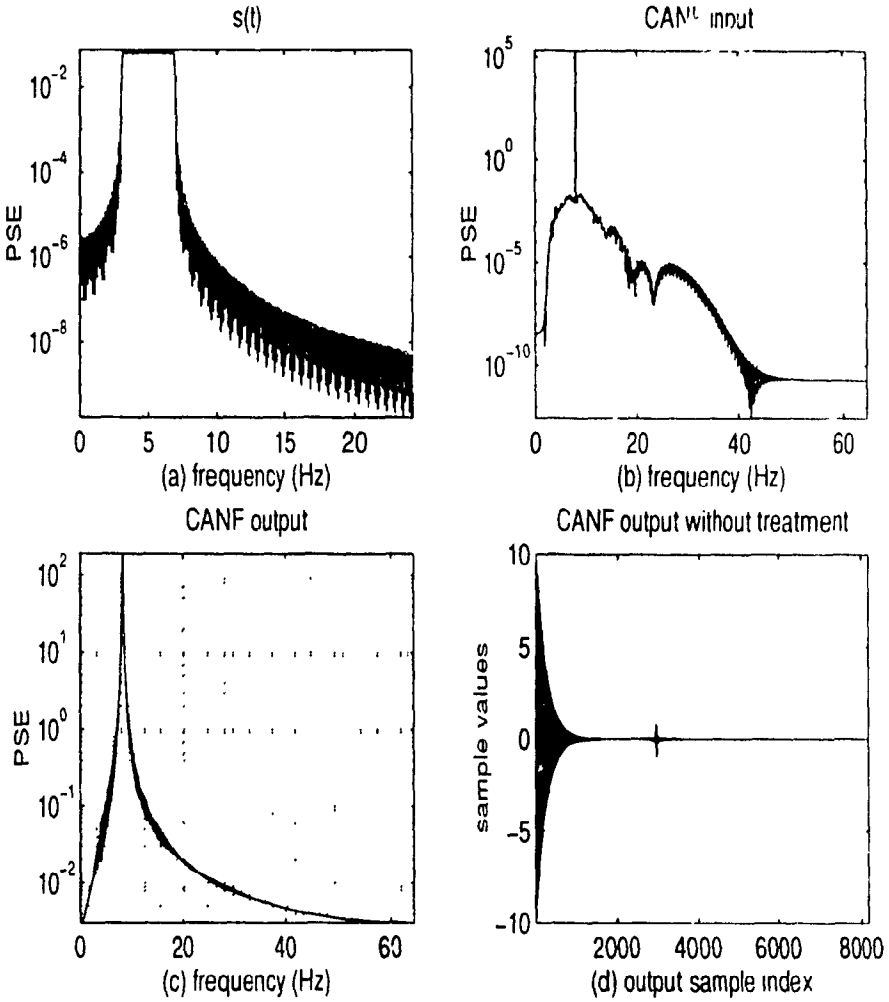

Figure 5.2: The power spectrum estimate of $s(t)$ is shown in this figure, as well as the effect of nonuniform sampling on the signal $u(t)$.

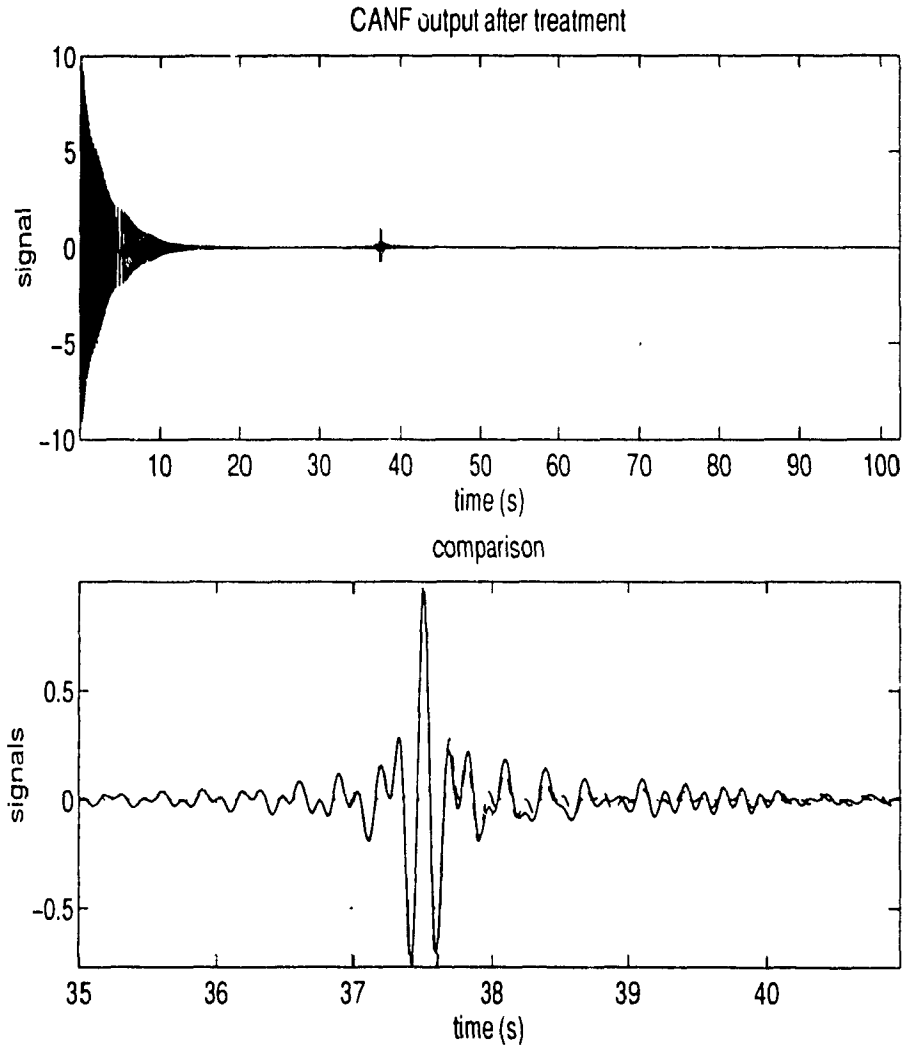

Figure 5.3: The signal $s(t)$ (before the addition of interference) is shown with dashes, and the recovery after time warping, filtering and interpolation with a continuous line.

The integral of the envelope provides the basis of the criterion to choose the nonuniform sampling points. Let

$$\Delta\gamma = \int_{t_k}^{t_{k+1}} A(t)dt \tag{5.10}$$

which is a fixed constant that ultimately defines the sampling rate. The sequence of nonuniform time instants $\{t_k\}$, obtained from Equation 5.10, is used to sample the signal. After sampling, the integral of the envelope changes to a straight line and the envelope to a constant in a new t' domain, shown in Figure 5.5. The subindices of the points $\{t_k\}$ are used for the abscissa axis in the t' domain. Figure 5.5 depicts the phase and shape of the AM/FM signal in the t' domain, along with the corresponding *PSF*. The AM/FM signal becomes a FM signal in the t' domain. A second transformation is then performed on the phase in the t' domain, so that the phase is sampled at the points where constant increments happen; if the phase is then drawn in a new t'' domain, with an abscissa axis defined by the subindex of the consecutive constant increments mentioned, a straight line represents now the phase, and the original AM/FM signal is a sinusoid with a constant envelope in the t'' domain. The corresponding shape and *PSF* are shown in Figure 5.6. This single sinusoid thus obtained can be suppressed or enhanced according to the application.

5.1.3 A time–varying envelope and a fixed-valued phase

The procedure proposed for this case assumes a time varying but known envelope, and the phase is a straight line. This is an AM signal, and the Figures 5.7, 5.8, and 5.9 show the steps to follow to transform the signal into a FM signal in the t' domain, and then into a single sinusoid with constant amplitude in the t'' domain. The transformation from the t domain to the t' domain proceeds in a similar manner as was shown in the last section, and the transformation from the t' domain to the t'' domain, where a FM signal is transformed into a single sinusoid, proceeds as was shown in Section 5.1.1. The inverse transformation, back into the original t domain, is also possible because the knowledge of the sets of points used for the transformations from domain to domain is kept.

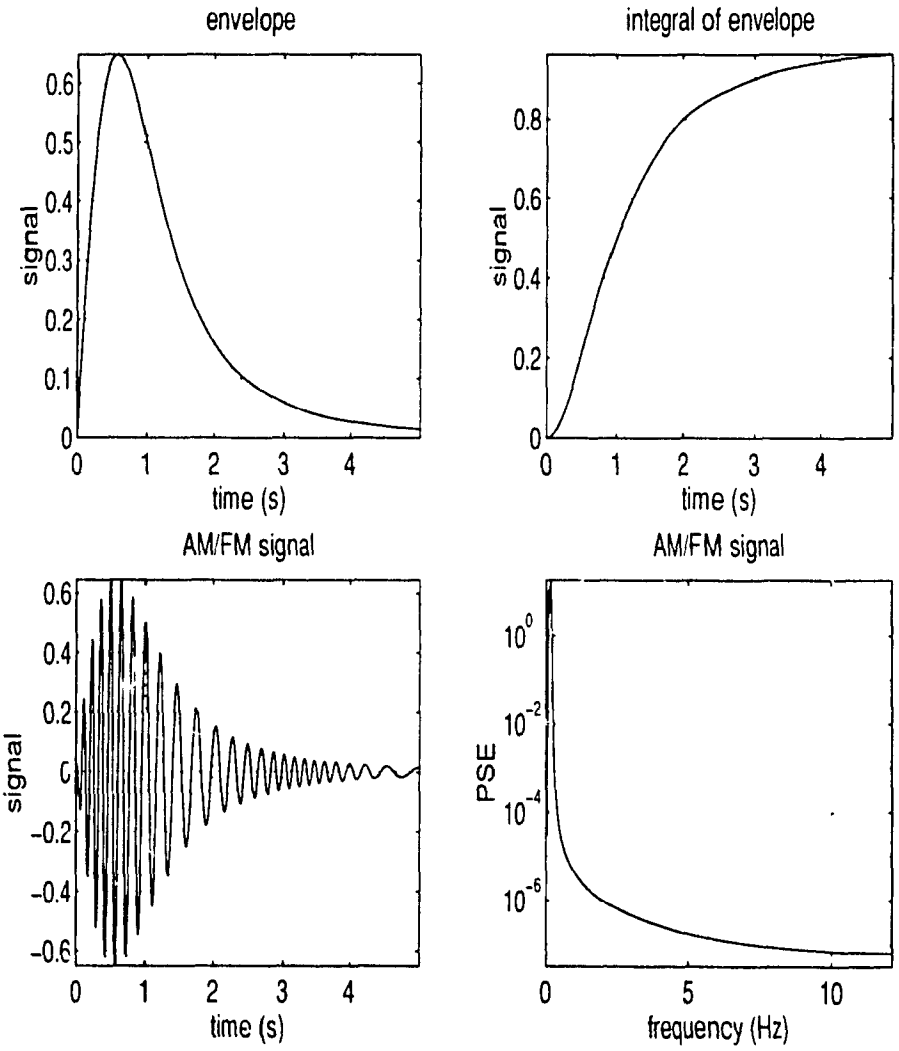

Figure 5.4: This figure shows an AM/FM signal, its power spectrum, the signal envelope, and the integral of the envelope.

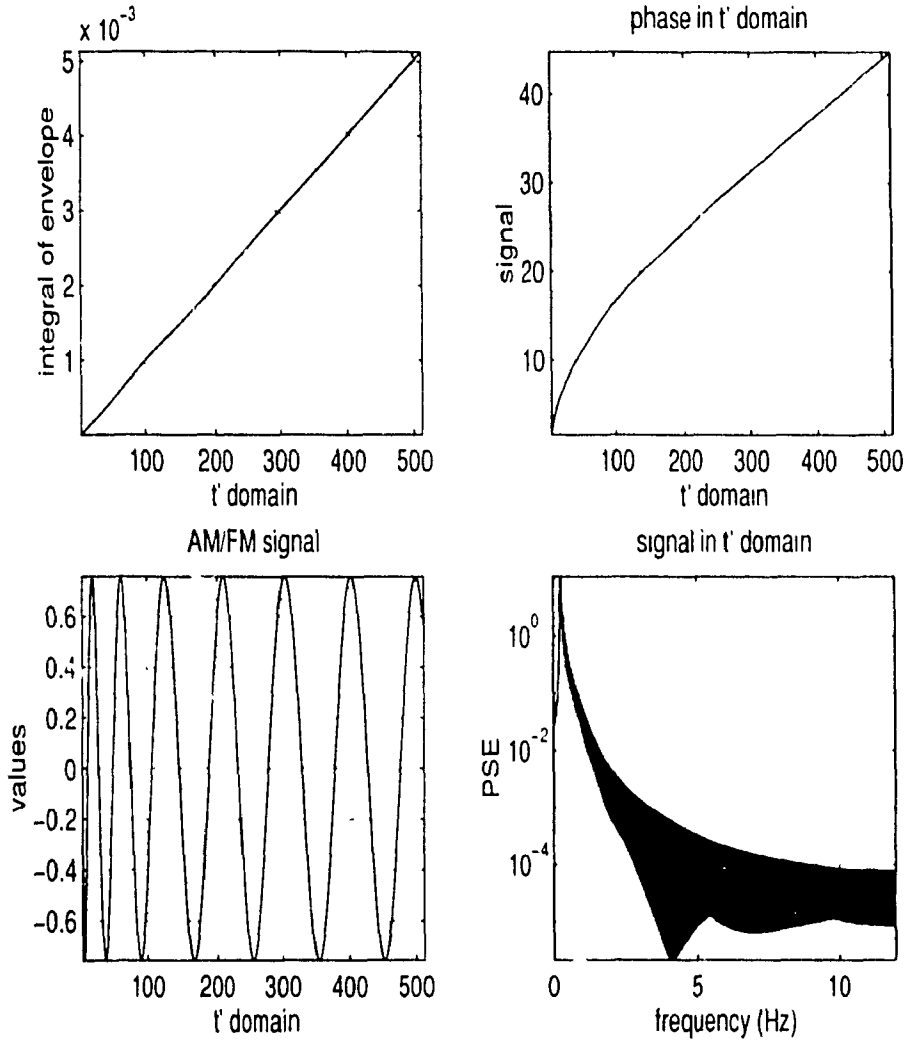

Figure 5.5: This figure shows the first step in the application of time warping to an AM/FM signal.

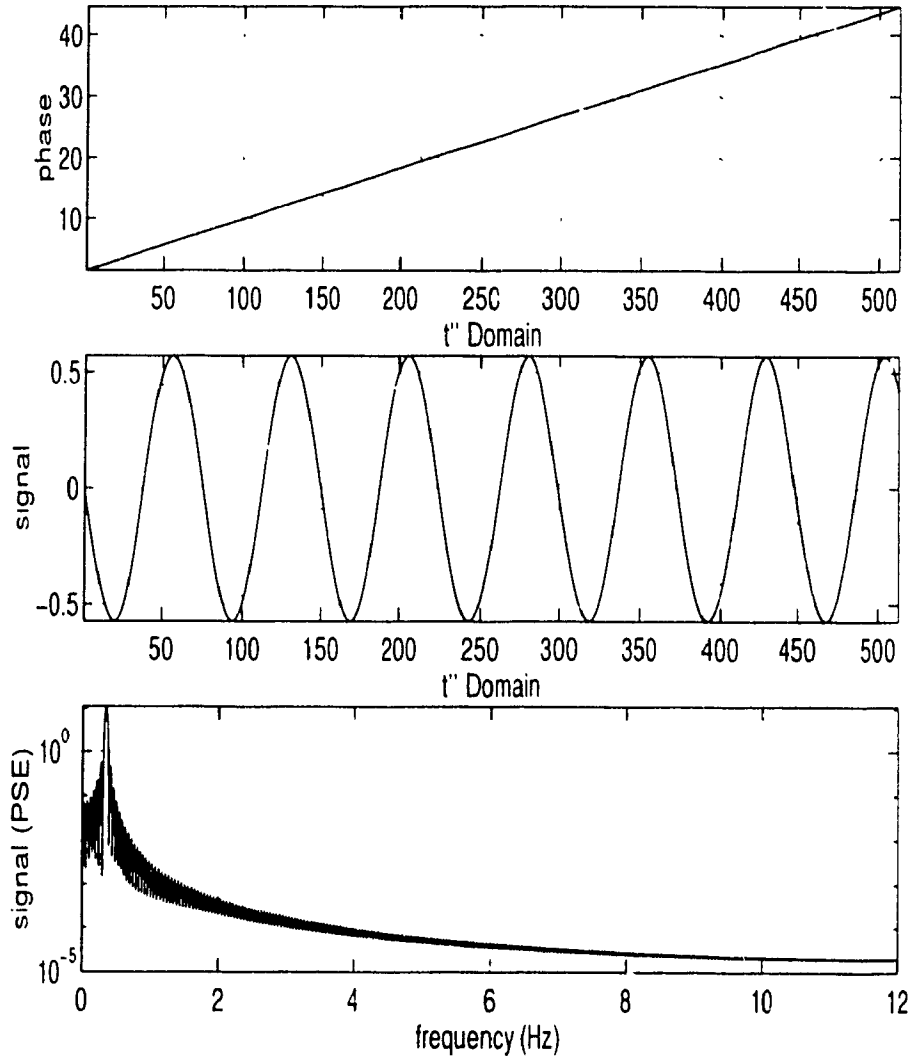

Figure 5.6: This figure shows the second step in the application of time warping to an AM/FM signal.

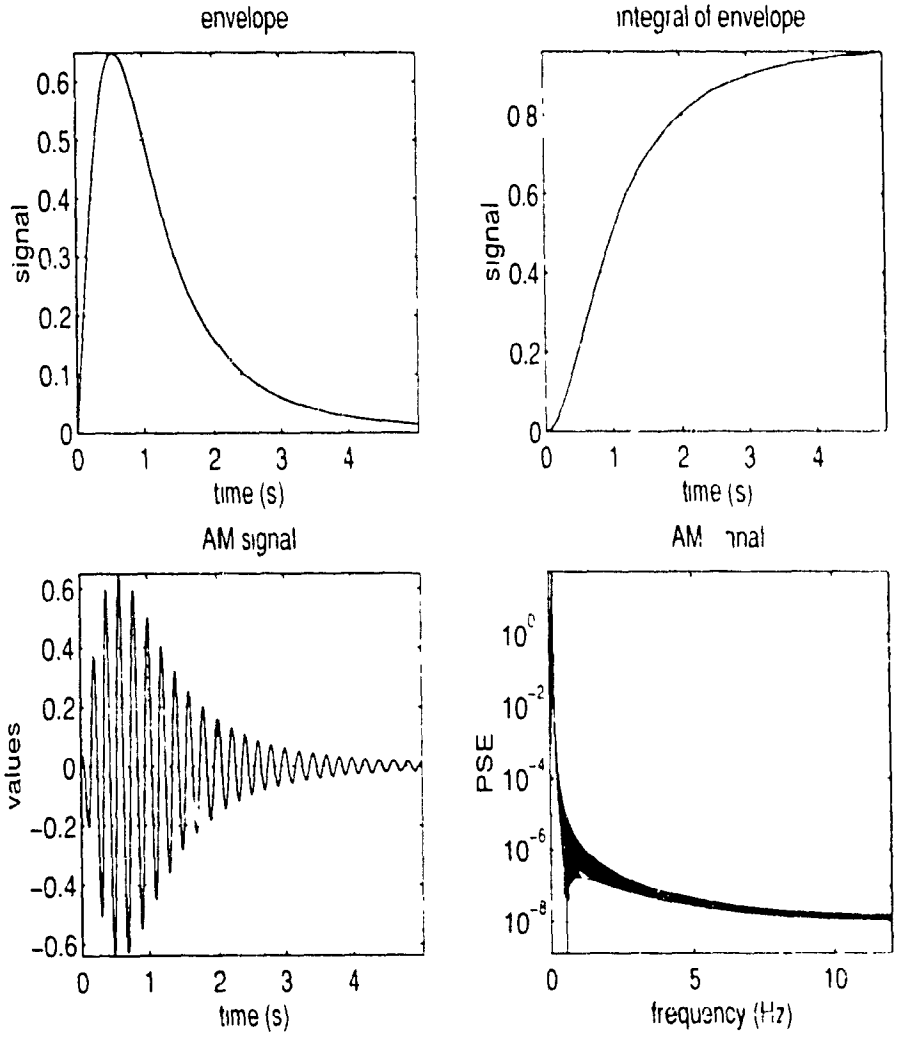

Figure 5.7: This figure shows the shape and the power spectrum of an AM signal along with its envelope and corresponding integral function

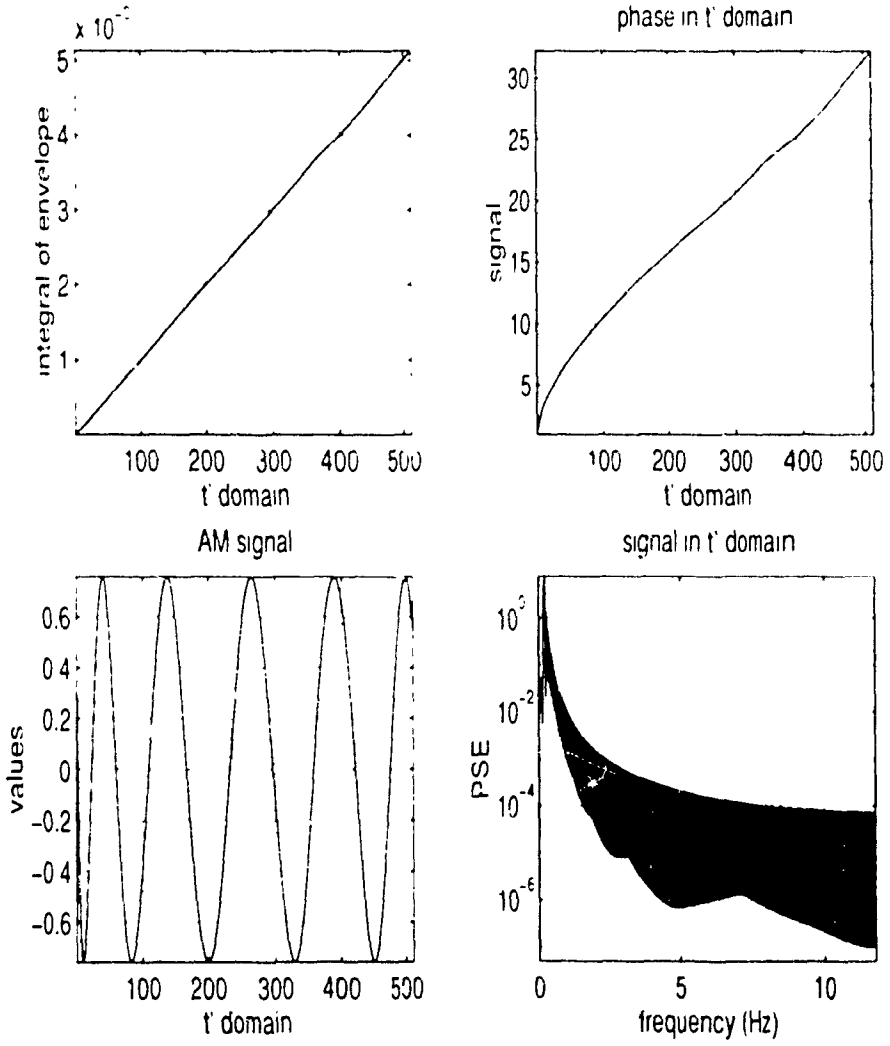

Figure 5.8: This figure shows an AM signal being transformed into a FM signal in a new domain t'. The corresponding shape and power spectrum in the new domain t' are shown, along with the phase.

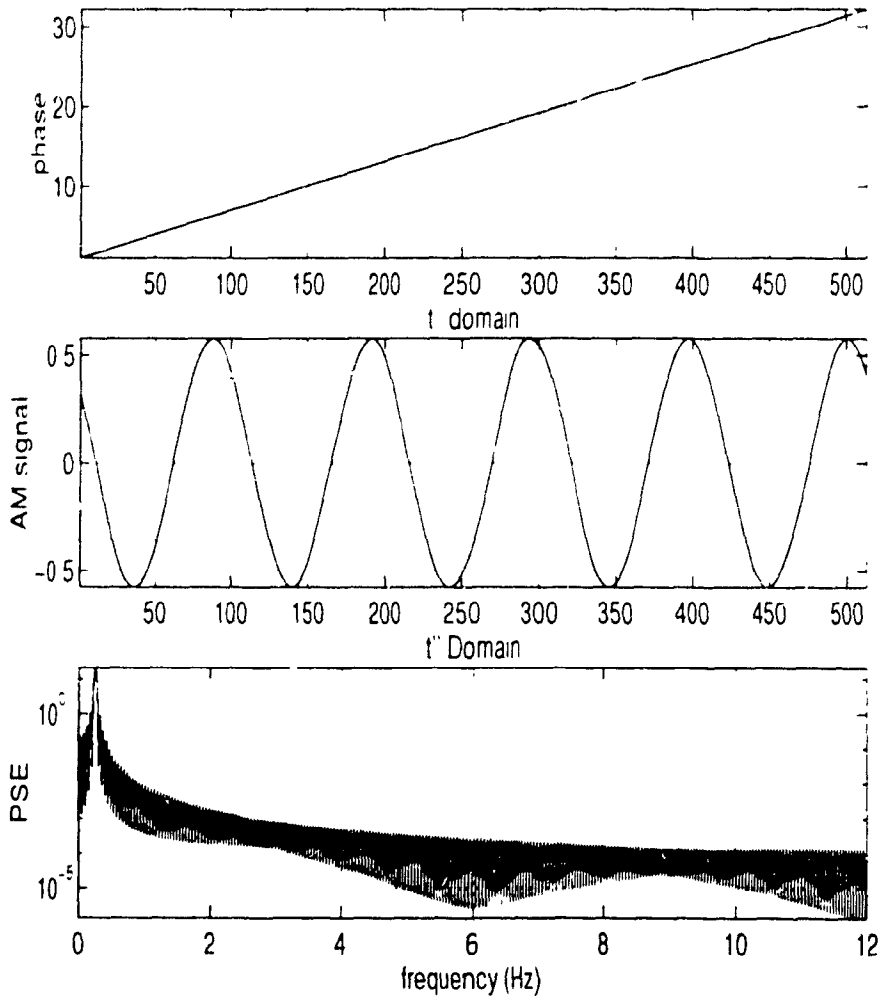

Figure 5.9: This figure shows the second step in the application of time warping to an AM signal.

5.2 Signal representation through the application of time warping

Another interesting application of the concept of time warping is in the representation of a signal as a finite sum of weighted sinc functions centered at nonuniform positions [101, 102]. The weights (coefficients of the sum) are nonuniform samples of a given signal taken at the nonuniform time positions obtained by a time warping criterion. In this section, a representation of a signal in terms of the samples of a second unrelated signal and a sum of the type mentioned above will be proposed. An intermediate function will be used to produce the nonuniform time positions where the sinc functions will be centered.

Let $z(t)$ be a signal bandlimited to the frequencies $|\omega| < \omega_z$ and belonging to the bandlimited finite energy space BL_2. Represent $z(t)$ in the form

$$z(t) = \Phi(t)\, x(t) \tag{5.11}$$

where $x(t)$ is bandlimited to ω_x. The spectral density $S_z(j\omega)$ given by the Fourier transform of $z(t)$ for the finite length observation interval I is

$$S_z(j\omega) = \begin{cases} \int_0^I \Phi(t)\, x(t) e^{-j\omega t} dt & |\omega| < \omega_m \\ 0 & |\omega| > \omega_m \end{cases} \tag{5.12}$$

Note that $\Phi(t)$ has to be bandlimited to ω_Φ, where $\omega_x + \omega_\Phi = \omega_m$; $\Phi(t)$ can be seen as a transformation over $x(t)$ or as an envelope. By definition, $\Phi(t)$ is a positive single valued function.

For the complete specification of $z(t)$, according to the WKS theorem, N samples are necessary, where

$$N = I\left[\frac{I}{\Delta t}\right] + 1 \tag{5.13}$$

with $\Delta t = \frac{\pi}{\omega_m}$ and I is a function that returns the smallest integer greater than or equal to the argument between the square brackets. Define now the function $\gamma(t)$ as

$$\frac{d\gamma(t)}{dt} = \Phi(t) \tag{5.14}$$

Replacing the last definition in Equation 5.12

$$S(j\omega) = \int_0^I x(t)e^{-j\omega t}d\gamma(t) \tag{5.15}$$

This is a Stieltjes integral that can be approximated by a Stieltjes sum using N equal step increments $\Delta\gamma = \gamma_{max}/N$, which is a constant, with

$$\gamma_{max} = \int_0^I \Phi(t)dt \tag{5.16}$$

Find the points $\{t_k\}$ that satisfy the following condition

$$\begin{aligned} \Delta\gamma &= \int_{t_k}^{t_{k+1}} \Phi(t)dt \\ &= \frac{\gamma_{max}}{N} \quad \forall\, k = 0 \qquad N-1 \end{aligned} \tag{5.17}$$

The location of the set $\{t_k\}$ depends on $\Phi(t)$. Once this set is obtained, the spectral density $S(j\omega)$ can be approximated as

$$S(j\omega) = \sum_{k=0}^{N-1} x(t_k)e^{-j\omega t_k}\Delta\gamma + r_e \tag{5.18}$$

where r_e is a residual error. If now the inverse Fourier transform is calculated,

$$\begin{aligned} z(t) &\approx \mathcal{F}^{-1}\{S_z(j\omega)\} \\ &= \frac{\Delta\gamma}{2\pi}\sum_{k=0}^{N-1} x(t_k)\int_{-\omega_m}^{+\omega_m} e^{j\omega(t-t_k)}d\omega + \mathcal{F}^{-1}\{r_e\} \\ &= \frac{\Delta\gamma}{2\pi}\sum_{k=0}^{N-1} x(t_k)\frac{2\sin[\omega_m(t-t_k)]}{t-t_k} + \mathcal{F}^{-1}\{r_e\} \\ &= 2\Delta\gamma f_m \sum_{k=0}^{N-1} x(t_k)\frac{\sin[\omega_m(t-t_k)]}{\omega_m(t-t_k)} + \mathcal{F}^{-1}\{r_e\} \\ z(t) &\approx 2\left[\frac{\gamma_{max}}{N}\right] f_m \sum_{k=0}^{N-1} x(t_k)sinc[\omega_m(t-t_k)] + \mathcal{F}^{-1}\{r_e\} \end{aligned} \tag{5.19}$$

If the functions $z(t)$ and $x(t)$ are provided, the transformation Φ could be taken as the ratio of these signals.

$$\Phi(t) = \frac{z(t)}{x(t)} \tag{5.20}$$

with the necessary restraint on $\Phi(t)$ to be a positive single valued function. If Φ is everywhere positive, then its integral is monotonically increasing, making possible the calculation of distinct and successive values t_k. To obtain $\Phi(t)$, the samples available for $z(t)$ and $x(t)$ (taken at the same time instants) should be used. The integral of Φ would be obtained, and from it the set of points $\{t_k\}$.

As an example for what has been proposed, consider now Figures 5.10 and 5.11. Two random signals, $z(t)$ and $x(t)$, the first with a bandwidth of 243 Hz, and the second with a bandwidth of 127 Hz, are shown in Figure 5.10 along with their corresponding power spectrums. In Figure 5.11, the signal $\Phi(t)$ is shown as well as its integral. The set $\{t_k\}$ is obtained from this integral by using Equation 5.17, and it is used to sample $x(t)$ and to center the sinc functions that appear in Equation 5.19. The representation of $z(t)$ is shown in the final plot of Figure 5.11. The number of points t_k used to represent $z(t)$ is the same as the minimum number of samples that according to the WKS theorem is needed to reconstruct $z(t)$. See Equation 5.13. It is also possible to increase the number of points t_k by increasing Λ in Equation 5.17, and the result would be an improved representation. The signal representation in Figure 5.11 uses $\Lambda = 28$, which is the minimum number of points to reconstruct $z(t)$ from uniform samples.

Figures 5.12 and 5.13 show a second example for the type of representation proposed in this section. This time, the signal $x(t)$ is a train of four triangular pulses.

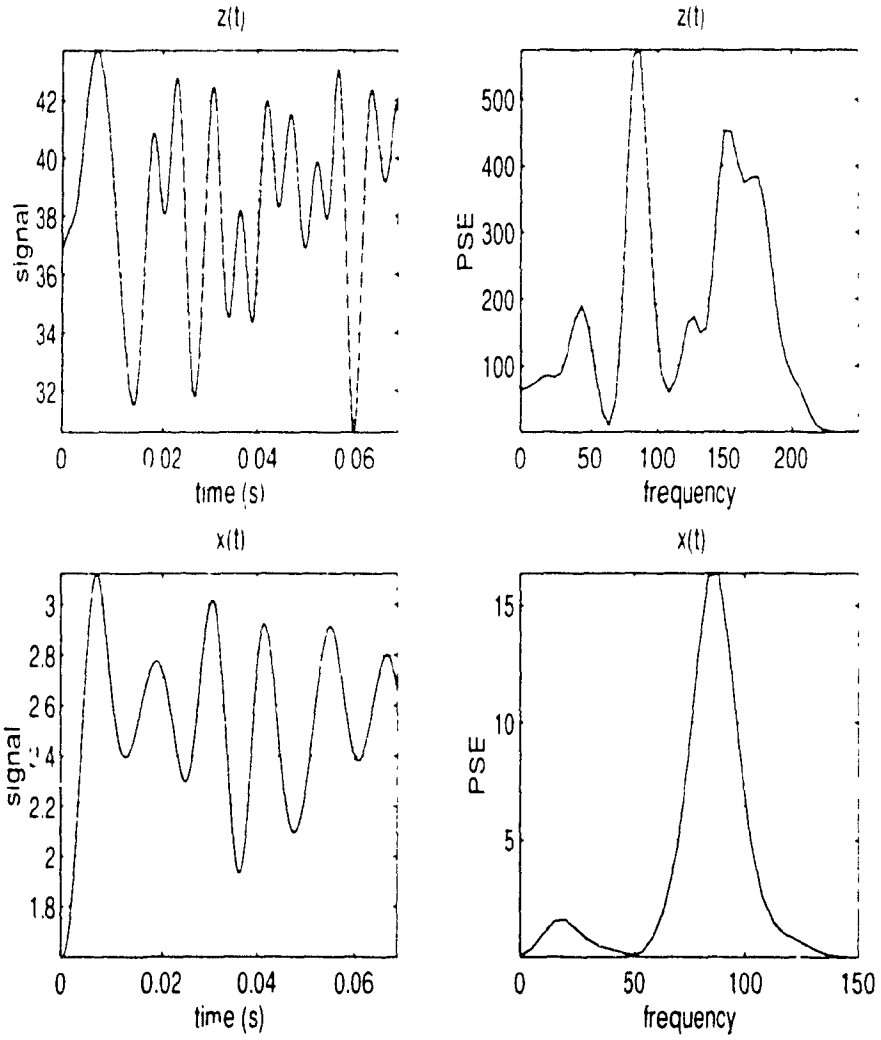

Figure 5.10: Signals $z(t)$ and $x(t)$ are shown in this figure, along with their corresponding power spectrums.

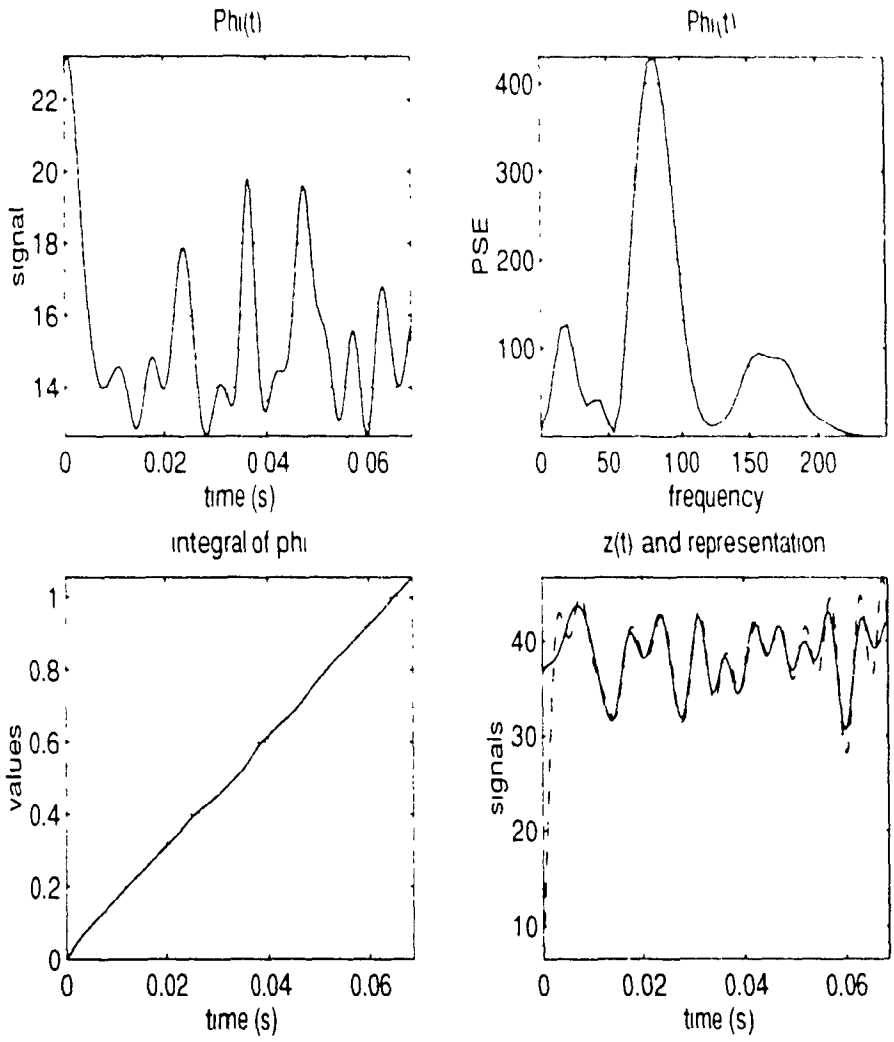

Figure 5.11: The function $\Phi(t)$ is shown here, as well as its integral. $z(t)$ is depicted as a continuous line and its representation as dashes in the final plot of this figure.

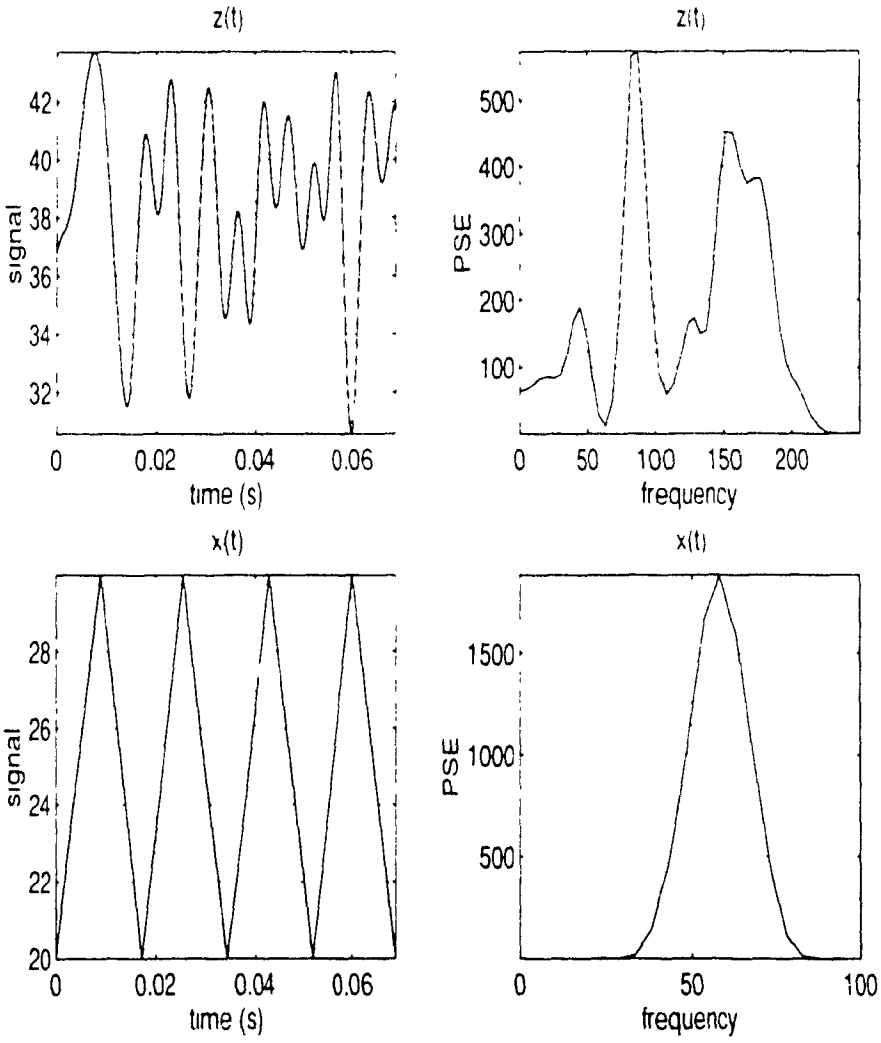

Figure 5.12: The signal $x(t)$ is a train of four triangular pulses. It is shown along with its power spectrum

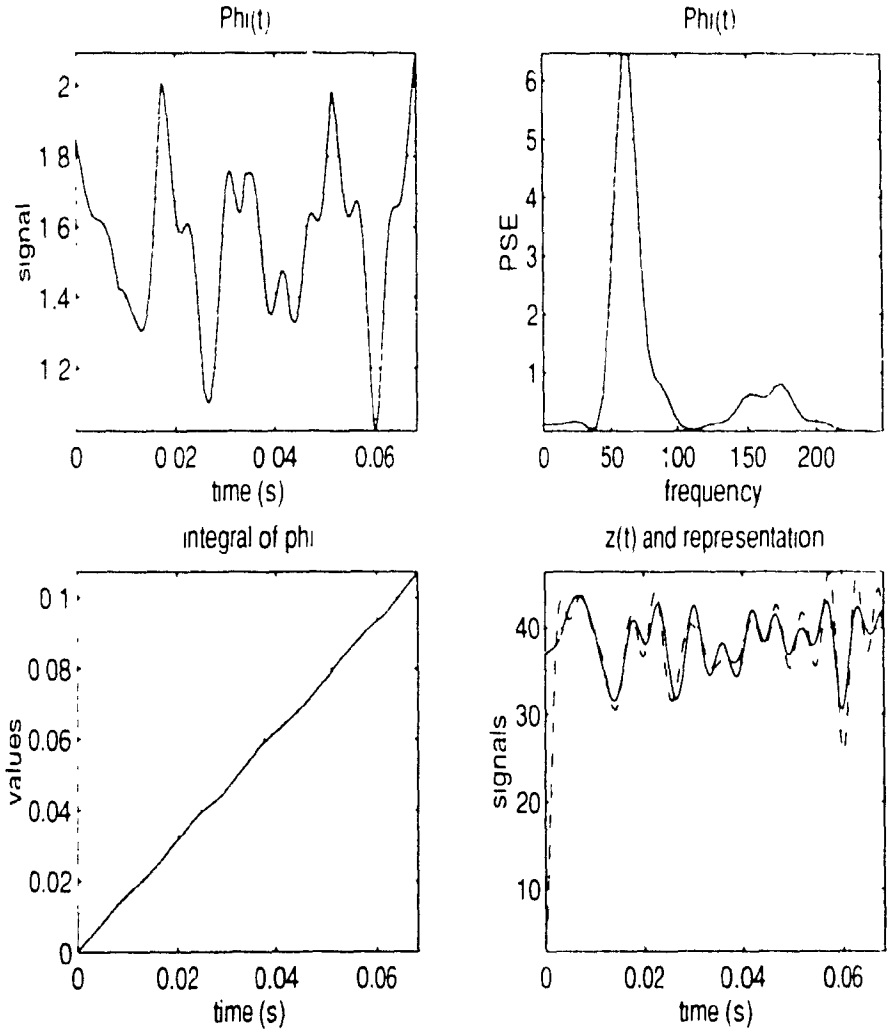

Figure 5.13: This figure shows the representation of $z(t)$ based on information obtained from a train of four triangular pulses. The signal is depicted as a continuous line and its representation as dashes in the final plot of this figure

Chapter 6

Conclusions

This thesis has been concerned with the applications of nonuniform sampling techniques based on the concept of time warping as well as with the predetermined nonuniform sampling defined by the root loci of orthogonal polynomials. The signal recovery from nonuniform samples has also been examined, and methods of reconstruction for short length intervals have been used within an iterative procedure to recover signals over longer intervals.

The following are the contributions that have been made by this research. They are accompanied by conclusions.

1. Definition of certain finite signal spaces from integral transformations based on orthonormal series expansions, for which the combination of Kramer's generalized sampling theorem and the theory of reproducing kernels produce sampling expansions whose coefficients are signal samples taken at the root loci of orthogonal polynomial. Results are obtained for the Laguerre, Hermite, Jacobi, and Bessel polynomials.

2. Extension of the SVD method of signal recovery to transformed domains other than Fourier, by considering the reproducing kernels associated with those domains. By this extension, transformations like sine, cosine and Hankel can exhibit their own version of the reconstruction method. The above mentioned finite signal spaces have their reproducing kernels, and by the same principle, the SVD method can be extended to these.

3. Extension of the SLE method of signal recovery to sampling expansions other than the WKS sampling theorem expansion. This generalization is as straightforward as the one concerning the SVD method, and it can be used for finite or infinite sampling expansions.

4. Use of the root loci of orthogonal polynomials in signal compression, FIR digital filter design, signal recovery from nonuniform samples, and signal representation by nonuniform sampling. The roots of the modified Laguerre polynomials, $R_n^{\alpha}(x)$, are included, and they form a mirrored image of the roots of the original polynomials.

5. The applicability of the SVD recovery method is extended from short length intervals to longer ones by the use of an on-line iterative procedure for the signal recovery from

nonuniform samples which rearranges the input sequence of samples into overlapping data blocks. The procedure is firstly employed for the case of uniform sampling patterns altered by jitter, but it is shown that it can also be used for the case of predetermined nonuniform sampling patterns originating from the root loci of orthogonal polynomials. To measure the deviation of time positions from those predetermined sampling patterns, a relative jitter parameter J_r is used instead of the parameter J corresponding to the uniform sampling case.

6. When the procedure mentioned above is used in conjunction with the SVD method, the overall performance in recovery is very good but the computational burden is higher with respect to the one obtained using the procedure with the SLE method. This suggests that the combination of the SLE method and the procedure is more convenient to use for the case $J < 1$ than the other combination because of the savings gained in computational complexity. For the case $1 < J < 3$ the combination of the SVD method and the procedure is more convenient than the other one because of the quality of the results, even though the computational complexity increases substantially.

7. Use of the time warping technique for the enhancement or suppression of an AM-FM or an AM signal.

8. Expansion of the concept of signal representation in terms of a finite sum of weighted sinc functions centered at nonuniform time positions. These nonuniform time instants are obtained by the time warping technique from information provided by: (1) the function whose representation is sought, and (2) another function, unrelated to the first one, from which samples will also be taken at those nonuniform time positions and will be used as the weights of the expansion.

The main contributions of this research are: (1) the derivation of sampling expansions whose coefficients are signal samples taken at the root loci of orthogonal polynomials, and (2) the introduction of an algorithm for the on-line iterative recovery of a signal from nonuniformly spaced samples.

Among the future research topics that can be explored concerning the themes studied in this thesis, we have the following

- Obtain sampling expansions for other systems of orthogonal polynomials with interesting characteristics, like the doubly orthogonal concentrated polynomials. The integral of the squared magnitude of these polynomials is maximum in an interval I at the expense of the same integral evaluated in another interval I'. The polynomials are orthogonal on both intervals, I and I' [103, 104].

- Improve the signal representation proposed for burst type signals by establishing a procedure that will use that representation as a first approximation. The goal of that procedure will be to diminish any existing misadjustment. Implement an algorithm that will process any number of transient signals, resulting in overall compression.

- Describe the system that will suppress or enhance an AM-FM or an AM signal using the time warping technique. This involves the solution of the synchronization problem for the phase (angle) and amplitude parts of the signal.

- Employ the signal representation in terms of a finite sum of weighted sinc functions centered at nonuniform time instants, in the signal recovery from irregularly spaced samples. Start with two sets $\{x(t_i)\}$ (samples) and $\{t_i\}$ (time positions), obtain a first estimation of uniform samples $\{x(nI)\}$ and use several iterations of the algorithm proposed in this thesis to recover the original signal, $x(t)$.

References

[1] A. L. Cauchy, "Memoire sur diverses formules d'analyse," *Comptes Rendus*, vol. 12, pp. 283–298, Janvier–Juin 1841.

[2] P. L. Butzer and R. L. Stens, "Sampling theory for not necessarily band-limited functions: a historical overview," *SIAM Review*, vol. 34, pp. 40–53, March 1992.

[3] A. J. Jerri, "The Shannon sampling theorem - its various extensions and applications: A tutorial review," *Proceedings of the IEEE*, vol. 65, pp. 1565–1596, Nov. 1977.

[4] A. I. Zayed, *Advances in Shannon's Sampling Theorem*, ch. 1, pp. 1–14. Boca Raton: CRC Press Inc., 1993.

[5] J. L. Yen, "On nonuniform sampling of bandwidth-limited signals," *IRE Transactions on Circuit Theory*, vol. 3, pp. 251–257, December 1956.

[6] D. J. Wingham, "The reconstruction of a band-limited function and its Fourier transform from a finite number of samples at arbitrary locations by singular value decomposition," *IEEE Transactions on Signal Processing*, vol. 40, pp. 559–570, March 1992.

[7] F. J. Beutler, "Sampling theorems and bases in a Hilbert space," *Information and Control*, vol. 4, pp. 97–117, 1961.

[8] F. J. Beutler, "Error free recovery of signals from irregularly spaced samples," *SIAM Review*, vol. 8, pp. 328–335, July 1966.

[9] F. J. Beutler and O. A. Z. Leneman, "Random sampling of random processes: Stationary point processes," *Information and Control*, vol. 9, pp. 325–346, 1966.

[10] O. A. Z. Leneman, "Random sampling of random processes: Impulse processes," *Information and Control*, vol. 9, pp. 347–363, 1966.

[11] O. A. Z. Leneman, "Random sampling of random processes: Optimum linear interpolation," *Journal of the Franklin Institute*, vol. 281, pp. 302–314, April 1966.

[12] O. A. Z. Leneman and J. B. Lewis, "Random sampling of random processes: Mean square comparison of various interpolators," *IEEE Transactions on Automatic Control*, vol. 11, pp. 396–403, July 1966.

[13] O. A. Z. Leneman and J. B. Lewis, "A note on reconstruction for randomly sampled data," *IEEE Transactions on Automatic Control*, vol. 11, p. 626, July 1966.

[14] K. Yao and J. B. Thomas, "On some stability and interpolatory properties of nonuniform sampling expansions," *IEEE Transactions on Circuit Theory*, vol. 14, pp. 404–408, December 1967.

[15] J. R. Higgins, "A sampling theory for irregularly spaced sample points," *IEEE Transactions on Information Theory*, pp. 621–622, September 1976.

[16] A. J. Willis, "SVD perturbation approach to estimation of bandlimited signal in presence of sample jitter," *Electronics Letters*, vol. 27, pp. 2204–2206, 21st November 1991.

[17] R. G. Wiley, "Recovery of bandlimited signals from unequally spaced samples," *IEEE Transactions on Communications*, vol. 26, pp. 135–137, January 1978.

[18] R. G. Wiley, "On an iterative technique for recovery of bandlimited signals," *Proceedings of the IEEE*, vol. 66, pp. 522–523, April 1978.

[19] F. A. Marvasti, "Spectral analysis of random sampling and error free recovery by an iterative method," *Transactions of the IECE of Japan*, vol. E 69, pp. 79–82, February 1986.

[20] F. A. Marvasti, M. Analoui, and M. Gamshadzahi, "Recovery of signals from nonuniform samples using iterative methods," *IEEE Transactions on Signal Processing*, vol. 39, pp. 872–877, April 1991.

[21] C. Cenker, H. G. Feichtinger, and H. Steier, "Fast iterative and non-iterative reconstruction of band-limited functions from irregular sampling values," in *Proceedings of the 1991 IEEE International Conference on Acoustics, Speech, and Signal Processing*, (Toronto), pp. 1773–1776, IEEE, 14–17 May 1991.

[22] K. Gröchenig, "Reconstruction algorithms in irregular sampling," *Mathematics of Computation*, vol. 59, pp. 181–194, July 1992.

[23] H. G. Feichtinger and K. Gröchenig, "Iterative reconstruction of multivariate band-limited functions from irregular sampling values," *SIAM Journal on Mathematical Analysis*, vol. 23, pp. 244–261, January 1992.

[24] E. I. Plotkin and M. N. S. Swamy, "Signal reconstruction from nonequally spaced samples with applications to jitter error reduction and bandwidth compression," in *Proceedings of ISSPA 87* (B. Boashash, ed.), (Brisbane, Australia), pp. 337–341, 24–28 August 1987.

[25] Y. Yoganandam, E. I. Plotkin, and M. N. S. Swamy, "An alternate method for the recovery of band-limited sequences from nonuniformly decimated versions," in

Proceedings of the 1993 Pacific Rim Conference on Communications, Computers, and Signal Processing, (Victoria, British Columbia), IEEE, 19-21 May 1993.

[26] E. I. Plotkin, M. N. S. Swamy, and Y. Yoganandam, "A novel iterative method for the reconstruction of signals from nonuniformly spaced samples," *Signal Processing*, vol. 37, pp. 203-213, May 1994.

[27] K. Horiuchi, "Sampling principle for continuous signals with time-varying bands," *Information and Control*, vol. 13, pp. 53-61, 1968.

[28] T. J. Deeming, "Fourier analysis with unequally-spaced data," *Astrophysics and Space Science*, vol. 36, pp. 137-158, 1975.

[29] E. van der Ouderaa and J. Renneboog, "Some formulas and applications of nonuniform sampling of bandwidth-limited signals," *IEEE Transactions on Instrumentation and Measurement*, vol. 37, pp. 353-357, September 1988.

[30] Y. Rahmat-Samii and R. L. Cheung, "Nonuniform sampling techniques for antenna applications," *IEEE Transactions on Antennas and Propagation*, vol. 35, pp. 268-279, March 1987.

[31] P. Sircar and T. K. Sarkar, "System identification from nonuniformly spaced signal measurements," *Signal Processing*, vol. 14, pp. 253-268, April 1988.

[32] J. A. Cadzow and E. M. Camardo, "Linear processing of nonuniformly sampled signals: A Fourier analysis," in *Conference Record of the Eleventh Annual Asilomar Conference on Circuits, Systems, and Computers*, (New York), pp. 322-326, IEEE, 1978.

[33] N. J. Malloy, "Non-uniform sampling for high resolution spectrum analysis," in *Proceedings of the 1984 International Conference on Acoustics, Speech, and Signal Processing*, (San Diego), pp. 6.8.1-6.8.4, IEEE, 1984.

[34] H. Wiese and K. G. Weil, "An efficient Fourier transform algorithm for frequency domains of several decades using logarithmically spaced time samples," *IEEE Transactions on Acoustics, Speech, and Signal Processing*, vol. 36, pp. 1096-1099, July 1988.

[35] P. C. Bagshaw and M. Sarhadi, "Analysis of samples of wideband signals taken at irregular, sub-Nyquist, intervals," *Electronics Letters*, vol. 27, pp. 1228-1230, 4th July 1991.

[36] F. Gori and G. Guattari, "Use of non-uniform samplings with a single correcting operation," *Optics Communications*, vol. 3, pp. 404-406, August 1971.

[37] P. Sircar and A. C. Ranade, "Nonuniform sampling and study of transient systems response," *IEE Proceedings - Part F*, vol. 139, pp. 49-55, February 1992.

[38] N. Sayiner, H. V. Sorensen, and T. R. Viswanathan, "A non-uniform sampling technique for A/D conversion," in *1993 IEEE International Symposium on Circuits and Systems*, (Chicago), pp. 1220–1223, IEEE, 3–6 May 1993.

[39] V.-E. Neagoe, "Chebyshev nonuniform sampling cascaded with the discrete cosine transform for optimum interpolation," *IEEE Transactions on Acoustics, Speech, and Signal Processing*, vol. 38, pp. 1812–1815, October 1990.

[40] Y. S. Zhu and S. W. Leung, "Systolic array implementations for Chebyshev nonuniform sampling," in *Proceedings of the 1992 International Conference on Acoustics, Speech, and Signal Processing*, (San Francisco), pp. 177–180, IEEE, 1992.

[41] J. Mark and T. Todd, "A nonuniform sampling approach to data compression," *IEEE Transactions on Communications*, vol. 29, pp. 24–32, January 1981.

[42] Y. C. Jenq, "Digital spectra of non-uniformly sampled signals with applications to digitally synthesized sinusoids," in *Proceedings of the 1987 International Conference on Acoustics, Speech, and Signal Processing*, (Dallas), pp. 16.9.1–16.9.3, IEEE, 1987.

[43] Y. C. Jenq, "Digital spectra of nonuniformly sampled signals: Fundamentals and high speed waveform digitizers," *IEEE Transactions on Instrumentation and Measurement*, vol. 37, pp. 245–251, June 1988.

[44] Y. C. Jenq, "Digital spectra of nonuniformly sampled signals—Digital look up tunable sinusoidal oscillators," *IEEE Transactions on Instrumentation and Measurement*, vol. 37, pp. 358–362, September 1988.

[45] Y. C. Jenq, "Digital spectra of nonuniformly sampled signals: A robust sampling time offset estimation algorithm for ultra high-speed waveform digitizers using interleaving," *IEEE Transactions on Instrumentation and Measurement*, vol. 39, pp. 71–75, February 1990.

[46] Y. C. Jenq, "Digital spectra of nonuniformly sampled signals: Theories and applications – Measuring clock/Aperture jitter of an A/D system," *IEEE Transactions on Instrumentation and Measurement*, vol. 39, pp. 969–971, December 1990.

[47] B. Summers, G. D. Cain, and A. Yardim, "FIR digital filter design using non-equispaced frequency sampling," *Electronics Letters*, vol. 25, pp. 338–339, 2nd March 1989.

[48] S. Bozic and F. Soltani, "FIR design by non-uniform sampling in frequency domain," *International Journal of Electronics*, vol. 65, no. 4, pp. 815–821, 1988.

[49] E. Angelidis and J. E. Diamessis, "A parallel interpolation method for designing FIR digital filters by nonuniform frequency samples," in *Proceedings of the 1993 International Conference on Acoustics, Speech, and Signal Processing*, (Minneapolis), pp. 105–108, IEEE, 1993.

[50] E. Hille, "Introduction to general theory of reproducing kernels," *Rocky Mountain Journal of Mathematics*, vol. 2, pp. 321-368, Summer 1972.

[51] N. Aronszajn, "Theory of reproducing kernels," *Transactions of the American Mathematical Society*, vol. 68, pp. 337-404, 1950.

[52] A. Papoulis, *Signal Analysis*, ch. 3, pp. 66-74, New York: McGraw-Hill, 1977.

[53] A. A. G. Requicha, "The zeros of entire functions: Theory and engineering applications," *Proceedings of the IEEE*, vol. 68, pp. 308-328, Mar. 1980.

[54] A. H. Zemanian, *Generalized Integral Transformations*, ch. 9, pp. 247-285, New York: Dover, 1987.

[55] F. A. Grünbaum, "A new property of reproducing kernels for classical orthogonal polynomials," *Journal of Mathematical Analysis and Applications*, vol. 95, pp. 491-500, 1983.

[56] G. Szegö, *Orthogonal Polynomials*, vol. XXIII of *Colloquium Publications*, ch. 4-5, pp. 57-106, New York City: American Mathematical Society, 1939.

[57] H. L. Krall and O. Frink, "A new class of orthogonal polynomials: The Bessel polynomials," *Transactions of the American Mathematical Society*, vol. 65, pp. 100-115, January-June 1949.

[58] S. D. Selvaratnam, *Shannon-Whittaker Sampling Theorems*, PhD thesis, University of Wisconsin, Milwaukee, August 1987.

[59] G. G. Walter, "Recent extension of the sampling theorem," in *Signal Processing Part I: Signal Processing Theory* (L. Auslander, T. Kailath, and S. Mitter, eds.), pp. 229-238, New York: Springer-Verlag, 1990.

[60] G. G. Walter and A. I. Zayed, "The continuous (α, β)-Jacobi transform and its inverse when $\alpha + \beta + 1$ is a positive integer," *Transactions of the American Mathematical Society*, vol. 305, pp. 653–664, February 1988.

[61] K. Yao, "Applications of reproducing kernel Hilbert spaces - bandlimited signal models," *Information and Control*, vol. 11, pp. 429–444, 1967.

[62] H. P. Kramer, "A generalized sampling theorem," *Journal of Mathematics and Physics*, vol. 38, pp. 68–72, 1959.

[63] J. Romero, E. I. Plotkin, and M. N. S. Swamy, "Reproducing kernels and the use of root loci of specific functions in the recovery of signals from nonuniform samples," *Signal Processing*, vol. 49, no. 1, pp. 11-23, 1996.

[64] A. J. Jerri, "Some applications for Kramer's generalized sampling theorem," *Journal of Engineering Mathematics*, vol. 3, pp. 103–105, April 1969.

[65] A. J. Jerri, *On Extension of the Generalized Sampling Theorem*, PhD thesis, Oregon State University, Corvallis, June 1967.

[66] M. Z. Nashed and G. G. Walter, "General sampling theorems for functions in reproducing kernel Hilbert spaces," *Mathematics of Control, Signals, and Systems*, vol. 4, pp. 363–390, 1991.

[67] J. Romero, E. I. Plotkin, and M. N. S. Swamy, "Using root distribution of specific functions in signal recovery from nonuniform samples," in *Proceedings of the 1994 Canadian Conference on Electrical and Computer Engineering* (C. R. Baird and M. E. El-Hawary, eds.), (Halifax), pp. 473–476, Canadian Society for Electrical and Computer Engineering, 25–28 September 1994.

[68] W. H. Press, S. A. Teukolsky, W. T. Vetterling, and B. P. Flannery, *Numerical Recipes in C: The Art of Scientific Computing*, ch. 2, p. 61. New York: Cambridge University Press, second ed., 1992.

[69] J. Bunch, J. Dongarra, C. Moler, and G. W. Stewart, *LINPACK User's Guide*, ch. 1, pp. 1.1–1.35. Philadelphia: Society for Industrial and Applied Mathematics, 1979.

[70] H. J. Landau, "Sampling, data transmission, and the Nyquist rate," *Proceedings of the IEEE*, vol. 55, pp. 1701–1706, October 1967.

[71] H. . G. Feichtinger, K. Gröchenig, and T. Strohmer, "Efficient numerical methods in non-uniform sampling theory," *Numerische Mathematik*, vol. 69, no. 4, pp. 423–440, 1995.

[72] J. J. Benedetto, "Frame decompositions, sampling, and uncertainty principle inequalities," in *Wavelets: Mathematics and Applications* (J. J. Benedetto and M. W. Frazier, eds.), pp. 247–304, Boca Raton: CRC Press Inc., 1994.

[73] H. G. Feichtinger and K. Gröchenig, "Theory and practice of irregular sampling," in *Wavelets: Mathematics and Applications* (J. J. Benedetto and M. W. Frazier, eds.), pp. 305–363, Boca Raton: CRC Press Inc., 1994.

[74] J. Romero and E. I. Plotkin, "An on-line method for signal recovery from nonuniform samples using block-rearrangement," in *Proceedings of the 1995 Canadian Conference on Electrical and Computer Engineering* (F. Gagnon, ed.), (Montréal), pp. 457–460, IEEE Canada, 5–8 September 1995.

[75] J. Romero and E. I. Plotkin, "On-line SVD-based iterative method for signal recovery from nonuniform samples," *Electronics Letters*, vol. 32, pp. 20–21, 4th January 1996.

[76] J. S. Lim, *Two-Dimensional Signal and Image Processing*, ch. 1, pp. 39–42. Englewood Cliffs, NJ: Prentice-Hall, 1990.

[77] J. Romero and F. I. Plotkin, "Nonuniform sampling based on the use of root loci of orthogonal polynomials," in *Proceedings of the 1995 Workshop on Sampling Theory and Applications*, (Jurmala (Latvia)), pp. 49–54, Institute of Electronics and Computer Science, 19–22 September 1995.

[78] W. J. Rozwod, C. W. Therrien, and J. S. Lim, "Design of 2-D FIR filters by nonuniform frequency sampling," *IEEE Transactions on Signal Processing*, vol. 39, pp. 2508–2514, November 1991.

[79] A. Zakhor and G. Alvstad, "Two-dimensional polynomial interpolation from nonuniform samples," *IEEE Transactions on Signal Processing*, vol. 40, pp. 169–180, January 1992.

[80] Angelidis and J. Diamessis, "A novel method for designing FIR digital filters with onuniform frequency samples," *IEEE Transactions on Signal Processing*, vol. 42, pp. 259–267, February 1994.

[81] V. Algazi and M. Suk, "On the frequency weighted least-square design of finite duration filters," *IEEE Transactions on Circuits and Systems*, vol. 22, pp. 943–953, December 1975.

[82] J. T. Kim, W. J. Oh, and Y. H. Lee, Design of nonuniformly spaced linear-phase FIR filters using mixed integer linear programming," *IEEE Transactions on Signal Processing*, vol. 44, pp. 123–126, January 1996.

[83] A. Antoniou, *Digital Filters: Analysis, Design, and Applications*, ch. 9, pp. 271–279, New York: McGraw-Hill, second ed., 1993.

[84] S. Haykin, *Adaptive Filter Theory*, ch. 11, pp. 402–417, Prentice-Hall Information and System Sciences Series, Englewood Cliffs, NJ: Prentice-Hall, second ed., 1991.

[85] R. A. Gopinath, "Thoughts on least squared-error optimal windows," *IEEE Transactions on Signal Processing*, vol. 44, pp. 984–987, April 1996.

[86] C. S. Burrus, A. W. Soewito, and R. A. Gopinath, "Least squared error FIR filter design with transition bands," *IEEE Transactions on Signal Processing*, vol. 40, pp. 1327–1340, June 1992.

[87] M. V. Spreckelsen and B. Bromm, "Estimation of single-evoked cerebral potentials by means of parametric modeling and Kalman filtering," *IEEE Trans. Biomedical Engineering*, vol. BME-35, pp. 691–700, Sept. 1988.

[88] A. Papoulis, "Error analysis in sampling theory," *Proceedings of the IEEE*, vol. 54, pp. 947–955, July 1966.

[89] B. H. Jansen and Y. S. Yeh, "Single trial evoked potential analysis by means of crosscorrelation and dynamic time-warping," *Signal Processing*, vol. 11, pp. 179–186, September 1986.

[90] J. T. Graf and N. Hubing, "Dynamic time warping comb filter for the enhancement of speech degraded by white gaussian noise," in *Proceedings of the 1993 IEEE International Conference on Acoustics, Speech, and Signal Processing*, (Minneapolis), pp. 339–342, IEEE, 1993. Volume II.

[91] M. K. Brown and L. R. Rabiner, "An adaptive, ordered, graph search technique for dynamic time warping for isolated word recognition," *IEEE Transactions on Acoustics, Speech, and Signal Processing*, vol. 30, pp. 535–544, August 1982.

[92] W. Philips, "ECG data compression with time-warped polynomials," *IEEE Transactions on Biomedical Engineering*, vol. 40, pp. 1095–1101, November 1993.

[93] W. Philips, "Coding properties of time-warped polynomial transforms," *Signal Processing*, vol. 37, pp. 229–242, 1994.

[94] J. J. Clark, M. R. Palmer, and P. D. Lawrence, "A transformation method for the reconstruction of functions from nonuniformly spaced samples," *IEEE Transactions on Acoustics, Speech, and Signal Processing*, vol. 33, pp. 1151–1165, October 1985.

[95] D. Cochran and J. J. Clark, "On the sampling and reconstruction of time-warped bandlimited signals," in *Proceedings of the 1990 International Conference on Acoustics, Speech, and Signal Processing*, (Albuquerque), pp. 1539–1541, IEEE, 3–6 April 1990.

[96] R. D. Gitlin, J. F. Hayes, and S. B. Weinstein, *Data Communications Principles*, ch. 5, pp. 306–309. Applications of Communications Theory, New York: Plenum Press, 1992.

[97] D. Wulich, E. I. Plotkin, and M. N. S. Swamy, "Synthesis of discrete time varying null filters for frequency-varying signals using the time-warping technique," *IEEE Transactions on Circuits and Systems*, vol. 37, pp. 977–990, August 1990.

[98] D. Wulich, E. I. Plotkin, and M. N. S. Swamy, "Constrained notch filtering of nonuniformly spaced samples for enhancement of an arbitrary signal corrupted by a strong FM interference," *IEEE Transactions on Signal Processing*, vol. 39, pp. 2359–2363, October 1991.

[99] D. Wulich, E. I. Plotkin, M. N. S. Swamy, and W. Tong, "PLL synchronized time varying constrained notch filter for retrieving a weak multiple sine signal jammed by FM interference," *IEEE Transactions on Signal Processing*, vol. 40, pp. 2866–2870, November 1992.

[100] W. Tong, E. I. Plotkin, D. Wulich, and M. N. S. Swamy, "Self-synchronized signal controlled constrained notch filter for rejection of nonstationary interference," in *Proceedings of the 1991 International Conference on Acoustics, Speech, and Signal Processing*, (Toronto), pp. 1937–1940, IEEE, 14–17 May 1991.

[101] E. I. Plotkin, L. M. Roytman, and M. N. S. Swamy, "Nonuniform sampling of bandlimited modulated signals," *Signal Processing*, vol. 4, pp. 295–303, 1982.

[102] E. I. Plotkin, L. M. Roytman, and M. N. S. Swamy, "Reconstruction of nonuniformly sampled band-limited signals and jitter error reduction," *Signal Processing*, vol. 7, pp. 151–160, October 1984.

[103] E. N. Gilbert and D. Slepian, "Doubly orthogonal concentrated polynomials," *SIAM Journal on Mathematical Analysis*, vol. 8, pp. 290–319, April 1977.

[104] A. Papoulis and M. S. Bertran, "Digital filtering and prolate functions," *IEEE Transactions on Circuit Theory*, vol. 19, pp. 674–681, November 1972.

[105] M. Lang and B.-C. Frenzel, "Polynomial root finding," *IEEE Signal Processing Letters*, vol. 1, pp. 141–143, October 1994.

[106] M. Lang and B.-C. Frenzel, "A new and efficient program for finding all polynomial roots," Tech. Rep. 9308, Electrical and Computer Engineering Department, Rice University, Houston, 15 April 1994.

[107] G. Sansone, *Orthogonal Functions*, p. 298. New York: Interscience Publishers, Inc., revised English ed., 1959.

[108] J. R. Rice, *Matrix Computations and Mathematical Software*, ch. 5, pp. 48–50. New York: McGraw-Hill, 1981.

[109] G. H. Golub and C. Reinsch, "Singular value decomposition and least squares solutions," *Numerische Mathematik*, vol. 14, pp. 403–420, 1970.

Appendix A

Functions and Constants

Several functions and constants that have been used in Chapter 2, are defined below. The notation follows references [54–57].

- Laguerre Transformation:

$$h_N = \Gamma(\alpha+1)\begin{pmatrix} N+\alpha \\ N \end{pmatrix}, \quad k_N = \frac{(-1)^N}{N!}, \quad w(x) = x^\alpha e^{-x}$$

- Jacobi Transformation: The weight function has already been indicated.

$$h_N = \frac{\Gamma(\alpha+N+1)\Gamma(\beta+N+1)}{N!\,\Gamma(\alpha+\beta+N+1)} \frac{2^{\alpha+\beta+1}}{\alpha+\beta+2N+1}$$

$$k_N = \frac{\Gamma(\alpha+N+1)}{N!\Gamma(\alpha+\beta+N+1)} \frac{1}{2^N} \frac{\Gamma(\alpha+\beta+2N+1)}{\Gamma(\alpha+N+1)}$$

- Hermite Transformation:

$$h_N = \pi^{\frac{1}{2}} 2^N N!, \quad k_N = 2^N, \quad w(x) = e^{-x^2}$$

- Bessel Transformation:

$$h_N = \frac{(-1)^{N+1}(b)^N N!\Gamma(\alpha)}{(2N+\alpha-1)\Gamma(N+\alpha-1)}, \quad k_N = \frac{\Gamma(2N+\alpha-1)}{b^N \Gamma(N+\alpha-1)}$$

$$\rho(x) = \frac{1}{2\pi j} \sum_{n=0}^{\infty} \frac{\Gamma(\alpha)}{\Gamma(\alpha+n-1)} \left(-\frac{b}{x}\right)^n$$

Note in the last equation, for the case $\alpha = 2$, $a \neq b$, $\rho(x) = e^{-\frac{b}{x}}$. Also, $j = \sqrt{-1}$.

Appendix B

Equivalence Between the Two Methods Utilized in Chapter 3

The two methods utilized in Chapter 3 give similar results in recovery from nonuniform samples, thus those methods may be considered as equivalent ones, as the following reasoning demonstrates. According to the SVD method [6], the solution to the reconstruction problem is

$$\underline{h}[t] = \underline{L}_r[t, n]\underline{q}[n]$$

where $\underline{q}[n]$ is the observations vector, and

$$L_r(t, n) = \sum_j u_j(t)\lambda_j^{-1}v_j(n)$$

is the kernel of the right inverse operator $\mathbf{L}_r$. Recall that $u_k(t)$ are functions centered at the time instants where the samples have been taken:

$$u_k(t) = \lambda_k^{-1}\sum_n v_k(n)K(t, t_n)$$

where $K(t, t_n)$ is the reproducing kernel evaluated at the time instant t and at the sample instant t_n. In the absence of jitter, if the samples are taken at the values given by the roots of the classical orthogonal polynomials of order $N + 1$,

$$K(t, t_n) = b(t_n)S_n(t)$$

where $b(t_n)$ is a normalization constant, and $S_n(t)$ is an element of the orthonormal set of functions derived from the reproducing kernel in Chapter 2. The eigenvalue-eigenvector equation [6]

$$KK_a[n, m]\underline{v}[m] = \lambda^2\underline{v}[n]$$

that defines the relationship among singular values, eigenvectors, and the matrix KK_a, simplifies when the samples are taken at the aforementioned values. Note that the entries of the matrix equal $K(t_n, t_m)$, and

$$K(t_n, t_m) = \begin{cases} b(t_n) & \text{if } n = m \\ 0 & \text{otherwise} \end{cases}$$

Therefore, the eigenvalue-eigenvector equation can be written as

$$\begin{bmatrix} b(t_1) & 0 & 0 & \cdots & 0 \\ 0 & b(t_2) & 0 & \cdots & 0 \\ \vdots & \vdots & \ddots & \vdots & \vdots \\ 0 & 0 & 0 & b(t_N) & 0 \\ 0 & 0 & 0 & 0 & b(t_{N+1}) \end{bmatrix} \underline{v}[m] = \lambda^2\underline{v}[n]$$

For the type of square matrix described above, the eigenvalues have the form $\lambda_i = b(t_i)$ and the eigenvectors

$$\underline{v}_1 = \begin{bmatrix} 1 \\ 0 \\ 0 \\ 0 \\ \vdots \\ 0 \\ 0 \end{bmatrix}, \underline{v}_2 = \begin{bmatrix} 0 \\ 1 \\ 0 \\ 0 \\ \cdot \\ 0 \\ 0 \end{bmatrix}, \underline{v}_3 = \begin{bmatrix} 0 \\ 0 \\ 1 \\ 0 \\ \\ 0 \\ 0 \end{bmatrix} \quad \cdots \quad \underline{v}_{N-1} \begin{bmatrix} 0 \\ 0 \\ \\ 0 \\ 1 \\ 0 \\ 0 \end{bmatrix}, \underline{v}_N \begin{bmatrix} 0 \\ 0 \\ 0 \\ \\ 0 \\ 1 \\ 0 \end{bmatrix}, \underline{v}_{N+1} \begin{bmatrix} 0 \\ 0 \\ 0 \\ \\ 0 \\ 0 \\ 1 \end{bmatrix}$$

The particular configuration of the λ's and of the eigenvectors simplify the expressions for $u_k(t)$ and for $L_i(t, n)$, as only one of the factors in the respective sum will be different from zero.

$$u_i(t) = \lambda_i^{-1} \sum_k v_i(n) h(t, t_k) = \lambda_i^{-1} \sum_k v_i(n) b(t_k) S_k(t) = \lambda_i^{-1} b(t_i) S_i(t)$$

Also, another expression that is simplified is

$$L_i(t, n) = \sum_i u_i(t) \lambda^{-1} v_i(n) = \lambda^{-1} u_i(t) = \lambda^{-1} b(t_i) S_i(t) = S_i(t)$$

Finally,

$$\underline{h}[t] = \underline{L}_i[t, n] \underline{q}[n] = \sum_n q(n) L_i(t, n) = \sum_n q(n) S_i(t)$$

which is equal to the reconstruction formula implemented by the sampling expansion approach. This result can be expected to be approximately valid even with small values of jitter.

Appendix C

Division by Zero in the Evaluation of Sampling Expansions

One particular problem found, when calculating the values of functions computationally from the kind of sampling expansions derived in this thesis, is the appearance of divisions by zero when the evaluation point is close to a polynomial root according to computer accuracy.

A solution to the above problem is to express the composing function present in the sampling expansion in an equivalent way, where it is absent from the denominator the factor that produces the division by zero.

As an illustration, consider the Laguerre-based sampling expansion derived in Chapter 2. The general expression for the composing function has been shown to be,

$$S_k(t) = \frac{t_k(t/t_k)^{\alpha/2}\exp(\frac{-(t-t_k)}{2})[-L^{\alpha}_{N+1}]}{(t-t_k)(N+1+\alpha)L^{\alpha}_{N}(t_k)} \tag{C.1}$$

so that the sampling expansion for a function f of finite support N is

$$f(t) = \sum_{k=1}^{N+1} f(t_k)S_k(t) \tag{C.2}$$

The polynomial $L^{\alpha}_{N+1}(t)$ can be expressed as:

$$\begin{aligned} L^{\alpha}_{N+1}(t) &= a_{N+1}t^{N+1} + a_N t^N + a_{N-1}t^{N-1} + \cdots + a_1 t + a_0 \\ &= a_{N+1}\left[t^{N+1} + \frac{a_N}{a_{N+1}}t^N + \frac{a_{n-1}}{a_{N+1}}t^{N-1} + \cdots + \frac{a_1}{a_{N+1}}t + \frac{a_0}{a_{N+1}}\right] \\ &= a_{N+1}[(t-t_1)(t-t_2)(t-t_3)\cdots(t-t_N)(t-t_{N+1})] \end{aligned}$$

where $\{r_i\}$ are the roots of the polynomial. Therefore,

$$L^{\alpha}_{N+1}(t) = a_{N+1}\prod_{l=1}^{N+1}(t-t_l)$$

For the Laguerre polynomials [51],

$$a_{N+1} = \frac{(-1)^{N+1}}{(N+1)!}$$

Combining the last results into the expression for the composing function:

$$\begin{aligned} S_k(t) &= \frac{t_k(t/t_k)^{\alpha/2}\exp(\frac{-(t-t_k)}{2})[-L^{\alpha}_{N+1}(t)]}{(t-t_k)(N+1+\alpha)L^{\alpha}_{N}(t_k)} \\ &= \frac{t_k(t/t_k)^{\alpha/2}\exp(\frac{-(t-t_k)}{2})(-1)a_{N+1}\prod_{l=1}^{N+1}(t-t_l)}{(t-t_k)(N+1+\alpha)L^{\alpha}_{N}(t_k)} \\ &= \frac{t_k(t/t_k)^{\alpha/2}\exp(\frac{-(t-t_k)}{2})\frac{(-1)^{N+2}}{(N+1)!}\prod_{l=1}^{N+1}(t-t_l)}{(t-t_k)(N+1+\alpha)L^{\alpha}_{N}(t_k)} \end{aligned}$$

For $l = k$, $t_l = t_k$. Therefore,

$$S_k(t) = \frac{(-1)^N t_k (t/t_k)^{\alpha/2} \exp(\frac{-(t-t_k)}{2}) \prod_{l=1, l\neq k}^{N+1} (t - t_l)}{(N+1)!(N+1+\alpha) L_N^{\alpha}(t_k)} \tag{C.3}$$

The product of factors present in the last formula needs for its evaluation the knowledge of the polynomial roots. A good program for finding polynomial roots is presented in [105]. On the other hand, when calculating polynomial coefficients from the roots, the computation can lead to large errors despite the fact that the polynomial may have the best numerical condition. To avoid this problem, a re-ordering of the roots (the so-called Leja ordering) can be used to correct this problem [106].

The final expression for the function f is

$$f(t) = \sum_{k=1}^{N+1} f(t_k) \left[\frac{(-1)^N t_k (t/t_k)^{\alpha/2} \exp(\frac{-(t-t_k)}{2}) \prod_{l=1, l\neq k}^{N+1} (t - t_l)}{(N+1)!(N+1+\alpha) L_N^{\alpha}(t_k)} \right] \tag{C.4}$$

Appendix D

Intermediate Algebraic Operations

Several relationships have been given in Chapter 2. The algebraic operations that justify those results are shown here.

D.1 Jacobi transformation

D.1.1 Composing function for the Jacobi transformation

What is left to do to find the composing function is to evaluate the integral

$$\int_{-1}^{1} |K(t,t_k)|^2 dx = \lim_{t \to t_k} K(t,t_k)$$

which will provide the normalizing constant. Let

$$\frac{2^{-\alpha-\beta}}{2N+\alpha+\beta+2} \frac{\Gamma(N+2)\Gamma(N+\alpha+\beta+2)}{\Gamma(N+\alpha+1)\Gamma(N+\beta+1)} = \Lambda(\alpha,\beta)$$

Now, we will have,

$$\begin{aligned}
\lim_{t \to t_k} K(t,t_k) &= \lim_{t \to t_k} [w(t)w(t_k)]^{\frac{1}{2}} \Lambda(\alpha,\beta) \left\{ \frac{P_{N+1}^{(\alpha,\beta)}(t) P_N^{(\alpha,\beta)}(t_k)}{(t-t_k)} \right\} \\
&= \Lambda(\alpha,\beta) w(t_k) P_N^{(\alpha,\beta)}(t_k) \left[\frac{d}{dx} P_{N+1}^{(\alpha,\beta)}(t) \right]_{t=t_k} \\
&= \Lambda(\alpha,\beta) w(t_k) P_N^{(\alpha,\beta)}(t_k) \left[\frac{N+\alpha+\beta+2}{2} \right] \left[P_N^{(\alpha+1,\beta+1)}(t) \right]_{t=t_k} \\
&= \Lambda(\alpha,\beta) w(t_k) P_N^{(\alpha,\beta)}(t_k) \left[\frac{N+\alpha+\beta+1}{2} \right] P_N^{(\alpha+1,\beta+1)}(t_k)
\end{aligned}$$

The composing function will be the ratio of Equation 2.26 and the last result, which appears in Equation 2.29.

D.1.2 The particular case $x = y$ in the reproducing kernel

The reproducing kernel for signals of finite support was established to be

$$K(x,y) = [w(x)w(y)]^{\frac{1}{2}} \Lambda(\alpha,\beta) \frac{P_{N+1}^{(\alpha,\beta)}(x) P_N^{(\alpha,\beta)}(y) - P_N^{(\alpha,\beta)}(x) P_{N+1}^{(\alpha,\beta)}(y)}{(x-y)}$$

When $x = y$, the L'Hôspital rule when applied gives

$$K(y,y) = \lim_{x \to y} [w(x)w(y)]^{\frac{1}{2}} \Lambda(\alpha,\beta) \frac{P_{N+1}^{(\alpha,\beta)}(x) P_N^{(\alpha,\beta)}(y) - P_N^{(\alpha,\beta)}(x) P_{N+1}^{(\alpha,\beta)}(y)}{(x-y)}$$

$$
\begin{aligned}
&= w(y)\Lambda(\alpha,\beta)\left\{P_N^{(\alpha,\beta)}(y)\left[\frac{d}{dx}P_{N+1}^{(\alpha,\beta)}(x)\right]_{x=y} - P_{N+1}^{(\alpha,\beta)}(y)\left[\frac{d}{dx}P_N^{(\alpha,\beta)}(x)\right]_{x=y}\right\} \\
&= w(y)\Lambda(\alpha,\beta)\left\{P_N^{(\alpha,\beta)}(y)\left[\frac{N+2+\alpha+\beta}{2}\right]P_N^{(\alpha+1,\beta+1)}(y) - \right. \\
&\quad \left. P_{N+1}^{(\alpha,\beta)}(y)\left[\frac{N+1+\alpha+\beta}{2}\right]P_{N-1}^{(\alpha+1,\beta+1)}(y)\right\}
\end{aligned}
$$

When using the reproducing kernel $K(x,y)$ in the SVD method (which justifies the title *reproducing kernel approach* to the procedure), the samples will be located at points y. If in the absence of jitter, and if these points y are roots of the Jacobi polynomial of order $N+1$, $K(y,y)$ simplifies to

$$
K(y,y) = w(y)\Lambda(\alpha,\beta)P_N^{(\alpha,\beta)}(y)\left[\frac{N+2+\alpha+\beta}{2}\right]P_N^{(\alpha+1,\beta+1)}(y)
$$

D.2 Hermite transformation

D.2.1 Composing function for the Hermite transformation

The normalization constant is calculated in the following way:

$$
\begin{aligned}
\int_{-\infty}^{\infty}|K(t,t_k)|^2dt &= \lim_{t\to t_k}\frac{\exp(-\left[\frac{t^2+t_k^2}{2}\right])H_{N+1}(t)H_N(t_k)}{2^{N+1}N!\sqrt{\pi}(t-t_k)} \\
&= \frac{\exp(-t_k^2)H_N(t_k)}{2^{N+1}N!\sqrt{\pi}}\lim_{t\to t_k}\left[\frac{H_{N+1}(t)}{(t-t_k)}\right] \\
&= \frac{\exp(-t_k^2)H_N(t_k)}{2^{N+1}N!\sqrt{\pi}}\left[\frac{d}{dx}[H_{N+1}(t)]\right]_{t=t_k}
\end{aligned}
$$

Making use of the equality $\frac{d}{dt}H_N(t) = 2NH_{n-1}(t)$ [54],

$$
\int_{-\infty}^{\infty}|K(t,t_k)|^2dt = 2(N+1)H_N(t_k)\frac{\exp(-t_k^2)H_N(t_k)}{\sqrt{\pi}2^{N+1}N!}
$$

Dividing Equation 2.27 by the last constant will produce Equation 2.30.

D.2.2 The particular case $x = y$ in the reproducing kernel

We have the following calculations for this case:

$$
\lim_{x\to y}K(x,y) = \lim_{x\to y}\frac{\exp(-\frac{x^2+y^2}{2})\{H_{N+1}(x)H_N(y) - H_N(x)H_{N+1}(y)\}}{2^{N+1}N!\sqrt{\pi}(x-y)}
$$

$$
\begin{aligned}
&= \frac{\exp(-y^2)}{2^{N+1}N!\sqrt{\pi}}\left[H_N(y)\left[\frac{d}{dx}H_{N+1}(x)\right]_{x=y} - H_{N+1}(y)\left[\frac{d}{dx}H_N(x)\right]_{x=y}\right] \\
&= \frac{\exp(-y^2)}{2^{N+1}N!\sqrt{\pi}}\left[H_N(y)2(N+1)H_N(y) - H_{N+1}(y)2NH_{N-1}(y)\right] \\
&= \frac{\exp(-y^2)}{2^{N+1}N!\sqrt{\pi}}\left[2(N+1)H_N^2(y) - 2NH_{N+1}H_{N-1}(y)\right] \\
K(y,y) &= \frac{\exp(-y^2)}{2^N N!\sqrt{\pi}}\left\{(N+1)H_N^2(y) - NH_{N+1}(y)H_{N-1}(y)\right\}
\end{aligned}
$$

When y is a root of the Hermite polynomial of order $N+1$:

$$
K(y,y) = \frac{\exp(-y^2)}{2^N N!\sqrt{\pi}}(N+1)H_N^2(y)
$$

D.3 Generalized Bessel transformation

D.3.1 The composing function for the Bessel transformation

The normalization constant is calculated in the following way:

$$
\begin{aligned}
\oint |K(t,t_k)|^2 dt &= \frac{(-1)^{N+1}\rho(t_k)\Gamma(N+a)y_N(t_k)}{(2N+a)N!\Gamma(a)}\left[\frac{d}{dt}y_{N+1}(t)\right]_{t=t_k} \\
&= \frac{(-1)^{N+1}\rho(t_k)\Gamma(N+a)y_N(t_k)}{(2N+a)N!\Gamma(a)}\frac{b(N+1)y_N(t_k)}{t_k^2[2(N+1)+a-2]}
\end{aligned}
$$

The following relationship has been used [57] in the last step:

$$
\frac{d}{dt}y_N(t) = \frac{1}{t^2(2N+a-2)}\left\{[N(2N+a-2)t - bN]y_N(t) + bNy_{N-1}(t)\right\}
$$

which when applied to the present case and evaluated at $t = t_k$ (a root of the polynomial of order $N+1$), will give

$$
\left[\frac{d}{dt}y_{N+1}(t)\right]_{t=t_k} = \frac{b(N+1)y_N(t_k)}{t_k^2[2(N+1)+a-2]}
$$

The normalizing constant will then be

$$
\oint |K(t,t_k)|^2 dt = \frac{(-1)^{N+1}\rho(t_k)\Gamma(N+a)y_N^2(t_k)b(N+1)}{(2N+a)N!\Gamma(a)t_k^2[2(N+1)+a-2]}
$$

Equation 2.28 when divided by this normalizing constant will give Equation 2.31. Note that, even though the reproducing kernel is complex, the composing function is real. The SVD method can not be used with the reproducing kernel because it is complex.

D.4 Laguerre transformation

The particular case $x = y$ in Equation 2.12 will now be analyzed for the Laguerre transformation. Taking the limit when $x \to y$,

$$\begin{aligned} K(y,y) &= \lim_{x\to y}(xy)^{\alpha/2}\exp(-\frac{x+y}{2})\frac{\Gamma(N+2)}{\Gamma(N+\alpha+1)}\left\{\frac{L_N^\alpha(x)L_{N+1}^\alpha(y)-L_{N+1}^\alpha(x)L_N^\alpha(y)}{(x-y)}\right\} \\ &= y^\alpha\exp(-y)\frac{\Gamma(N+2)}{\Gamma(N+\alpha+1)}\left\{\left[\frac{d}{dx}L_N^\alpha(x)\right]_{x=y}L_{N+1}^\alpha(y) - \right. \\ &\quad \left.\left[\frac{d}{dx}L_{N+1}^\alpha(x)\right]_{x=y}L_N^\alpha(y)\right\} \end{aligned}$$

The following identity will be useful [56]:

$$\frac{d}{dx}L_N^\alpha(x) = \frac{1}{x}\left[NL_N^\alpha(x) - (N+\alpha)L_{N-1}^\alpha(x)\right]$$

Using the last identity in the present development,

$$\begin{aligned} K(y,y) &= y^\alpha\exp(-y)\frac{\Gamma(N+2)}{\Gamma(N+\alpha+1)}\left\{\frac{1}{y}\left[NL_N^\alpha(y)-(N+\alpha)L_{N-1}^\alpha(y)\right]L_{N+1}(y) - \right. \\ &\quad \left.\frac{1}{y}\left[(N+1)L_{N+1}^\alpha(y)-(N+\alpha+1)L_N^\alpha(y)\right]L_N^\alpha(y)\right\} \\ &= y^\alpha\exp(-y)\frac{\Gamma(N+2)}{\Gamma(N+\alpha+1)}\{((N+\alpha+1)/y)[L_N^\alpha(y)]^2-(L_{N+1}^\alpha(y)/y)L_N^\alpha(y) \\ &\quad -((N+\alpha)/y)L_{N-1}^\alpha(y)L_{N+1}^\alpha(y)\} \\ &= y^\alpha\exp(-y)\frac{\Gamma(N+2)}{\Gamma(N+\alpha+1)}\{((N+\alpha+1)/y)[L_N^\alpha(y)]^2-(L_{N+1}^\alpha(y)/y)[L_N^\alpha(y) \\ &\quad +(N+\alpha)L_{N-1}^\alpha(y)]\} \\ &= y^{\alpha-1}\exp(-y)\frac{\Gamma(N+2)}{\Gamma(N+\alpha+1)}\{(N+\alpha+1)[L_N^\alpha(y)]^2-L_{N+1}^\alpha(y)[L_N^\alpha(y)+ \\ &\quad (N+\alpha)L_{N-1}^\alpha(y)]\} \end{aligned}$$

When y is a root of the Laguerre polynomial $L_{N+1}^\alpha(x)$, then

$$K(y,y) = y^{\alpha-1}\exp(-y)\frac{\Gamma(N+2)}{\Gamma(N+\alpha+1)}(N+\alpha+1)[L_N^\alpha(y)]^2$$

Appendix E

Modified Laguerre Polynomials

E.1 Definition and calculation of composing function

Define the modified Laguerre polynomials as

$$R_n^\alpha(x) = L_n^\alpha(\nu_n - x) \tag{E.1}$$

where ν_n is the largest root of $L_n^\alpha(x)$.
The condition of orthogonality and normalization for Laguerre polynomials is [56]:

$$\int_0^\infty e^{-x} x^\alpha L_n^\alpha(x) L_m^\alpha(x) dx = \Gamma(\alpha+1) \begin{pmatrix} n+\alpha \\ n \end{pmatrix} \delta_{nm} \tag{E.2}$$

Now, let $x = \nu_n - y$, therefore

$$\begin{aligned} \int_{-\infty}^{\nu_n} e^{-(\nu_n - y)} (\nu_n - y)^\alpha L_n^\alpha(\nu_n - y) L_m^\alpha(\nu_n - y) dy &= \Gamma(\alpha+1) \begin{pmatrix} n+\alpha \\ n \end{pmatrix} \delta_{nm} \\ \int_{-\infty}^{\nu_n} e^{-(\nu_n - y)} (\nu_n - y)^\alpha R_n^\alpha(y) L_m^\alpha(\nu_n - y) dy &= \Gamma(\alpha+1) \begin{pmatrix} n+\alpha \\ n \end{pmatrix} \delta_{nm} \\ &= \Phi(\alpha, n) \delta_{nm} \end{aligned} \tag{E.3}$$

The last equation indicates that $R_n^\alpha(y)$ is orthogonal in the interval $]-\infty, \nu_n]$ with respect to the weighting function $e^{-(\nu_n - y)}(\nu_n - y)^\alpha$. Rewriting Equation E.3,

$$\int_{-\infty}^{\nu_n} \frac{e^{-(\nu_n - y)/2} (\nu_n - y)^{\alpha/2} L_n^\alpha(\nu_n - y)}{[\Phi(\alpha, n)]^{1/2}} \frac{e^{-(\nu_n - y)/2} (\nu_n - y)^{\alpha/2} L_m^\alpha(\nu_n - y)}{[\Phi(\alpha, n)]^{1/2}} dy = \delta_{nm}$$

This means that the orthonormal sequence defined by

$$\psi_m(y) = \frac{e^{-(\nu_n - y)/2} (\nu_n - y)^{\alpha/2} L_m^\alpha(\nu_n - y)}{[\Phi(\alpha, m)]^{1/2}}$$

define an orthonormal series expansion expressed by

$$f = \sum_{m=0}^{\Lambda} F(m) \psi_m(y)$$

with f being of finite support N, if we follow the ideas presented in Chapter 2. If instead of ν_n it is used ν_{N+1}, the orthonormal sequence obtained will be of the form

$$\frac{e^{-(\nu_{N+1} - y)/2} (\nu_{N+1} - y)^{\alpha/2} L_m^\alpha(\nu_{N+1} - y)}{[\Phi(\alpha, m)]^{1/2}}$$

which will be defined in the interval $]-\infty, \nu_{N+1}]$. ν_{N+1} is the largest root of the polynomial $L_{N+1}^\alpha(y)$. Calculating now the reproducing kernel.

$$
\begin{aligned}
K(x,y) &= \sum_{n=0}^{N} \psi_n(y)\psi_n(x) \\
&= \sum_{n=0}^{N} \left(\frac{e^{-(\nu_{N+1}-y)/2}(\nu_{N+1}-y)^{\alpha/2} L_n^{\alpha}(\nu_{N+1}-y)}{[\Phi(\alpha,n)]^{1/2}} \times \right. \\
&\quad \left. \frac{e^{-(\nu_{N+1}-x)/2}(\nu_{N+1}-x)^{\alpha/2} L_n^{\alpha}(\nu_{N+1}-x)}{[\Phi(\alpha,n)]^{1/2}} \right) \\
&= \sum_{n=0}^{N} \frac{e^{-\nu_{N+1}} e^{(x+y)/2}[(\nu_{N+1}-y)(\nu_{N+1}-x)]^{\alpha/2} L_n^{\alpha}(\nu_{N+1}-y) L_n^{\alpha}(\nu_{N+1}-x)}{\Phi(\alpha,n)} \\
&= e^{-\nu_{N+1}} e^{(x+y)/2}[(\nu_{N+1}-y)(\nu_{N+1}-x)]^{\alpha/2} \sum_{n=0}^{N} \frac{L_n^{\alpha}(\nu_{N+1}-y) L_n^{\alpha}(\nu_{N+1}-x)}{\Phi(\alpha,n)}
\end{aligned}
$$

From [107],

$$
\begin{aligned}
\sum_{n=0}^{N} \frac{L_n^{\alpha}(x) L_n^{\alpha}(y)}{\Phi(\alpha,n)} &= \frac{\Gamma(N+2)}{\Gamma(N+\alpha+1)} \frac{L_{N+1}^{\alpha}(y) L_N^{\alpha}(x) - L_{N+1}^{\alpha}(x) L_N^{\alpha}(y)}{(x-y)} \\
&= I
\end{aligned}
$$

If the following change of variables is performed in the last equation,

$$
\begin{aligned}
x &= \nu_{N+1} - x' \\
y &= \nu_{N+1} - y'
\end{aligned}
$$

one will have,

$$
\begin{aligned}
I &= \frac{\Gamma(N+2)}{\Gamma(N+\alpha+1)} \frac{L_{N+1}^{\alpha}(\nu_{N+1}-y') L_N^{\alpha}(\nu_{N+1}-x') - L_{N+1}^{\alpha}(\nu_{N+1}-x') L_N^{\alpha}(\nu_{N+1}-y')}{(\nu_{N+1}-x') - (\nu_{N+1}-y')} \\
&= \frac{\Gamma(N+2)}{\Gamma(N+\alpha+1)} \frac{R_{N+1}^{\alpha}(y') L_N^{\alpha}(\nu_{N+1}-x') - R_{N+1}^{\alpha}(x') L_N^{\alpha}(\nu_{N+1}-y')}{y'-x'}
\end{aligned}
$$

Substituting now to find the reproducing kernel, one will have,

$$
\begin{aligned}
K(x,y) &= e^{-\nu_{N+1}} e^{(x+y)/2}[(\nu_{N+1}-y)(\nu_{N+1}-x)]^{\alpha/2} \frac{\Gamma(N+2)}{\Gamma(N+\alpha+1)} \times \\
&\quad \frac{R_{N+1}^{\alpha}(y) L_N^{\alpha}(\nu_{N+1}-x) - R_{N+1}^{\alpha}(x) L_N^{\alpha}(\nu_{N+1}-y)}{y-x}
\end{aligned} \tag{E.4}
$$

with $-\infty < x, y < \nu_{N+1}$. Choosing now $y = t_k$, where t_k is one of the $N+1$ roots of $R_{N+1}(y)$, the expression for the reproducing kernel changes to

$$K(x,t_k) = e^{-\nu_{N+1}} e^{(x+t_k)/2}[(\nu_{N+1}-t_k)(\nu_{N+1}-x)]^{\alpha/2}\frac{\Gamma(N+2)}{\Gamma(N+\alpha+1)} \cdot \left[\frac{R^{\alpha}_{N+1}(x)L^{\alpha}_{N}(\nu_{N+1}-t_k)}{(x-t_k)}\right] \tag{E.5}$$

To find the composing function corresponding to the reproducing kernel already found, one needs only to calculate the normalization constant:

$$\begin{aligned}\int_{-\infty}^{\nu_{N+1}} |K(x,t_k)|^2 dx &= \lim_{x\to t_k} e^{-\nu_{N+1}} e^{(x+t_k)/2}[(\nu_{N+1}-t_k)(\nu_{N+1}-x)]^{\alpha/2}\frac{\Gamma(N+2)}{\Gamma(N+\alpha+1)} \cdot \\ &\quad \frac{L^{\alpha}_{N}(\nu_{N+1}-t_k)R^{\alpha}_{N+1}(x)}{(x-t_k)} \\ &= e^{-\nu_{N+1}+t_k}(\nu_{N+1}-t_k)^{\alpha}\frac{\Gamma(N+2)}{\Gamma(N+\alpha+1)}L^{\alpha}_{N}(\nu_{N+1}-t_k) \cdot \\ &\quad \left[\frac{d}{dx}R^{\alpha}_{N+1}(x)\right]_{x=t_k} \\ &= e^{-\nu_{N+1}+t_k}(\nu_{N+1}-t_k)^{\alpha}\frac{\Gamma(N+2)}{\Gamma(N+\alpha+1)}L^{\alpha}_{N}(\nu_{N+1}-t_k) \cdot \\ &\quad \left[\frac{d}{dx}L^{\alpha}_{N+1}(\nu_{N+1}-x)\right]_{x=t_k}\end{aligned}$$

Applying the relationship for the first derivative of a Laguerre polynomial [56],

$$\frac{d}{dx}L^{\alpha}_{N+1}(\nu_{N+1}-x) = \frac{(-1)}{\nu_{N+1}-x}\left[(N+1)L^{\alpha}_{N+1}(\nu_{N+1}-x) - (N+\alpha+1)L^{\alpha}_{N}(\nu_{N+1}-x)\right]$$

With $x = t_k$, a root of $R^{\alpha}_{N+1}(x)$, the last expression simplifies to

$$\left[\frac{d}{dx}L^{\alpha}_{N+1}(\nu_{N+1}-x)\right]_{x=t_k} = \frac{(N+\alpha+1)L^{\alpha}_{N}(\nu_{N+1}-t_k)}{\nu_{N+1}-t_k}$$

Substituting in the equation for the normalization constant,

$$\int_{-\infty}^{\nu_{N+1}} |K(x,t_k)|^2 dx = \frac{e^{-\nu_{N+1}+t_k}(\nu_{N+1}-t_k)^{\alpha-1}\Gamma(N+2)[L^{\alpha}_{N}(\nu_{N+1}-t_k)]^2(N+\alpha+1)}{\Gamma(N+\alpha+1)} \tag{E.6}$$

The composing function will then be of the form (after dividing Equation E.5 by Equation E.6),

$$S_k(x) = \frac{e^{(x-t_k)/2}(\nu_{N+1}-t_k)^{1-\alpha/2}(\nu_{N+1}-x)^{\alpha/2}L^{\alpha}_{N+1}(\nu_{N+1}-x)}{(x-t_k)L^{\alpha}_{N}(\nu_{N+1}-t_k)(N+\alpha+1)} \tag{E.7}$$

$$= \frac{e^{(x-t_k)/2}(\nu_{N+1}-t_k)^{1-\alpha/2}(\nu_{N+1}-x)^{\alpha/2}R^{\alpha}_{N+1}}{(x-t_k)L^{\alpha}_{N}(\nu_{N+1}-t_k)(N+\alpha+1)} \tag{E.8}$$

E.2 The particular case when $x = y$ in the reproducing kernel

Consider the expression for the reproducing kernel (Equation E.1) with $\alpha = 0$.

$$K(x,y) = e^{-\nu_{N+1}} e^{(x+y)/2}(N+1)\left[\frac{R_{N+1}(y)L_N(\nu_{N+1}-x) - R_{N+1}(x)L_N(\nu_{N+1}-y)}{y-x}\right]$$

Making $x = y$,

$$\begin{aligned}
K(y,y) &= -e^{\nu_{N+1}} e^{y}(N+1)\left\{R_{N+1}(y)\left[\frac{d}{dx}L_N(\nu_{N+1}-x)\right]_{x=y} - L_N(\nu_{N+1}-y)\cdot\right. \\
&\quad \left.\left[\frac{d}{dx}L_{N+1}(\nu_{N+1}-x)\right]_{x=y}\right\} \\
&= e^{\nu_{N+1}} e^{y}(N+1)\left\{R_{N+1}(y)\left[\frac{N}{\nu_{N+1}-x}(L_N(\nu_{N+1}-x) - L_{N-1}(\nu_{N+1}-x))\right]\right. \\
&\quad \left. - L_N(\nu_{N+1}-y)\left[\frac{N+1}{\nu_{N+1}-x}(L_{N+1}(\nu_{N+1}-x) - L_N(\nu_{N+1}-x))\right]\right\}_{x=y} \\
&= \frac{e^{-\nu_{N+1}+y}(N+1)}{\nu_{N+1}-y}\{NR_{N+1}(y)[L_N(\nu_{N+1}-y) - L_{N-1}(\nu_{N+1}-y)] - \\
&\quad (N+1)L_N(\nu_{N+1}-y)[R_{N+1}(y) - L_N(\nu_{N+1}-y)]\} \\
&= \frac{e^{-\nu_{N+1}+y}(N+1)}{\nu_{N+1}-y}\{(N+1)[L_N(\nu_{N+1}-y)]^2 - R_{N+1}(y)[L_N(\nu_{N+1}-y) + \\
&\quad NL_{N-1}(\nu_{N+1}-y)]\}
\end{aligned}$$

If y is a root of $R_{N+1}(y)$, then

$$K(y,y) = \frac{e^{\nu_{N+1}+y}(N+1)^2[L_N(\nu_{N+1}-y)]^2}{\nu_{N+1}-y}$$

Appendix F

Computational Complexity of SVD and SLE Methods

F.1 SLE method

The computational work performed in the solution of the system $A\underline{x} = \underline{b}$ by Gaussian elimination is divided in three steps: calculation of multipliers, elimination, and back substitution [108].

1. If we consider only divisions and multiplications as the relevant operations, for the first step there are $\frac{(n-1)(n-2)}{2}$ operations, where n is the number of equations.

2. For the second step, there are $\frac{n(n-1)(2n-1)}{6}$ operations.

3. For the last step, there are $\frac{(n-1)(n-2)}{2} + \frac{n(n+1)}{2} + n$ operations.

The final number of operations is given by the sum of the three counts,

$$\lambda_{SLE} = \frac{2n^3 + 6n^2 - 8n + 12}{6}$$

The last equation is restrained to the system of linear equations. If the number of operations needed to calculate the coefficients of the system is included, n^2 more operations have to be summed to the last result. Therefore,

$$\begin{aligned} \mu_{SLE} &= \lambda_{SLE} + n^2 \\ &= \frac{2n^3 + 12n^2 - 8n + 12}{6} \end{aligned} \tag{F.1}$$

F.2 SVD method

The operation counts for the SVD method will be based on the second version of the method, that was presented in Section 3.1. There are five steps. Assume for the calculations that $m = p$.

1. The formation of matrix B takes m^2 multiplications.

2. The second step is executed in two main stages, according to the algorithm proposed in [109]. The first stage consists in the application of Householder transformations to reduce matrix B to a bidiagonal form, and the second stage consists in the application of a variant of the QR algorithm to find the singular values of the bidiagonal matrix. There is an intermediate step between both stages, which consists in the initialization of the matrices U and V, which contain the left and the right singular vectors of B. The reduction to bidiagonal form has $\frac{4}{3}m^3$ floating point multiplications. The initialization for matrices U and V implies $\frac{4}{3}m^3$ multiplications. In the second stage, the rotations that are used to reduce the bidiagonal matrix to diagonal form must be multiplied into the arrays of singular vectors. If r designates the number of rotations, then the amount of multiplications performed is $8mr$. The number r is difficult to

estimate. The reduction of the kth superdiagonal element requires no more than k rotations. There are approximately m superdiagonal elements that must be reduced until they are considered to be zero by a given convergence criterion. Thus, if s is the maximum number of iterations required to reduce a superdiagonal element, $r \leq \frac{1}{2}sm^2$ [69].

3. The third step takes $2m^3 + m$ operations.

4. The fourth step takes $2m^2$ operations.

5. The fifth step takes m^2 operations.

The approximate number of operations (counting only divisions and multiplications) for the SVD method, for a set of m nonuniform samples is

$$\begin{aligned} \mu_{SVD} &= m^2 + \frac{8}{3}m^3 + 8mr + 2m^3 + m + 2m^2 + m^2 \\ &= \frac{14m^3 + 12m^2 + 24mr + 3m}{3} \end{aligned} \tag{F.2}$$